DIFFERENTIAL CELLULAR RESPONSES TO METAL OXIDE BASED NANOPARTICLES AND POTENTIAL BIOMEDICAL APPLICATIONS

by

Cory L. Hanley

A thesis

submitted in partial fulfillment

of the requirements for the degree of

Master of Science in Biology

Boise State University

Summer 2009

The thesis presented by Cory L. Hanley entitled “Differential cellular responses to metal oxide based nanoparticles and potential biomedical applications” is hereby approved:

Denise Wingett Advisor	Date
Alex Punnoose Committee member	Date
Kevin Feris Committee member	Date
Juliette Tinker Committee member	Date
John R. Pelton Dean of the Graduate College	Date

DEDICATION

To my parents, John and Gwen Hanley

ACKNOWLEDGEMENTS

I would like to extend my deepest gratitude to my advisor, Dr. Denise Wingett, for her continued encouragement and support throughout the course of my graduate career. Her guidance and expertise were paramount to my learning and scientific accomplishments and for this I am forever grateful. I would like to most sincerely thank Dr. Alex Punnoose, who not only spearheaded this collaborative nano-based project, but also inspired success by enthusiastically sharing his knowledge, resources and unyielding support, and to members of Dr. Punnoose's lab for graciously supplying me with the nanomaterials used in my research. Special thanks and recognition goes to my committee members, Dr. Kevin Feris for his mentoring and contributions to my project, especially with regard to the bacterial studies, and Dr. Juliette Tinker for her assistance and support. I would also like to thank our blood donors and NIH grant support, without which my research would not have been possible.

I wish to extend thanks to my labmates, Janet Layne and Ashley Masterson, for their continued friendship and support throughout this process, and to Alma Hodzic for her friendship and guidance in the beginning of my graduate scientific career. Special thanks to Janet Layne, for allowing me to include some of her cancer cell experiments in my research. Finally, I would like to thank all members of the Boise State University Biology Department who supported me in my graduate school endeavors.

AUTOBIOGRAPHY

I was born on January 22, 1977 to John and Gwen Hanley and spent my life growing up between Anchorage, Alaska and Ketchum, Idaho. After graduating from high school, I attended Boston College where I majored in Psychology. After college, I lived and worked in Washington, D.C. and San Francisco, CA before deciding to return to Idaho and enrolling at Boise State University to take post-baccalaureate science classes. It was while taking Immunology from Dr. Denise Wingett that I developed a true passion for molecular biology and immunology and decided to pursue a Master's of Science in Biology degree. After graduating I plan on pursuing a career as an Associate Research Scientist in immunology or a related field.

EDUCATION

Boise State University, Boise, Idaho- M.S. Biology- August, 2009

Boston College, Chestnut Hill, Massachusetts- B.A. Psychology- May, 1999

PUBLICATIONS

- Reddy, K.M., Feris, K., Bell, J., Wingett, D., **Hanley, C.** and Punnoose, A. (2007) Selective toxicity of zinc oxide nanoparticles to prokaryotic and eukaryotic systems. *Appl Phys Lett* **90**: 213901-213902
- **Hanley, C.**, Layne, J., Punnoose, A., Reddy, K.M., Coombs, A., Coombs, I., Feris, K. and Wingett, D. (2008) Preferential killing of cancer cells and activated human T cells using ZnO nanoparticles. *Nanotechnology* **19**(29): 295103-13
- Wang, H., Wingett, D., Engelhard, M., Feris, K., Reddy, K.M., Turner, P., Layne, J., **Hanley, C.**, Bell, J., Tenne, D., Wang, C. and Punnoose, A. (2009) Fluorescent dye encapsulated ZnO particles with cell-specific toxicity for potential use in biomedical applications. *Journal of Material Science*: *Materials in Medicine* 20**(1): 11-22**
- **Hanley, C**., Coombs, A., Coombs, I., Punnoose, A., Thurbur, A. and Wingett, D. (2009) The influences of cell type and ZnO NP size on immune cell cytotoxicity and cytokine induction, *in preparation*

ABSTRACT

The multidisciplinary field of nanotechnology has allowed for unprecedented exploration and manipulation of molecular, sub-molecular, and atomic structures and advancements in this field are revolutionizing scientific thought and applications. Within the field of nanotechnology, the branch of nanobiotechnology focuses on studying the effects of nanomaterials on biological systems and to elucidate how nanomaterials interact with cells and cellular components. Nanoparticles are a particular type of nanomaterial whose dimensions measure 100 nanometers and are shown to possess unique size-dependent physical, chemical and biological properties compared to their bulk counterparts. Metal oxide nanoparticles, such as those made from ZnO, are a type of nanomaterial found in many different industrial products such as sunscreen, food preservatives and clothing. Due to the prevalence of ZnO nanoparticles in the environment, there is an urgent need to gain an understanding of how these particles interact with biological systems, and due to the fact that nanoparticles are within the range of many different naturally occurring biological molecules, research investigating nanoparticle-cell interactions may offer innovative approaches for the development of novel biomedical applications.

This research focuses on examining the effects of metal oxide based nanoparticles, including ZnO, on immune cells and investigates cell-specific responses

and mechanisms of toxicity. Collectively, our results demonstrate differential ZnO NP toxicity based on cell-type, activation status, and NP size with highly proliferative/rapidly diving cells (e.g. cancer cells and activated T cells) killed at lower concentrations of ZnO nanoparticles compared to normal cells. In addition, an inverse relationship between nanoparticle size and cytotoxicity was observed. Further, these results implicate ROS production as a major mechanism of ZnO-NP induced cytotoxicity capable of inducing apoptosis in human immune cells, and reveal ZnO NP induce pro-inflammatory cytokine production (e.g. IFN-γ, TNF-α and IL-12). Exploitation of the preferential nanoparticle-mediated toxicity observed in these studies may provide a foundation for the design and development of novel ZnO nanoparticle based biomedical applications and therapeutics for the treatment of human diseases, such as cancer and autoimmune disorders.

TABLE OF CONTENTS

LIST OF TABLES

LIST OF FIGURES

LIST OF ABBREVIATIONS

Ab	Antibody
Ag	Antigen
APC	Antigen Presenting Cell
ATP	Adenosine Triphosphate
CD	Cluster of Differentiation
CD40L	CD40 Ligand
CeO_2	Cerium dioxide
DCFH-DA	2',7'-Dichlorofluorescein Diacetate
DEG	Diethylene Glycol
DNA	Deoxyribonucleic Acid
E. coli	Escherichia coli
ELISA	Enzyme-linked Immunosorbent Assay
ETC	Electron Transport Chain
FACS	Fluorescent-Activated Cell Sorting
FBS	Fetal Bovine Serum
FDA	Food and Drug Administration
Fe^{2+}	Ionic Iron
FITC	Fluoroscein Isothiocyanate

FS	Forward-Scatter
g	Gram
GSH	Glutathione
H_2O_2	Hydrogen Peroxide
IC_{50}	50% Inhibitory Concentration
IFN-γ	Interferon Gamma
Ig	Immunoglobulin
IL-12	Interleukin-12
L	Liter
LAK	Lymphokine-Activated Killer Cell
MFI	Mean Fluorescent Intensity
MHC I	Major Histocompatibility Complex I
MHC II	Major Histocompatibility Complex II
mL	Mililiter
Mono	Monocytes
NAC	N-Acetyl Cysteine
ng	Nanogram
NO	Nitric Oxide
NP	Nanoparticle
NK	Natural killer cell
O_2	Molecular Oxygen
O_2^-	Superoxide Anion

$\cdot O_2^-$	Superoxide Radical
OH·	Hydroxide Radical
PBMC	Peripheral Blood Mononuclear Cells
PBS	Phosphate Buffer Saline
PE	Phycoerithryn
PI	Propidium iodide
PMA	Phorbol 12-Myristate 13-Acetate
QD	Quantum Dot
ROS	Reactive Oxygen Species
S. aureus	Staphylococcus aureus
SiO_2	Silicon Dioxide
SnO_2	Tin Dioxide
SOD	Superoxide Dismutase
SSC	Side-Scatter
T_C	Cytotoxic T Cell
TCR	T Cell Receptor
TEM	Transmission Electron Microscopy
T_H	T Helper Cell
Th1	T Helper Cell Type 1
Th2	T Helper Cell Type 2
TNF-α	Tumor Necrosis Factor Alpha
uL	Microliter

XPS	Photoelectron Spectroscopy
XRD	X-Ray Diffraction
ZnO	Zinc oxide

INTRODUCTION

Scientific advancements in biology and biotechnology have enabled the molecular and sub-molecular examination of intracellular dynamics and intercellular interactions, resulting in the development of new and improved biomedical devices and therapeutic interventions. The ability to investigate sub-atomic, atomic and molecular materials and structures has led to the emerging field of nanotechnology, a multidisciplinary industry concerned with researching, developing and utilizing nanometer (nm) sized materials. As many naturally occurring biological structures are found in the nanometer range, the integration of biology and nanotechnology provides a platform by which significant contributions to the development of new diagnostic agents and devices, and targeted therapeutic treatments may be achieved. Nano-sized materials, such as nanoparticles (NP), can exhibit unusual properties such as alterations in chemical reactivity and other physical characteristics not predicted for larger particles made from the same material (Feringa 2000). The altered properties of NP, coupled with their similarity in size to many biological structures, allow for their interactions with biomolecules both on the cell surface and within the cell, and may potentially affect cellular responses in a dynamic and selective manner. As such, it is necessary to identify and characterize the effects of NP on various biological systems and cell types and evaluate the possibility of exploiting NP for use in novel biomedical applications.

Nanotechnology and Nanomaterials

Nanotechnology encompasses many different scientific disciplines, including computer science, engineering, physics, chemistry and biology, and has revolutionized scientific applications in all these areas. Explosive growth in the field of nanotechnology has resulted in phenomenal global market spending on research and products, increasing from $8.6 billion in 2004 to upwards of $18 billion in 2008 (approximately $8.4 billion in government funding, $8.4 billion in corporate funding and $1.6 billion in venture capitalist funding), and is estimated to exceed more than $2.5 trillion dollars worldwide by the year 2014 (Lux Research Inc 2009). In response to this rapid growth and the widespread use of nano-based products, federally funded organizations, such as the National Nanotechnology Initiative (NNI), have been created to monitor and support the research and development of nanomaterials and nanostructures. As stated in the White House press release upon the formation of the NNI, "These developments [in nanotechnology] are likely to change the way almost everything - from vaccines to computers to automobile tires to objects not yet imagined - is designed and made" (NNI 2009).

Unlike bulk materials, whose behaviors are dictated and predicted based on the laws of classical physics and the properties of individual molecules, the properties and characteristics of nanomaterials are governed by laws of both quantum and classical physics. This phenomenon is attributed to "quantum effects" in which the behaviors of a materials are altered in response to significant reductions in material size (Singh and Nalwa 2007). As the size of a material is reduced to the nano-scale, there is an increase in the surface area to volume ratio, and a greater percentage of atoms are expressed on the

surface of nanomaterials compared to micron-sized bulk materials (Cao 2004). The consequences of this phenomenon are the unique properties observed in many nanomaterials such as changes in reactivity, conductivity, and light diffraction. An example of these changes is illustrated when comparing the properties of bulk copper compared to nano-sized copper structures. Although bulk copper (e.g. wire, ribbon, etc.) is malleable and highly conductive, when reduced to the nano-scale (less than 50 nm) copper loses both its malleability and conductive abilities (Takata, Lee, Lim, Kim and Tsuji 2007). Another example is the discrepancy observed in suspensions of alumina NP, which have been shown to have increased thermal conductivity compared to suspensions of micron-sized alumina particles (Oesterling et al. 2008).

The term "nanotechnology" is a 20th century idiom, however evidence for utilization of nanomaterials can be found in early civilization artifacts. Archaeologists and museum scientists have discovered that 10th century Persian artisans used metallic (e.g. silver and copper) NP in ceramic glazes to give the pottery an illustrious and iridescent finish, with results dependent on size, shape, and the distribution of the metallic clusters in the glaze (Erhardt 2003). This technique, which spread throughout Europe by the 14th century, was accomplished by the breakdown of metal salts and oxides during the firing process (Erhardt 2003). Although the molecular basis for the distinctive properties exhibited by these nanomaterials (namely, increased optical refractivity and surface reactivity) was not understood at the time, modern science has revealed these desirable qualities are ascribed to the nanometer-sized particles found in these glazes.

The central scientific concepts which led to the creation of nanotechnology were first described by Scottish physicist, James Clerk Maxwell, in 1867, whose work

revolutionized theories explaining the laws of thermodynamics and electromagnetic behavior (Maxwell and Niven 2003). His theories, stating that molecular movement is predicted by the laws of probability, and not certainty, created a foundation upon which nanotechnology was developed (Maxwell and Niven 2003). From that time through the first quarter of the 20th century, significant progress was made towards the understanding of atomic/sub-atomic behavior, all of which contributed to the concepts upon which nanotechnology is built. However, it was a seminar given by Richard Feynman in 1959 entitled "There's Plenty of Room at the Bottom" which is credited as catalyzing the creation of nanotechnology (Wilkinson 2004). In this presentation, Dr. Feynman discussed the possibility of manipulating materials at the atomic and molecular scale, and addressed the potential issues associated with this, such as the fact that matter on this scale behaves differently than it would on a larger scale (Feynman 1959).

Nanomaterials and nano-based products are becoming increasingly prevalent and can already be found in a variety of different industrial applications, ranging from electronics and laser-based applications to anti-microbial band-aids and anti-reflective coatings for glass (Osman, Rardon, Friedman, and Fanor-Vega 2006). Specific types of nanomaterials, such as those made from metal oxides, have been found to possess specific properties, such as increased conductivity, changes in color and transparency, which make them useful in a wide-range of industrial products, including water-repellent clothing, biosensors, electronics and cosmetics (Cao 2004).

ZnO is a type of naturally occurring metal oxide frequently found in a variety of different products such as paints, adhesives, sunscreens, cosmetics, and as an anti-microbial agent in ointments and rubber (Nohynek, Dufour and Roberts 2008). When

reduced to the nano-scale, ZnO exhibits distinctive optical and electronic properties, and demonstrates superior transparency and UV adsorption/blocking abilities compared to bulk ZnO (Cross, Innes, Roberts, Tsuzuki, Robertson and McCormick 2007). Due to the increasing use of nanomaterials in industrial applications, a thorough understanding of the mechanisms by which nano-sized materials interact and impact various cell types is critical from both a toxicological standpoint and for enabling the discovery of potential applications for these materials.

Nanobiotechnology and Nanoparticles

Nanobiotechnology is a specific branch of nanotechnology aimed at investigating potential biological applications for nanomaterials and exploring how nano-sized materials and structures interact with and affect biological systems (McNeil 2005). As many important biological entities, such as DNA and proteins, fall within the nanometer size range, nanomaterials (e.g. NP) are being designed to interact with specific biological components allowing for improved precision and efficiency in molecular manufacturing and control. The use of nanomaterials in biological applications may provide new approaches and exciting possibilities for genomics, information storage, energy conservation and medicine. Current applications under investigation include biosensing, tumor imaging, and targeted drug delivery (e.g. antibody-NP conjugates) (Angeli et al. 2008; Dinauer, Balthasar, Weber, Kreuter, Langer and von Briesen 2005). Researching new applications for different types of nanomaterials in a biological context is an integral part of nanobiotechnology, and exploiting the specific properties of nanomaterials may

enable new approaches for manipulating and eliciting specific biological responses (Lowe 2000).

NP (particles 100 nm or less in any two dimensions) are among the nanomaterials that may be best suited for biological applications due to their size being in the range of many biological entities and their unique size-dependent properties (Zhang, Gu, Chan, Wang, Langer and Farokhzad 2008). NP are highly diversified, come in a variety of different shapes and sizes and are made from an assortment of materials. All these factors contribute to the unique size-dependent physical, chemical, and biological properties observed in NP which distinguish them from their micron-sized bulk counterparts (McNeil 2005). Additionally, many types of NP have a propensity to form micrometer-sized aggregates (called nanopowders), which affect both the solubility and behavior of these materials (Roca and Haes 2008). Metal oxide NP, in particular, have wide-spread applications and are frequently found in many different commercial products ranging from sunscreens and cosmetics (e.g. TiO_2, Fe_3O_4 and ZnO) to dental fillers (e.g. SiO_2) and photovoltaic cells (e.g. CdS, CdSe and ZnS) (Brayner, Ferrari-Iliou, Brivois, Djediat, Benedetti and Fievet 2006; Donaldson 2006).

Examples of some NP dependent properties include superparamagnetism observed in certain types of magnetic NP, surface plasmon resonance in various metal NP, and the quantum confinement of semiconductor NP (Donaldson 2006). These differences are further illustrated in the altered characteristics observed in gold NP which appear reddish-black in color and are capable of conducting electricity, compared to micron-sized bulk gold which is yellow in color and non-conductive (Wilson 2008). The distinctive chemical and physical properties observed in NP warrants further

investigation into the biological effects of specific types of NP to various cellular systems and cell types under physiologically relevant conditions and identifying different types of NP suited for biological applications (Schmid 2004). To this end, much research is being conducted to evaluate potential biological applications for various types of NP, ranging from drug delivery and biosensing to even utilizing NP as drugs themselves (Bogunia-Kubik and Sugisaka 2002). Examples of NP specifically useful for biotechnology and nanomedicine include fullerenes (e.g. bucky balls and carbon tubes), liposomes, nanoshells, dendrimers, nanorods, superparamagnetic NP, and quantum dots (QDs) (Roco 2003).

QDs, or nanocrystals, are semiconductor NP (e.g. CuO_2, Fe_2O_3, Au, ZnO, etc.) being explored for biotechnological applications, specifically for use in biosensing, cell-labeling/tumor imaging and drug delivery due to their distinctive electronic and fluorescent properties and reduced tendency to photobleach (Vashist, Tewari, Bajpai, Bharadwaj and Raiteri 2006). The novel properties possessed by QDs are due to valence electron band holes, or excitons, which are confined in all three spatial dimensions in these particles (Ashammakhi 2006). As many types of metal NP and metal oxide NP are QDs, these NP (e.g. ZnO NP) are gaining recognition and utility not only for expansion on traditional applications, but also for new biomedical purposes.

Nanomedicine and Biomedical Applications of NP

Nanomedicine is similar to nanobiotechnology in that both encompass investigating the impact of nanomaterials on biological systems. However, nanomedicine specifically describes the intersection of nanotechnology and medical science, and is

focused on developing and utilizing nanomaterials to target specific cellular and sub-cellular components for disease prevention, treatment and damaged tissue repair (Moghimi, Hunter and Murray 2005; Ashammakhi 2006). In contrast to many conventional therapeutics (e.g. radiation, chemotherapy and surgery), nanomedicine offers highly selective approaches to eliminate or repair specific cells and examples of the types of nanomedicines under investigation include NP biological mimetics, the creation of "nanomachines" (e.g. structures made from interchangeable DNA parts and DNA scaffolds), nano-scale devices used for drug release, biosensors for use in laboratory diagnosis (e.g. QD), polymetric nano-constructs for use as molecular switches, tissue engineering, and creating NP-antibody conjugates for targeted delivery of drugs, genetic elements and diagnostic agents to specific cells and tissues (Navalakhe and Nandedkar 2007; Riehemann, Schneider, Luger, Godin, Ferrari and Fuchs 2009). Additionally, NP may be useful modalities for targeting and killing specific disease causing cells (e.g. tumor and auto-reactive cells) while leaving normal cells and tissues unharmed, and with fewer adverse side effects compared to conventional treatments (Cho, Wang, Nie, Chen and Shin 2008).

Thus far, findings from several published *in vitro* studies examining the ability of engineered NP to selectively destroy disease-causing pathogens and cancer cells have revealed promising results (Emerich and Thanos 2007). One approach involves using porous, biologically compatible ceramic NP (e.g. silica, alumina, titania, etc.) to encapsulate anti-cancer photosensitive drugs (Salata 2004). Cytotoxicity is achieved using a laser beam, which causes the photosensitive drugs to release reactive oxygen species (ROS) which are cytotoxic to the targeted tumor cells, and surface modifications

(e.g. attaching antibodies to the surface) allow targeted delivery and uptake of the NP/drug complex to tumor cells (Salata 2004). Exploring different types of NP materials for use in nanomedicines may reveal innovative methods for treating human diseases such as cancer, autoimmune disease, neurodegenerative disorders and infection. However, before any nanomedicine can be employed, a detailed understanding of how NP interact and effect different types of cells is critical and is one of the major goals of our research.

NP and Toxicity

The development and industrial exploitation of NP is progressing at an extremely rapid rate and potential applications are being continually discovered. However, information regarding mechanisms of NP toxicity to different cell types and biological systems lags behind this prolific growth. Understanding the effects of NP on cell systems is imperative as the unique behaviors and characteristics observed in many nano-sized materials can potentially render an otherwise benign substance toxic to cells at the same concentration (Nair et al. 2008). For example, a recently published study showed CdS NP to be toxic to mammalian Chinese Hamster Lung (CHL) cells at lower concentrations compared to micron sized CdS particles (Li et al. 2009). As with the introduction of any new material that displays unusual and unorthodox behaviors, there is a need to increase knowledge and awareness of the potential environmental impacts and toxic effects. The toxicity of a given substance is monitored and recorded by the Federal Drug Administration which has established a list of "Generally Recognized as Safe" (GRAS) substances which is a record of substances shown by rigorous *in vitro* and *in vivo*

scientific studies to be safe under the conditions of their accepted use and are thus exempt from the usual Federal Food, Drug, and Cosmetic Act (FFDCA) food additive tolerance requirements (Angeli et al. 2008). Lately, concern has been raised over the evaluation guidelines used to assess the safety of commonly accepted nano-sized GRAS substances, as most toxicological data collected was conducted using bulk sized materials and did not take the special characteristics of nanomaterials into consideration (Fischer and Chan 2007). Recently published research suggests NP toxicity is largely dependent on chemical composition (e.g. subsequent ion dissolution and NP catalyzed cell-surface reactions), potential for ROS formation, NP size/shape, and specific NP-cell interactions (Guo et al. 2008; Dobrovolskaia and McNeil 2007). As such, additional research is needed to investigate the factors influencing NP toxicity to specific cell types and to elucidate mechanisms of NP-induced cytotoxicity.

Although ZnO is a GRAS substance and has been shown to be relatively nontoxic in bulk form (micron-sized particles and larger), recently published studies have demonstrated ZnO NP toxicity in both eukaryotic and prokaryotic cell types. In one study, researchers tested the effects of various metal oxide NP (e.g. TiO_2, Al_2O_3, SiO_2 and ZnO) to several strains of bacteria (*E. coli*, *B. subtilis* and *P. fluorescens*) and found significant differences in toxicity in all metal oxide NP tested (except for TiO_2) compared to their respective micron-scaled counterparts. Interestingly, of all the metal oxide NP types used in this study, ZnO NP were shown to be the most toxic to all bacterial strains tested (Jiang, Mashayekhi and Xing 2009). Another recently published study found ZnO NP display selective toxicity to different bacterial strains, namely increased susceptibility in *S. aureus* compared to *E. coli*. In addition, this study demonstrated that prokaryotic

cells were killed at lower concentrations of ZnO NP compared to primary human T cells (Reddy, Feris, Bell, Wingett, Hanley and Punnoose 2007).

Other published studies examining the effects of metal oxide NP, specifically ZnO NP, on eukaryotic cells have demonstrated significant cytotoxicity in various mammalian cells, and research suggests the production of ROS may be a predominant mechanism of toxicity (Limbach, Wick, Manser, Grass, Bruinink and Stark 2007). In order to better predict toxic potential of NP due to oxidative stress, the hierarchical oxidative stress model was developed which uses a three-tiered system based on the levels of ROS produced in response to ZnO NP, CeO_2 NP and TiO_2 NP (Xia et al. 2008a). In tier 1, low levels of ROS produced initiate the upregulation of the Nrf2 transcription factor responsible for mediating the expression of antioxidant response elements (ARE) in promoter phase 2 genes. This chain of events acts as a compensatory mechanism to protect against ROS-induced cell damage. If exogenous sources of ROS overwhelm tier 1 mechanisms, an inflammatory response is elicited in which ROS induce redox-sensitive signaling pathways (e.g. MAP-kinases, NF-κB cascades and pro-inflammatory cytokine expression such as IL-12, IFN-γ and TNF-α). Finally, if ROS are produced in excess of what is required to induce a tier 2 response, mitochondrial inner membrane electron transfer and permeability are disrupted, resulting in ROS-induced cell death by both apoptotic and necrotic pathways.

Although ZnO NP have been shown to be toxic to eukaryotic cells, the majority of research testing the ZnO NP toxicity to mammalian cells has been done on immortalized cell lines and up until now, there have been only limited *in vitro* studies evaluating ZnO NP cytotoxicity to primary human cells. Additionally, little is known

about the factors influencing ZnO NP-mediated toxicity to specific immune cell types such as ROS formation and mechanisms of ZnO NP-induced cell death (e.g. apoptosis and necrosis). ZnO toxicity to both eukaryotic and prokaryotic cells has been established, with varying toxicity thresholds observed for different strains of bacteria. Given the integral role of the immune system in treating and preventing disease and maintaining host integrity and the phenotypic diversity present amongst immune cells, it is reasonable to assume not all immune cells will respond the same to ZnO NP treatment and is an issue that requires further examination.

The Immune System and Host Health

The immune system acts to protect and defend animals from pathological, potentially disease-causing entities such as viruses, bacteria, parasites, and mutated/aberrant cells (i.e. cancer cells) by means of highly complex and tightly regulated physical, chemical and biological mechanisms (U.S. Department of Health and Human Services 2003). A key aspect of the immune system is the ability to distinguish "self" from "nonself", or put another way, the ability to recognize and ignore normal healthy "self" cells and to identify and destroy "foreign" non-self cells and entities (Mannie 1999). This requires the coordinated action of many different types of cells called leukocytes, commonly known as "white blood cells" (WBC). Immune system malfunctioning results in the emergence of disease-processes such as autoimmune disease (where the immune cells attack and destroy normal healthy tissue) or in the case of immune system failure, the emergence of opportunistic infections and cancer (Cohn 2005). Evaluating the effects of commonly used NP, such as ZnO NP, on immune cells

and elucidating mechanisms of immune cell-NP interactions may ultimately allow for creating targeted NP treatments for these diseases and provides critical information on how ZnO NP impact the human immune system.

Innate Versus Adaptive Immunity

The immune system is broadly broken up into two intricately related groups, innate immunity and adaptive immunity (Huston 1997). Innate immunity refers to those defense mechanisms which serve as the "first line of defense" against foreign entities upon initial exposure. Components of the innate immune system are preventive in nature and are present before exposure to an infectious pathogen and are extremely fast in nature (Uthaisangsook, Day, Bahna, Good and Haraguchi 2002). An important distinction between innate and adaptive immune response is that innate immune mechanisms are non-specific, as they do not recognize specific pathogens but rather provide general barriers against infection or recognize general classes of molecular markers commonly found on classes of pathological organisms (Uthaisangsook et al. 2002). Examples include physical barriers such as the skin and mucous membranes, physiological barriers such as temperature and pH, and biological barriers by way of cells that act to contain and/or destroy pathogens and small non-cellular debris via internalization and the release of various chemicals and cytokines (Mayer 2006). Additionally, the inflammatory response acts as a barrier against foreign invasion by containment, activation, and recruitment of immune cells to the area of infection (Mayer 2006).

When cells of the innate immune system recognize general "foreign" proteins they respond by either engulfment and intracellular destruction of the foreign material

(called phagocytosis), or by direct killing processes using chemicals mediators injected into target cells (Mayer 2006). After phagocytosis of a pathogen has occurred, a piece of the pathogen (an antigen (Ag)) is expressed on the phagocyte cell surface in a process known as Ag-presentation (Mayer 2006). Certain immune cells, namely dendritic cells (DC), macrophages/monocytes and B cells are known as professional antigen presenting cells (APC), and are responsible for presenting Ag to T lymphocytes (cells of the adaptive immune response) and activating Ag-specific immune responses (Bowers 2006a). A crucial aspect of immune response involves the release of soluble proteins called cytokines by immune cells in response to their encounter with foreign Ag, which serve as a means of cell-to-cell communication and are critical for proper immune system functioning (Mulloy and Rider 2006). Cytokines recognize and bind to specific receptors found on the surfaces of neighboring cells (paracrine), cells located distantly (endocrine) or on the secreting cell itself (autocrine) (Parkin and Cohen 2001). Binding of a cytokine to its receptor causes cell "activation", a process by which the cell progresses through the cell cycle, divides and proliferates and carries out various biological processes. Cells of the innate immune system include mast cells, eosinophils, basophils, neutrophils, DC, macrophages/monocytes, and natural killer (NK) cells (Mayer 2006).

In contrast to innate immunity, adaptive immunity is highly selective and diverse, and is capable of immunologic memory, a process by which arsenals of "memory" cells are formed for protection against future Ag exposure (Pancer and Cooper 2006). Additionally, cells of the adaptive immune response, namely T and B cell lymphocytes, are able to recognize and distinguish self from nonself (Pancer and Cooper 2006) and are capable of recognizing an infinite number of Ag (molecular markers specific to a

particular pathogen or foreign material) for the elimination of cells or entities displaying the specific Ag (Pancer and Cooper 2006). Once a specific Ag has been encountered, "memory" cells are created and remain dormant in circulation. In the event of a second encounter with the same Ag, memory cells become activated and rapidly proliferate to mount an attack against the foreign invader (Pancer and Cooper 2006). A functional adaptive immune system requires cooperation between B cells and T cells. While B cells serve as APC and produce Ag-specific antibodies to eliminate pathogens, T cells are activated after recognizing Ag presented by APC (Krogsgaard and Davis 2005). Although cells of the adaptive immune response are slower to take effect initially, once activated they are powerful weapons in fighting infection and disease (Pancer and Cooper 2006). Our research focuses on the effects of ZnO NP on T cells, B cells, NK cells and monocytes as a representative panel of immune cells with varying phenotypes and diverse biological functions.

Mechanisms of Cellular-Uptake: Endocytosis and Phagocytosis

Endocytosis describes the active (ATP-dependent) process used by cells for importing selected substances present in the extracellular environment (e.g. macromolecules, pathogens, membrane lipids, integral proteins and other particulate matter), and endocytic pathways are used by viruses, toxins and symbiotic micro-organisms to gain entry into cells (Doherty and McMahon 2009). Endocytic mechanisms serve many important cellular functions including the uptake of extracellular nutrients, regulation of cell-surface receptor expression, maintenance of cell polarity, and preservation of host health by eliminating potentially harmful bacteria and activating the

immune response by Ag-presentation (Seabra, Mules and Hume 2002; Doherty and McMahon 2009). During endocytosis, materials are taken into the cell by invagination of the plasma membrane, resulting in the formation of new membrane-bound vesicles containing the ingested substances (called endosomes), and are transported to various intracellular locations including digestive organelles (e.g. lysosomes) for degradation and cytoplasmic storage within endocytic compartments (Doherty and McMahon 2009). Additionally, endocytosis can occur by both clathrin-mediated and clathrin-independent processes, the former which is associated with the cytosolic protein clathrin, a large protein that assists in the formation of clathrin-coated pits on the inner surface of the plasma membrane. Endocytosis is generally subdivided into three groups: pinocytosis, receptor-mediated endocytosis, and phagocytosis (Decuzzi and Ferarri 2007), although disagreement exists among scientists about how endocytosis should be classified and some literature describes receptor-mediated endocytosis as a type of pinocytosis and considers phagocytosis as a separate cellular process altogether. Almost all cells of the body are capable of pinocytosis (also known as fluid endocytosis), an important cellular function by which cells engulf a portion of the extracellular fluid and all suspended and/or dissolved solutes, macromolecules, and small particulate matter. Unlike receptor-mediated endocytosis (RME), where ingestion of certain substances (e.g. cell surface proteins, viruses, etc.) is triggered by a ligand binding to its specific cell receptor, pinocytosis is non-specific as whatever substances/solutes are found within the area of invagination are brought into the cell from the extracellular environment (Lodish, Beck, Zipurksy, Matsudaira, Baltimore and Darnell 2000). RME is a highly complex and tightly regulated process used by most cells for the internalization of extracellular molecules

(e.g. proteins, viruses, transmembrane receptors, ion channels, etc.) in response to ligands binding to complementary cell-surface receptors and allows for precise regulation of the interactions between the cell and its environment. For example, regulation of cell sensitivity to specific extracellular ligand-mediated cues is achieved by RME, resulting in removal of certain transmembrane receptors so they are no longer available for these interactions (Doherty and McMahon 2009). Subsequent to ligand-receptor binding, clathrin-pits invaginate into the cell and bud off to yield ligand-receptor complexes in clathrin-coated vesicles (CCVs), and once transported from the cell membrane, are uncoated and the contents of the vesicles delivered to their target locations (Decuzzi and Ferrari 2008).

Phagocytosis is a special type of actin-dependent endocytosis used by specific immune cells, namely neutrophils, DC and monocytes/macrophages, as a major immune defense mechanism for the envelopment and internalization of large foreign particulates (usually >250 nm in size), bacteria, dead and/or dying cells, etc. (May and Machesky 2001). Phagocytosis requires recognition and binding of the material to specific plasma membrane receptors (e.g. Fc receptors, mannose receptors, scavenger receptors, etc.) capable of triggering intracellular uptake (usually by formation of F-actin driven pseudopods) of the membrane bound particle in vesicles called phagosomes. Subsequent to ingestion, phagosomes typically fuse with endosomes and/or lysosomes, exposing their contents to hydrolytic enzymes for digestion and intracellular processing of the material results in cell surface Ag-presentation (expression of a conserved protein sequence) on the phagocyte surface (May and Machesky 2001).

T Cells and Their Role in the Immune Response

T cells and B cells belong to a specific group of white blood cells called lymphocytes (Beilhack and Rockson 2003). T cells are named after the thymus gland which is the tissue in which they mature, and it is here that T cells migrate (after originating in the bone marrow) and begin to express an Ag-specific binding receptor on their surface called the T cell receptor (TCR) (Medema and Borst 1999). T cells play an integral role in both the innate and mammalian acquired immune responses by coordinating and activating immune cells from both arms of the immune system against a specific Ag and have direct, Ag-specific cytotoxic killing abilities. T cells are unique in that they almost only recognize and become activated by Ag presented in the context of a specific type of cell-membrane molecule, called a major histocompatibility complex (MHC) (Hummell 1994). Once activated, T cells are responsible for a myriad of activities which include mounting a specific defense against the foreign pathogens, direct killing of virally infected cells or tumor cells, and regulation of the T cell mediated response (Beilhack and Rockson 2003). T cells are divided into two subpopulations: T helper cells (T_H) and cytotoxic T cells (Tc) (Huston 1997). T_H cells express a CD4 receptor on their surface and are thus named $CD4^+$ T cells, while T_C cells express a CD8 receptor and are named $CD8^+$ T cells. $CD4^+$ T_H cells recognize Ag presented in the context of MHC II, a protein found on the surface of APC cells, while $CD8^+$ T_C cells recognize Ag presented by MHC I, a protein found on all nucleated cells (Medema and Borst 1999). T_C cells possess direct cytotoxic capabilities toward virally infected cells and cancer/tumor cells and are the cells involved in tissue rejection after transplantation (Behrens et al. 2004).

Additionally, all T cells are defined as either memory T cells or naïve T cells, a classification based on prior exposure to a specific Ag (Surh and Sprent 2008).

$CD4^+$ T Helper (T_H) Cells

T helper cells (T_H) comprise a subset of T lymphocytes responsible for orchestrating the immune response (Cohn 2005) and are also referred to as $CD4^+$ T cells due to the expression of a membrane glycoprotein molecule found on their surface called the cluster of differentiation (CD) type 4 (Schepers, Arens and Schumascher 2005). Unlike other types of immune cells, T_H cells are unique in that they do not phagocytose and/or have any direct cytotoxic abilities (Behrens et al. 2004) but instead are capable of recognizing Ag presented in the context of MHC class II proteins found on the surface of APCs, namely B cells, DCs and macrophages/monocytes (Krogsgaard and Davis 2005). Once T_H cells bind to the Ag-MHC II complex, they release numerous cytokines which bind to specific receptors located on the membranes of various cell types, and activate and direct immune cell activity involved in inflammation and pathogen elimination (Wieder, Braumuller, Kneilling, Pichler and Rocken 2008). In addition to activating a host of different immune cells, cytokines direct the differentiation of T helper cells into two different subsets, type 1 (Th1) and type 2 (Th2) (Fishman and Perelson 1999).

Th1 Versus Th2

Activated T_H cells secrete various cytokines which result in the activation and proliferation of other immune cells and initiate differentiation of T helper cells into two classes, Th1 and Th2 (Bowers 2006b). Th1 and Th2 differ in the cytokines they secrete,

which impacts the type of immune response produced, either a humoral, B-cell/antibody-based response, or a cellular, inflammatory-based response (Bowers 2006b). Th1 induction occurs in the presence of IL-2 and TNF-α, cytokines secreted mainly from macrophages/monocytes and DC (Fishman and Perelson 1999) and stimulate cells involved in the inflammatory response (e.g. macrophages/monocytes, DC and NK) to proliferate and secrete pro-inflammatory cytokines such as IL-12, IFN-gamma, etc. (Guo et al. 2004) At the same time, Th1 cells inhibit the production of IL-4, a major cytokine involved in promoting Th2 differentiation, thereby preserving and maintaining the Th1 response (Fishman and Perelson 1999).

The primary function of Th2 cells is to stimulate B cell proliferation and induce B-cell antibody class switching resulting in increased antibody production against a particular pathogen (Liberman, Refojo and Arzt 2003; Kondo 2003). The cytokines secreted by Th2 cells (e.g. IL-4, IL-5, IL-6, IL-10 and IL-13) serve to activate B cells and maintain the Th2 response by inhibition of cytokines critical for Th1 differentiation and result in Ag elimination and clearance of invading pathogens from the host (Sallusto, Palermo, Hoy and Lanzavecchia 1999; Fishman and Perelson 1999).

Memory Versus Naïve T Cells

T cells clones of antigenically-stimulated cells are called memory T cells, while T cells that have not yet encountered peripheral cognate Ag are called naïve T cells (Surh and Sprent 2008) and these T cell subsets are distinguished from each other based on their response to Ag and expression of specific cell surface markers. Memory T cells, characterized by the expression of the cell surface marker CD45RO ($CD45RO^{+}$), persist

after Ag exposure and remain dormant and inactive until a secondary encounter takes place (Surh and Sprent 2008). Unlike memory T cells, naïve T cells (Th_0) have not encountered cognate Ag, and are non-prolific quiescent cells characterized by the expression of the cell-surface marker CD45RA ($CD45RA^+$ cells) (Zimmermann, Prevost-Blondel, Blaser and Pircher 1999). Naïve T cells circulate throughout the body in a state of homeostasis until encounter with novel Ag, and upon activation adopt an activated or "memory" phenotype. The process of aging skews the memory to naive T cell ratio in favor of memory cells, which is partly responsible for the reduced ability of geriatric populations to effectively fight infection and disease (Surh and Sprent 2008). Both memory and naïve T cells are critical elements of the immune response; memory T cells allow for a fast response to previously encountered Ag, while naïve T cells are slower to respond, but enable the host to fight novel pathogens.

T Cell Activation

All mature T cells express the T cell receptor (TCR) on their surface, which is required for the ability of T cells to recognize and respond to Ag presented by APCs (Rojo, Bello and Portoles 2008). Each TCR is composed of two transmembrane polypeptides, α and β or γ and δ, with $\alpha\beta$ bearing T cells being the more common type (Modlin and Sieling 2005). Each TCR subunit has one variable and one constant domain, and at the end of each TCR are hypervariable loops that recognize Ag presented by MHC (Godfrey, Rossjohn and McCluskey 2008). Additionally, each TCR molecule is associated with a molecule called CD3, a complex critical for T cell signal transduction, made up of five transmembrane polypeptides (γ, ε, δ, ζ, and η) which come together to

form three dimers (γε, δε, and ζζ or ζη) (Rojo et al. 2008) . A correctly assembled TCR-CD3 complex is essential for T cell activation since the TCR is necessary for recognition of Ag (Feito, Jimenez-Perianez, Ojeda, Sanchez, Portoles and Rojo 2002). TCRs are capable of distinguishing self from non-self through the recognition of both endogenous (i.e. tumor cells and virally infected cells) and exogenous (i.e. bacteria) foreign molecules. Upon pathogen recognition, APCs engulf and digest the foreign material into smaller peptides which are expressed on the surface of the APC in the context of a MHC molecule, and circulating T cells are able to recognize and bind to foreign peptide/MHC complexes, resulting in T cell activation and subsequent pathogen clearance (Lindquist and Schraven 2006).

CD28 is a surface molecule constitutively expressed on 80% of all $CD4^+$ T cells and is a co-stimulatory signal for further activation of T cells (Blair et al. 1997). CD28 is comprised of disulfide-linked homodimeric glycoproteins, although some studies have demonstrated the ability of CD28 to function in its monomer form as well (Bour-Jordan and Blueston 2002). CD28 binds to the B7 protein expressed on the surface of activated B cells, monocytes and T cells (Lenschow, Walunas and Bluestone 1996). The CD28/B7 pathway plays a major role in T cell activation, especially when activated by low Ag concentrations or weak Ag as binding of the TCR/CD3 complex to a specific peptide/MHC complex lowers the activation threshold required for T cell activation (Bour-Jordan and Blueston 2002). Activation by CD3 alone requires the cross linking of approximately 8000 TCRs, as opposed to activation by CD3/CD28, which requires the cross-linking of approximately 1000 TCRs (Blair et al. 1997). The CD28/B7 co-stimulatory signaling pathway plays other important roles in T cell activation, such as

stabilization of IL-2 mRNA (critical for T cell growth), increased expression of Bcl-X_L (an anti-apoptotic protein that promotes cell survival), and in the early development and differentiation of Th1 and Th2 cells (Bour-Jordan and Blueston 2002; Lenschow et al. 1996).

B Cells and Their Role in the Immune Response

B cells and T cells fall in the class of immune cells known as lymphocytes which are the principal cell types involved in the adaptive immune response. B cells make up approximately 10% of the immune cell population, and can be identified by cell surface expression of the CD19 marker (Goldsby, Kindt, Osborne and Kirby 2003). The primary function of B cells is the production of antibodies (Ab) which are Ag-specific immunoglobulins whose role is to immobilize and target foreign, pathogenic entities for destruction (Bowers 2006a). Unlike T cells, which only recognize Ag presented by an MHC molecule, B cells are able to recognize soluble Ag in its cognate native form (Chaplin 2006) and are a type of APC whose principal function is to activate immune cells against a specific Ag and mount an Ag-specific immune response (Alam 1998).

There are two ways in which B cells can be activated to produce Ab, the first type is T cell-independent and occurs when the B cell receptor (BCR) recognizes and binds to either soluble Ag circulating in the blood or bound Ag presented in the context of an MHC molecule on immune cells (e.g. macrophages/monocytes), and the second type is T cell dependent and occurs when a B cell recognizes and binds to a T_H cell (specifically a Th2 cell) previously activated or "primed" by Ag (Goldsby et al. 2003). The result of B cell activation is rapid proliferation of B cells, increased Ab production against the

specific Ag, and cytokine induction in order to further stimulate other B cells and activate other immune cells (Beilhack and Rockson 2003).

Natural Killer (NK) Cells and Their Role in the Immune Response

Natural killer (NK) cells are large, granular, cytotoxic lymphocytes capable of detecting and eliminating a wide range of tumor cells and, to some extent, virally infected cells (Parham 2005). NK cells make up ~2% of the immune cell population (~5-10% of all lymphocytes), and play a critical role in the innate immune response (Alam 1998). NK cells express several cell surface markers (CD16, CD56, Fc receptors, etc.) integral for proper NK cell functioning which involves the release of cytotoxic molecules called perforin and granzyme (a type of protease). In response to encounter with a virally-infected or cancer cell, NK cells release these cytotoxic molecules and perforin proteins form pore-like structures in the membrane of the target cell. Granzymes and associated molecules are then able to enter and induce cell death by both apoptotic and necrotic processes (Caligiuri 2008). The mechanisms by which NK cells identify potential target cells involve the ability of NK cells to recognize cellular abnormalities, specifically a reduction in MHC I surface expression (seen in many cancer and virally-infected cells), and the Fc region of specific Ab directed against tumor and viral Ag found on the surface of aberrant target cells (called cell-mediated cytotoxicity) (Middleton, Curran and Maxwell 2002). In addition to direct destruction of mutated cells by granzymes and perforin, activated NK cells secrete cytokines (e.g. IFN-γ and TNF-α) involved in activating other types of immune cells (Le Page, Genin, Baines and Hiscott 2000).

Monocytes and Their Role in the Immune Response

Monocytes are mononuclear cells responsible for the non-Ag specific recognition and elimination of foreign, potentially pathogenic entities (e.g. bacteria, large particulate matter, cellular debris, etc.) by a highly metabolic process known as phagocytosis (Dobrovolskaia and McNeil 2007), and play an important role in the innate immune defense, inflammation and tissue remodeling (Volk, Reinke and Docke 1999). Phagocytosis results in the containment and destruction of pathogenic entities by enzymatic digestion and ROS production, and subsequent Ag-presentation is critical for immune cell activation (Dobrovolskaia and McNeil 2007). Monocytes make up ~3-8% of circulating leukocytes and two main subsets of monocytes have been identified based on differences in phenotype and function (Uthaisangsook et al. 2002). Classical monocytes are characterized by high levels of CD14 surface expression (called $CD14^{++}$), and release specific cytokines (e.g. IFN-α, TNF-α, IL-1, IL-6, etc.) in response to encounter with Ag. These cytokines serve to activate other immune cells and initiate differentiation of $CD14^{++}$ monocytes into pro-inflammatory $CD14^{+}CD16^{+}$ monocytes (Le Page et al. 2000). $CD14^{+}CD16^{+}$ non-classical monocytes (derived from $CD14^{++}$ monocytes) are specifically associated with inflammation, exhibit increased TNF-α secretion, and upon stimulation and activation, rapidly proliferate and migrate from the blood to the site of assault where they differentiate into tissue-specific macrophages and DC for engulfment of foreign material (Mayer 2006; Ziegler-Heitbrock 2007). Phagocytosis is initiated by both receptor-and non-receptor mediated processes, the former involving recognition of pathogens via specific cell surface receptors such as mannose-receptors, scavenger-receptors and Fc receptors. Mannose receptors allow for recognition and phagocytosis of

bacteria by binding terminal mannose and fucose residues of glycoproteins and glycolipids present in microbial cell walls, a feature that distinguishes bacteria from mammalian cells whose glycoproteins and glycolipids contain terminal sialic acid or N-acetylgalactosamine residues instead of mannose and fucose (Kantari, Pederzoli-Ribeil and Witko-Sarsat 2008). Similar to mannose-receptors, scavenger-receptors are able to detect various microbes as well as low-density lipoprotein (LDL) particles. Monocytes also recognize pathogens via Fc receptors which bind the Fc region of Ab attached to infected cells and microorganisms (called opsonization) to stimulate phagocytosis in a process known as Ab-dependent phagocytosis (Kantari et al. 2008). In addition to Ag processing and presentation for immune cell activation, monocytes are capable of producing high levels of reactive oxygen species (ROS) for intracellular destruction of engulfed pathogenic material located within phagosomes. Fusion of phagosomes with digestive enzyme containing lysosomes initiates assemblage of NADPH oxidase subunits which catalyze the synthesis of superoxide anion (O_2^-) in a process called the respiratory burst. Conversion of O_2^- to hydrogen peroxide (H_2O_2) by superoxide dismutase (SOD) results in pathogen killing and the importance of this mechanism is illustrated in a genetic condition known as chronic granulomatous disease (CGD), a genetic condition in which the gene encoding NADPH oxidase is defective or missing, resulting in chronic bacterial infections (Ziegler-Heitbrock 2007).

Inflammation and Immune System Activation

Inflammation is the complex sequence of biological events due to tissue damage caused by a wound, invading pathogens, or other foreign material and is characterized by

redness, heat, swelling and pain (Martin and Leibovich 2005). The symptoms associated with inflammation are due to three major inflammatory responses, vasodilation, increased capillary permeability, and influx of phagocytes (Martin and Leibovich 2005). These responses, which are initiated by a complex series of events involving the secretion of various cytokines and chemokines, have evolved to allow expedient immune cell access to the area of infection for intended clearance of the pathogen (Mackay 2001).

Cytokines are soluble low molecular weight signaling molecules (proteins, peptides or glycoproteins) secreted by cells for the purposes of cell-to-cell communication and immune system regulation (Bellanti, Kadlec and Escobar-Gutierrez 1994). Although not strictly confined to the immune system, cytokines are essential to the development and modulation of both the innate and adaptive immune responses. For example, in response to encountering a pathogen, cells of the innate immune system secrete specific cytokines which act to activate and recruit other immune cells to help fight the foreign pathogen (Mulloy and Rider 2006). Once secreted from a cell, cytokines bind to specific cell-surface receptors located on adjacent cells (paracrine), cells in a distant location (endocrine), or even the secreting cell itself (autocrine) (Mackay 2001). Binding of a cytokine to its ligand produces intracellular cell-signaling cascades which result in the up- or down-regulation of genes, transcription factors, and release or inhibition of other cytokines and/or cytokine receptors (Mulloy and Rider 2006). The effects produced by a particular cytokine depends on many factors, such as cell type, cytokine concentration, the absence of specific receptors for that particular cytokine and the downstream signaling events that occur due to receptor binding (Alfano and Poli 2005).

Cytokines play an integral role in inflammation and stimulating immune cell activation to fight infection. Although the inflammatory response is designed as a protective measure against exposure to foreign, potentially disease causing entities, unresolved inflammation (often due to exposure to innocuous substances) can have serious and often fatal consequences and is an important consideration when designing new therapeutic treatments (Uthaisangsook et al. 2002). Manipulating the inflammatory response so that immune cell activation against a specific entity is achieved, is one way in which more targeted therapeutic treatments for disease may be accomplished. In summary, cytokines are critical in directing and coordinating the immune response and three important immunomodulating cytokines described in this research are IFN-γ, TNF-α and IL-12.

IFN-γ

Interferon-γ (IFN-γ , originally called "macrophage-activating factor") is an acid-labile, soluble cytokine that is biologically active in its dimerized form, with each monomer being comprised of six α-helices (Schroder, Hertzog, Ravasi and Hume 2004). IFN-γ is secreted by NK cells, $CD4^+$ T_H cells (specifically Th1 cells), $CD8^+$ T_C cells and DC and has anti-viral, immunoregulatory and anti-tumor properties (Schroder et al. 2004). IFN-γ binds to receptors found on the surfaces of almost all cells of the body (with receptor number varying by cell type) to produce a variety of different physiological and cellular responses which include, but are not limited to, activating macrophages and monocytes to increase Ag presentation and lysozyme activity, suppression of the Th2 response and promotion of Th1 response, increases in MHC I

expression, promotion of leukocyte migration by increasing adhesion and binding, activation of NK cells, and up regulation of various transcription factors involved in immunomodulation (Tau et al. 2000).

TNF-α

Tumor necrosis factor-α (TNF-α) is a trimeric, 17 kilo-Dalton (kd) (it is 17 kD in its secreted form, and 27 kD in its transmembrane noncleaved form) inflammatory cytokine with pleiotrophic effects (Wajant, Pfizenmaier and Scheurich 2003). For example, the effects of TNF-α can be both growth stimulatory, as seen in the case of neutrophil stimulation during inflammation, and growth inhibitory, as seen in neutrophil apoptosis upon TNF- α binding to the TNF-R55 receptor (Gaur and Aggarwal 2003). TNF-α is produced and secreted by a variety of different cell types including neutrophils, T cells, NK cells, and macrophages/monocytes, and receptors for TNF-α are found on most cells of the body (Wajant et al. 2003). TNF-α is involved in many different biological processes including maintenance of circadian rhythms, replacement and remodeling of injured tissues via fibroblast stimulation, fighting pathogenic infections, and inducing cell death of cancer-causing cells (Locksley, Killeen and Lenardo 2001). However, over-abundant and chronic exposure to TNF-α has been shown to have detrimental effects for host health such as pernicious vascular permeability (as seen in septic shock), over-activation of immune cells leading to pathologic clot formation, and has been shown to play an important role in carcinogenesis (Mocellin and Nitti 2008).

IL-12

Interleukin 12 (IL-12 is a heterodimeric, cytokine composed of four alpha helices and encoded by two separate genes, IL-12A (p35) and IL-12B (p40) secreted primarily by B cells, DC, macrophages/monocytes and to a lesser extent, T cells (Maranda and Robak 1998). IL-12 is involved in a variety of different functions including stimulation of T cell differentiation (Th1) and proliferation, IFN-γ and TNF-α induction by T cells and NK cells, and reduction of IL-4 mediated suppression of IFN-γ (Goriely and Goldman 2007). Additionally, IL-12 has clinical relevancy and is being investigated as a potential adjuvant for IL-2 adoptive lymphokine-activated killer cell (LAK cell) immunotherapy as it reduces the doses of IL-2 required and thus decreases toxicity associated with IL-2 treatment (Lissoni, Pittalis, Roselli, Rovelli and Vigano 1996).

Although too much inflammation can be detrimental to the integrity of an organism, some inflammation can be beneficial in stimulating an immune response against disease causing cells. For example, inflammation stimulates immune cells such as monocytes, neutrophils, etc., to produce ROS which induces cytotoxicity in pathogens or infected cells and results in robust immune responses against invading entities (Uthaisangsook et al. 2002).

Reactive Oxygen Species (ROS)

Reactive oxygen species (ROS) are molecules and ions containing unpaired valence shell electrons and constitute a type of free radical specifically involving oxygen (Bergamini, Gambetti, Dondi and Cervellati 2004). The unpaired valence shell electrons make ROS highly reactive, and although ROS play an important role in cell signaling,

excess ROS (called oxidative stress) can result in significant cellular damage which can ultimately lead to cellular demise by both necrotic and apoptotic processes (Davies 2000). Types of ROS formed as a result of the sequential reduction of molecular oxygen include superoxide radical ($\cdot O_2^-$)superoxide anion (O_2^-), hydrogen peroxide (H_2O_2) and the hydroxyl radical (OH·) (Bergamini et al. 2004).

Sources of ROS are both exogenous and endogenous in nature. Exogenous mediators of intracellular ROS production such as UV light and ionizing radiation exert their deleterious effects by damaging DNA, proteins and lipids resulting in cell damage, cell death and in some instances the creation of malignant cells (if genes responsible for controlling cell growth and replication are damaged). Although excessive ROS production can result in cell damage and death, ROS play a critical role in many normal cellular functions. For example, ROS can be formed as a necessary intermediate in various enzyme reactions and WBC (e.g. neutrophils, macrophages/monocytes, etc.) utilization of ROS for host defense mechanisms and cellular communication (e.g. nitric oxide) (Valko, Leibfritz, Moncol, Cronin, Mazur and Telser 2007).

A major endogenous source of ROS are mitochondria, which produce H_2O_2 from $\cdot O_2^-$ as a natural by-product of ATP production as oxygen is reduced along the electron transport chain (Bergamini et al. 2004). This can damage cells both directly and indirectly as H_2O_2 interacts with Fe^{2+} or other catalytic metals (a process known as the Fenton reaction) and is converted into the highly destructive OH· radical (Bacic, Spasojevic, Secerov and Mojovic 2008). The metabolism and detoxification of drugs, pollutants and ingested particular matter (collectively called xenobiotics) can also serve

as a major endogenous source of free radicals which is important to consider when new drugs and novel materials are being evaluated for utilization (Valko et al. 2007).

Cellular processes, in the form of intracellular enzymes, have evolved to neutralize the potentially harmful effects of ROS produced in physiologically moderate amounts. These enzymes include superoxide dismutase, catalase, and the glutathione enzymes (e.g. glutathione-peroxidase, glutathione-reductase and S-glutathione transferase) (Willcox, Ash and Catignani 2004). Superoxide dismutase is found in both the mitochondrial matrix and cytoplasm and catalyzes the formation of H_2O_2, O_2 and water from the potent highly damaging superoxide radicals ($\cdot O_2^-$) produced in the electron transport chain. Under conditions in which superoxide dismutase becomes overwhelmed (e.g. during oxidative stress), excessive amounts of H_2O_2 are produced resulting in the formation of $OH^{\cdot}$ via the Fenton reaction (Benzie 2000).

Catalase is localized in digestive organelles known as peroxisomes and exerts its antioxidant effects by reacting with H_2O_2 to catalyze the formation of O_2 and water (Djordjevic 2004). Glutathione is an important antioxidant tri-peptide synthesized from the amino acids L- cysteine, L-glutamic acid and glycine, and in its reduced state participates in conjugation reactions to remove various toxic metabolites and donates electrons to unstable ROS molecules (Devasagayam, Tilak, Boloor, Sane, Ghaskadbi and Lele 2004).

During oxidative stress glutathione precursors become depleted and glutathione production is insufficient in neutralizing the ROS generated. To combat diminished glutathione levels, exogenous supplemental cysteine rich compounds, such as N-acetyl cysteine (NAC) can be used to restore glutathione precursor reserves for conversion by

specific enzymes and replenishment of glutathione stores (Townsend, Tew and Tapiero 2003).

Excessive ROS production has been implicated in a variety of different human diseases such as cancer, atherosclerosis and neurodegenerative disorders, and exerts its damaging effects by reacting with cellular components, causing cell death by both necrotic and apoptotic processes.

Cell Death: Apoptosis and Necrosis

Cell death can occur by two different mechanisms, apoptosis and necrosis. Apoptosis is a type of programmed cell death or "cell suicide" involving a predictable series of biochemical events and morphological changes such as decreased cell volume, modification of the cytoskeleton resulting in membrane blebbing, chromatin condensation and DNA fragmentation (Winoto 1997). Subsequent to these changes, the apoptotic cell breaks into small membrane-bound particles called apoptotic bodies which signal phagocytic immune cells (e.g. macrophages and monocytes) to engulf the apoptotic bodies, avoiding the release of cellular contents into the surrounding tissue and induction of a local inflammatory response (Elmore 2007). Unlike apoptosis, necrosis is not programmed by the cell, but is cell death due to overwhelming injury from which the cell is unable to recover. In necrosis, the damage incurred causes the cell to swell and burst, spilling its cellular contents into the surrounding environment and the dispersed cellular debris triggers an inflammatory response in an effort to clear the debris and remove the offending stimulus (Proskuryakov, Gabai, Konoplyannikov, Zamulaeva and Kolesnikova 2005). Apoptosis is essential in maintaining homeostasis and host health and

is critical for cell differentiation during embryogenesis. Additionally, apoptosis is responsible for sustaining a stable number of cells in the body, controlling the growth of aberrant mutated cells and is one of the mechanisms by which immune cells, namely NK and T_C cells, induce cytotoxicity. Also, the absence of apoptosis (due to genetic mutations, for example) can have dire consequences for the organism resulting in the development of diseases such as cancer and autoimmunity (Kam and Ferch 2000).

In conclusion, the utilization of NP (specifically metal oxide NP) is ever-increasing, and NP are already found in many different commercial products. Due to their unique properties, it is essential to elucidate the effects and mechanisms of NP-biological interactions and investigate the biomedical potential of different types of particles on various cell types and systems. Evaluating parameters influencing NP toxicity ensures the safe use of NP for various industrial applications and may allow for the creation of new and improved therapeutic treatments for disease. Our immediate goal is to examine the differential toxic effects of metal oxide NP, specifically ZnO NP, on primary human immune cells. The main hypothesis of this research is that ZnO NP toxicity is dependent on various parameters including cell type, NP size, and cell-activation state. Additionally, our research evaluated specific mechanisms of toxicity, cell death and the inflammatory potential of ZnO NP in immune cells. Exploitation of these observations may enable the development of novel treatments for disease, which is the long term goal of our research.

EXPERIMENTAL PROCEDURES

Preparation and Characterization of ZnO NP

ZnO NP utilized in all experiments were synthesized in diethylene glycol (DEG) via forced hydrolysis of zinc acetate (Reddy et al. 2007). In brief, zinc acetate was dissolved in DEG, and nanopure water was added under magnetic stirring. Subsequently, the system was heated at 160 ºC under reflux for 90 min. After cooling, the resulting product was removed from DEG via centrifugation and washed with ethanol several times before drying for 24 h at 50 °C, resulting in a powder sample. The sample crystal phase, crystallite size and morphology were characterized via x-ray diffraction (XRD), and transmission electron microscopy (TEM) (Hanley et al. 2008; Reddy et al. 2007). The NP powder was weighed and reconstituted in phosphate buffered saline (PBS) solution to the desired stock concentration. After reconstitution, NP were sonicated for 10 min and immediately vortexed prior to addition to cell culture samples. For all experiments, except for those directly comparing effects of NP size on cell viability and ROS production, 8 or 13 nm ZnO NP were used as specified.

Different sized ZnO NP were synthesized as described above and sizes altered by modifying the hydrolysis molar ratio of water to zinc acetate with ratios of 2.4, 6.1, 12.2, and 36.6 yielding NP with average diameters of 4 nm, 8 nm, 13 nm, and 20 nm, respectively. The corresponding particle size for all four NP sizes analyzed reveals a narrow size distribution and XRD patterns indicate all of the ZnO samples are well indexed to pure wurtzite crystallite phase of ZnO. Furthermore, the average crystallite

sizes estimated using the peak widths (full width at half maximum) of the XRD patterns agree well with TEM results.

Preparation of FITC-Doped ZnO NP

FITC encapsulated ZnO (FITC-ZnO) particles were synthesized by forced hydrolysis and condensation of FITC-binding silane and silicate to obtain the FITC-SiO_2 core (Burns, Ow and Weisner 2006), and the ZnO surface layer formed using zinc salt (Wang et al. 2009). The core-shell structure of the ~200 nm sized FITC-ZnO particles and the presence of a surface layer of 13 nm sized ZnO NP were confirmed using TEM, XRD and x-ray photoelectron spectroscopy (XPS) studies, and fluorescence properties were investigated using photoluminescence spectroscopy and flow cytometry (Wang et al. 2009).

Preparation of SnO_2 and CeO_2 NP

SnO_2 NP were synthesized by our collaborators using methodologies nearly identical to those described for ZnO NP preparation (Reddy et al. 2007). Briefly, SnO_2 NP were synthesized in diethylene glycol (DEG) via forced hydrolysis of tin chloride and the resulting product was removed from DEG via centrifugation and washed with ethanol several times before drying for 24 h at 50 °C, resulting in a powder sample of ~4-8 nm sized NP. CeO_2 NP were synthesized from cerium nitrate by sol-gel preparation resulting in a ~9 nm NP powder sample. For use in mammalian cell cultures, NP were weighed and reconstituted in phosphate buffered saline (PBS) solution to the desired stock

concentration, sonicated for 10 min, and immediately vortexed prior to addition to cell samples.

Immune Cell Isolation and Cell Culture

Isolation of Peripheral Blood Mononuclear Cells (PBMC)

For isolation of PBMC (peripheral blood mononuclear cells) and immune cell subsets, written informed consent was obtained from all blood donors and the University Institutional Review Board approved this study. PBMC were obtained via Ficoll-Hypaque (Histopaque-1077, Sigma, St Louis, MO) gradient centrifugation using heparinized phlebotomy samples (Coligan 1995). After removal of the leukocyte layer, cells were washed three times with Hank's buffer (Sigma, St. Louis, MO) and resuspended to a final concentration of 1-2 x 10^6 cells/mL in RPMI-1640 (Sigma) containing 10% fetal bovine serum (FBS) and cultured at 37° C and 5% CO_2.

Primary $CD4^+$ T Cell Isolation

After isolation of human PBMC, $CD4^+$ T cells were purified using negative immunomagnetic selection per manufacturer's instructions using a cocktail of antibodies against CD8, CD14, CD16, CD19, CD56, and glycophorin A (StemCell Technologies, Vancouver, BC) with collection of unlabeled T cells (typically >97% $CD4^+$ and >90% viable as assessed by flow cytometry). Purified $CD4^+$ cells were cultured in RPMI/10% FBS and suspended at a final concentration of 1-2 x 10^6 cells/mL.

Primary $CD14^+$ Monocyte Isolation

PBMCs were obtained by Ficoll-Hypaque density centrifugation as described above and $CD14^+$ cells isolated from the mixed cell suspension. Negative immunomagnetic selection was performed according to the manufacturer's protocol using a cocktail of antibodies directed against CD2, CD3, CD16, CD19, CD20, CD56, CD66b, CD123, glycophorin A (StemCell Technologies, Vancouver, BC). For optimal cell recovery, PBMCs were first blocked with anti-human CD32 (Fcγ RII) blocker reagent before labeling with the antibody cocktail and running through the column. Collection of $CD14^+$ monocytes was typically >97% viable as assessed by flow cytometry. Purified monocytes were then cultured in RPMI/10% FBS at 5×10^5 cells/mL in 200 μL total volume in 96-well microtiter plates at 37° C and 5% CO_2.

Jurkat Lymphoma, Hut-78 Leukemic, and U937 Monocytic Cancer Cell Lines

The Jurkat lymphoma T cell, Hut-78 leukemic T cell and U937 monocytic cancer cell lines (ATTC, Rockville, MD) were cultured in RPMI 1640 supplemented with 10% FBS (Jurkat) or 20% FBS (U937) and 2 mM L-glutamine, 1.5g/L sodium bicarbonate, 4.5 g/L glucose, 10 mM HEPES, and 1.0 mM sodium pyruvate. Cells were maintained in log phase at 37° C and 5% CO_2 and seeded at 5×10^5 cells/well in 96-well plates for individual experiments.

Antibodies (Ab) and Flow Cytometry

Flow cytometric analyses were performed using a 4-color Epics XL flow cytometer (Beckman Coulter, Fullerton, CA). Immunofluorescent staining was

accomplished by harvesting cells plated at a concentration of 1 x 10^6 cells/mL into FACS buffer and centrifuging for 10 min at 2000 rpm to pellet cells. After supernatant removal, cells were resuspended in FACS buffer and stained with fluorescently labeled Ab (Beckman Coulter, Fullerton, CA). Appropriate concentrations of each Ab were determined by titration for optimal staining prior to experimental use. Cells were incubated with the appropriate fluorescent Ab for 30 min at 4°C, washed two times, harvested into FACS buffer and immediately analyzed. Ten thousand events gated on the parameters of size (forward scatter - FS) and granularity (side scatter - SSC) were analyzed, and expression of the percentage of positively staining cells or the mean fluorescence intensity (MFI) determined by comparisons to isotype controls. In PBMC cultures, individual cell types were distinguished from one another based on differential Ab staining and FS and SSC properties. T cells were defined as $CD3^+$; T_H defined as $CD3^+$,$CD4^+$; naïve T cells defined as $CD3^+$,$CD45RA^+$; memory T cells defined as $CD3^+$, CD45RO; B cells defined as $CD19^+$,$CD3^-$; NK cells defined as $CD56^+$,$CD16^+$, $CD3^-$, or $CD56^+$, $CD3^-$; and monocytes defined as $CD14^+$,$CD3^-$. To prevent indiscriminate Ab staining of monocytes via Fc receptors, 100 μL of heat-inactivated human AB serum was added to experimental samples immediately prior to staining.

T Cell Activation and Culture Conditions

Purified $CD4^+$ cells were cultured in RPMI/10% FCS at 1 x 10^6 cells/mL in 200 μL total volume and activated using immobilized CD3 Ab (1.0 μg/well of clone OKT3, ATCC, Rockville, MD) +/- CD28 Ab (0.25 μg/well of clone CD28.2 (PharMingen, San Diego, CA) in 96-well tissue culture plates. Cultures were treated with freshly prepared

and sonicated NP, or left untreated for varying lengths of time and analyzed using flow cytometry and a microplate reader. T cell activation was verified by detecting an increase in membrane CD40L protein expression using flow cytometry.

Cell Viability Assays

Flow Cytometric Analysis of Immune Cell Viability

To assess the effect of ZnO NP on PBMC and isolated immune cell viability, two different flow cytometric assays were employed. In the first assay, cells identified were stained and identified using fluorescently labeled Ab and viability determined by staining with 50 μg/mL of propidium iodide (PI), a fluorogenic dye used to monitor losses in cell membrane integrity, for 10 min prior to analysis. Fluorescent CountBright® counting beads (Invitrogen, Carlsbad, CA) were added to samples to enable determinations of absolute cell numbers, and flow cytometry used to evaluate changes in PI staining and quantify cell death. NP were excluded from the analysis based on absence of fluorescence signal and light forward scatter (FS) and side scatter (SSC) characteristics. In experiments testing the effects of micron-sized bulk ZnO on cell viability, purified $CD4^+$ T cells were left untreated or treated with various concentrations of commercially available (Sigma Aldrich, St. Louis, MO) bulk ZnO powder or laboratory synthesized ZnO NP resuspended in PBS, cultured for 20-24 h, and viability assessed using PI and analyzed by flow cytometry. Identical conditions to those just described were used for experiments testing the effects of SnO_2 NP and CeO_2 NP on T cell viability, except that only one concentration (e.g. 10 mM) of either SnO_2 NP or CeO_2 NP was evaluated.

A second viability assay, the LIVE/DEAD viability assay for mammalian cells (Invitrogen, Eugene, OR) was used to verify results seen using PI. Per manufacturer's protocol for flow cytometry, purified $CD4^+$ T cells were dually stained with two fluorescently labeled probes that enable the simultaneous determination of live and dead cells in a sample. Calcein AM was used to stain live cells as it fluoresces only when cleaved by intracellular esterases, and EthD-1 was used to identify dead/dying cells as it exclusively enters cells with disrupted cell membranes.

Flow Cytometric Analysis of Bacterial Viability

Two different strains of bacteria (*E. coli* and *S. aureus*) were provided by our collaborator, Dr. Kevin Feris, for determination of bacterial cell viability. Bacterial cultures (*E.coli* and *S. aureus*) were grown for 3 h in LB medium and subsequently treated with ZnO NP resuspended in PBS. After 15 h of treatment, a two color live/dead BacLight® bacterial viability kit (Molecular Probes, Carlsbad, CA) was used to determine cell viability as analyzed by flow cytometry. The ratio of dead to live bacteria remaining in the culture following NP exposure was determined by simultaneously staining with PI and a green fluorescent dye, Syto9, that intensely stains cells with intact membranes and, to a lesser extent, cells with damaged membranes. Populations of live (green) and dead (red) bacteria were discriminated based on green and red fluorescence staining profiles and changes in FS and SSC characteristics.

Alamar Blue Viability Assay

The Alamar Blue viability assay, which utilizes the fluorogenic redox indicator dye, Alamar Blue, was also used to evaluate NP-induced cytotoxicity. This dye becomes fluorescent upon reduction by mitochondrial enzymes in metabolically active (live) cells. Cells were seeded into 96-well plates at 5 x 10^5 cells/mL in a final volume of 200 μL and treated with ZnO NP for 18 h. Alamar Blue (20 μL) was added to cultures for an additional 6 h of culture for a total NP-exposure time of 24 h. A BioTek® spectrophotometer was used with an excitation/emission at 530/590 nm to monitor and record changes in fluorescence and viability was normalized to fluorescence values from control wells.

Determination of IC_{50} Values for Immune Cells

To determine the concentration at which 50% of cells remain viable (IC_{50}), experiments were performed testing the effects of varying concentrations of ZnO NP on cell viability. To determine the IC_{50} values for purified T cell and monocytes, cells were treated with varying concentrations of ZnO NP (1 mM, 5 mM and 10 mM for T cells and 0.0625 mM, 0.25 mM, 0.5 mM and 1 mM for monocytes) for 22-24 h and viability assessed using the Alamar Blue assay. The program GraphPad Prism® 5.0 was used to calculate IC_{50} values for purified $CD4^+$ T cells and $CD14^+$ monocytes by plotting cell viabilities against the logarithm of NP concentration and using a nonlinear regression analysis to fit a variable slope dose-response curve. For cells found in mixed PBMC cultures, cell types were identified using fluorescently labeled antibodies against specific plasma membrane markers and viabilities determined by PI uptake and flow cytometry.

To calculate IC_{50} values for these flow cytometric experiments, cell viabilities were plotted against NP concentrations and a linear regression analysis used to determine IC_{50} values.

Reactive Oxygen Species (ROS) Assays

ROS Detection

To assay for NP-induced ROS production in primary lymphocytes and monocytes, cultures of mixed PBMC were obtained from whole blood treated with an ammonium chloride lysing solution (1.5 M NH_4Cl, 0.1 M $NaHCO_3$, 0.01 EDTA) used to lyse red blood cells and centrifuged for 10 min at 4°C to remove erythrocytic debris. PBMC were counted, resuspended in phenol red-free RPMI to a final concentration of 1 x 10^6 cells/mL and treated with 1 mM or 5 mM of ZnO NP (8 nm). To evaluate ROS production, cells were loaded with 5 μM of the oxidation-sensitive dye, 2',7'-dichlorofluorescein diacetate (DCFH-DA, Invitrogen, Carlsbad, CA) for 20 min prior to analysis. The oxidation product of DCFH-DA has an excitation/emission maxima of ~495 nm/529, enabling detection both by using a microplate reader and flow cytometry (Luo et al. 2002). In flow cytometric analyses, $CD3^+$ lymphocytes and $CD14^+$ monocytes were identified based on FS and SSC gating and staining with fluorescently labeled Ab, allowing for simultaneous cell identification and evaluation of ROS production. Additionally, ROS production in PBMC cultures was measured after several different NP-exposure times (6 h – 24 h) to assess the kinetics of NP-induced oxidative stress. To compare NP-induced ROS in primary cells with cancer cells, Hut-78 T leukemic cells were treated with ZnO NP and ROS measured using similar methodology as described

for primary cells. As a positive control for ROS production in all cell types tested, untreated (no NP) cells were loaded with DCFH-DA and activated with PMA (25 ng/mL) for 1 h prior to analysis.

In parallel experiments investigating the effect of NP size on ROS production, bulk cultures of PBMC were treated with various concentrations (5 mM and 10 mM) of different sized ZnO NP (4, 13, and 20 nm), loaded with DCFH-DA and ROS production analyzed using a fluorescent microplate reader as described by others (Hong and Liu 2004; Onaran, Sencan, Demirtas, Aydemir, Ulutin and Okutan 2008).

ROS Quenchers

To determine the role of ROS in NP-induced cell death, primary purified $CD4^+$ T cells and $CD14^+$ monocytes were seeded in a 96-well plates at a concentration of 5×10^5 cells/mL and treated with the ROS scavenger, N-acetyl cysteine (NAC, Sigma Aldrich, St. Louis, MO). NAC was made as a stock solution in sterile nanopure water and added to cells at a final concentration of 5 mM. Cells were pretreated with NAC for 2 h to allow time for NAC to enter the cells before treating with various concentrations of 8 nm ZnO NP for 24 h. Viability was determined using the Alamar Blue cytotoxicity assay and a fluorescent microplate reader.

Confocal Microscopy

Apoptosis Versus Necrosis

Mechanisms of ZnO NP-induced cytotoxicity were evaluated by confocal microscopy using two different fluorescent staining techniques; acridine orange and

Vybrant® Apoptosis Assay Kit #2- AlexaFluor® annexinV/propidium iodide by Invitrogen (Eugene, OR). Acridine orange stains double stranded DNA and allows for visualization of nuclear morphology. Invitrogen's Vybrant annexin V assay makes use of two different fluorescently labeled probes, annexin V and PI, to differentiate between live, necrotic and apoptotic cells. Briefly, Jurkat T cells were suspended in complete RPMI-1640 medium and plated at 5×10^5 on poly-D lysine coated glass bottom culture dishes (P35GC-1.5 mm-14 mm-C) supplied by MatTek Corporation (Ashland, MA). Samples were left untreated, treated with 0.3 mM ZnO NP, or with 100 nM okadaic acid as a positive control for apoptosis. Following a 20 h incubation at 37° C (5% CO2), cells were washed and stained with annexin V Ab/PI per manufacturer's protocol or stained with 5 μg/ mL acridine orange (AO) for 10 min at 37° C, followed by washing and resuspension in PBS. Cells were visualized using a Zeiss LSM 510 META laser scanning confocal microscope (Zeiss, Germany). Images were acquired using factory-set dichronics (an argon laser set and two helium neon lasers) with either 63 × Plan Apochromat 1.4 oil DIC or 100× Plan Fluar 14.5 oil objective. Image acquisition and processing was performed using the LSM 510 META software.

NP Association with Immune Cells

NP-cell interactions were investigated using both flow cytometric analysis and visualization using confocal microscopy. Bulk cultures of PBMC were left untreated or treated with 5 mM FITC-doped ZnO NP for 16 h and cell types identified by staining with fluorescently labeled Ab. Cell identification and FITC-NP/cell associations were assessed using flow cytometry and both the percentage of fluorescent cells (FACS%) and

mean fluorescence intensity (MFI) values for $CD3^+$ T cells, $CD4^+$ T_H cells, $CD19^+$ B cells and $CD14^+$ monocytes determined.

To examine NP intracellular localization versus extracellular plasma membrane association, confocal microscopy was used to calculate the average number of FITC-doped NP/z-series slice in both Jurkat T and monocytic U937 cells. Cells were suspended in RPMI-1640 medium and plated at 5×10^5 cells/mL on poly-L lysine coated glass-bottom culture dishes (P35GC-1.5 mm-14 mM-C) supplied by MatTek Corporation (Ashland, MA) for a 24 h to allow cellular adherence to plates. Jurkat T cell lymphoma cells were left untreated and treated with 0.5 mM FITC-doped ZnO NP for 8 h at 37° C (5% CO_2). Cells from the monocytic cancer U937 cell line were left untreated and treated with 0.3 mM FITC-doped ZnO for 20 h using identical parameters as above. Following incubation, cells were washed with PBS and stained with fluorescent Ab for cell identification; fluorescent anti-CD14 PE for U937 and fluorescent anti-CD3 for Jurkat. After staining, cells were washed twice with PBS to remove excess Ab and reduce fluorescent background signal before being visualized using a Zeiss LSM 510 META laser scanning confocal microscope (Zeiss, Germany). Images were acquired using factory-set dichronics (an argon laser set and two helium neon lasers) with either 63x Plan Apochromat 1.4 oil DIC or 100x Plan Fluar 14.5 oil objective. Image acquisition and processing was performed using LSM 51- META software. FITC-doped ZnO NP were counted in multiple images for each cell type by examining individual slices from a Z-series image. Orthogonal viewing was performed to verify intracellular localization of NP compared to extracellular membrane association.

Enzyme-Linked Immunosorbent Assay (ELISA)

To investigate the effect of ZnO NP treatment on cytokine production, a sandwich enzyme linked immunosorbent assay (ELISA) was employed to allow for detection and quantification of soluble cytokine released into culture medium. Human IFN-γ, TNF-α and IL-12 were measured in primary peripheral blood mononuclear (PBMC) cells at a concentration of 1 x 10^6 cells/mL. PBMC were left unactivated or activated with 1000 U/mL of IFN-γ (Peprotech, Rocky Hill, NJ) for 14 h and subsequently treated with varying concentrations of 8 nm ZnO NP (0.05 mM, 0.1 mM and 0.2 mM) for 24 h. Control (no activation and no NP treatment) samples were also included to allow for background cytokine expression. Following incubation, cell-free supernatant was harvested via successive 10 min centrifugations (2,000 rpm, 7,000 rpm and 13,000 rpm) and cell supernatants stored at -80° C until analysis. ELISA was performed by the UMAB Cytokine Core Laboratory (Baltimore, MD), with all samples analyzed in triplicate and cytokine production expressed in pg/mL. IL-12 expression was measured in PBMC left unactivated or activated with IFN-γ (1000 U/mL) both alone and in the presence of ZnO NP. Expression of IFN-γ and TNF-α was assessed as described above except that exogenous IFN-γ was not added to cell culture samples.

Data Analysis

All data was analyzed using SAS, Inc. software (Cary, NC). Data for Figures 2, 4, 5, 6, 7, 8, and 10 were analyzed using repeated measures analysis of variance (ANOVA) with post hoc comparisons and significance levels defined as $p < 0.05$. Repeated measures of variance analyses were used when two or more measurements of the same

type were made on the same subject to determine statistical differences between the means and to allow separation of within-subject variation from between subject variation. Data for Figures 12, 13, and 18 were analyzed using a two-way analysis of variance (ANOVA) to test for overall statistical significance of the model and post hoc comparisons were used to test for statistically significant effects of treatment on cell viability ($p < 0.05$).

RESULTS

ZnO NP Display Cytotoxic Effects in T Cells Compared to Bulk ZnO

To determine if reduction of ZnO to the nano-scale alters the biological effects of ZnO, we performed experiments comparing the effects of bulk micron-sized ZnO and ~13 nm sized ZnO NP on isolated primary human $CD4^+$ T cell viability. ZnO NP were synthesized and characterized by our collaborators in the Punnoose lab by collection of ZnO NP powder after separation from DEG medium via centrifugation. In agreement with the XRD results (Reddy et al. 2007), transmission electron microscopy (TEM) measurements were carried out to further investigate ZnO particle size and shape (Figure 1A) and average particle size of the NP estimated using the Scherrer relation was found to be ~13 nm, with a range of particle sizes (7-19 nm) observed (Figure 1B).

Experiments were performed testing identical concentrations of both ZnO NP and bulk ZnO suspended in a phosphate buffered saline (PBS) solution on human $CD4^+$ T cells. Dual-color flow cytometry was used to simultaneously identify cells and assess cell viability using propidium iodide (PI), a red fluorescent nuclear stain that enters only cells with disrupted plasma membranes (Figure 2). No appreciable loss of viability was observed in T cells treated with micron-sized bulk ZnO powder at any concentration tested, conversely, ZnO NP treatment caused significant decreases in viabilities at concentrations ≥ 5 mM ($p=0.0001$). This data indicates that T lymphocyte cytotoxicity is limited to ZnO in the nanoscale size range, as no significant effect of bulk ZnO powder was found at any of the concentrations tested (0.5 – 10 mM).

Differential ZnO NP Toxicity to *E. coli* and *S. aureus*

For bacterial studies performed by our collaborator, Dr. Kevin Feris, ZnO NP and bulk ZnO powders were suspended in diethylene glycol (DEG) to desired stock concentrations and two different bacterial strains, *E. coli* and *S. aureus*, were treated with varying concentrations of ~13 nm sized ZnO NP. Results from these studies demonstrated a differential inhibition of colony forming units (CFU) between the two bacterial strains in response to ZnO NP treatment, with *S. aureus* exhibiting greater CFU inhibition at lower concentrations compared to *E. coli* (Reddy et al. 2007).

To confirm ZnO NP definitively kill bacteria as opposed to merely inhibiting their growth, we performed experiments in which bacteria were treated with 5 mM NP (*E. coli*) or 2 mM NP (*S. aureus*) for 15 h and viability was determined using a 2-color live/dead BacLight® bacterial viability kit (Invitrogen, Eugene, OR) in which populations of live and dead bacteria were discriminated based fluorescence staining profiles. As seen in Figure 3, substantial losses in viability were observed in both types of bacteria, with *S. aureus* being the most susceptible (>59% loss of viability) followed by *E. coli* (>30% loss in viability). This data combined with additional bacterial studies contributed by our collaborator, Dr. Kevin Feris, and our own T cell viability demonstrate that T cells are significantly less susceptible to ZnO NP-induced toxicity compared to both *E. coli* and *S. aureus* at the same concentrations tested ($p=0.000$) (Reddy et al. 2007). Collectively, these results indicate that ZnO NP toxicity occurs in a cell-dependent manner, with significant differences in viability observed among different strains of prokaryotes (*S. aureus* are killed at lower NP concentrations compared to *E. coli*) and between prokaryotes and eukaryotes (T cells are more resistant to NP treatment compared to both

strains of bacteria) (Reddy et al. 2007). To expand our understanding of factors affecting ZnO NP toxicity, we conducted experiments to investigate the parameters affecting ZnO NP toxicity in primary human immune cells.

Preferential Killing of Activated Versus Unactivated T Cells

To determine if differential toxicity to ZnO NP is dependent upon the microenvironment or signaling status of eukaryotic cells, toxicity effects were determined in resting primary human T cells and compared to cells activated through the T cell receptor (TCR). Signal transduction through the TCR pathway is recognized as an essential event required for resting T cells to enter the cell cycle and proliferate (Foell, Hewes and Mittler 2007) and a second signal provided by ligation through the CD28 receptor protein augments TCR signaling and enables maximal T cell activation and proliferation. For these studies, normal peripheral blood $CD4^+$ T cells were isolated using negative immunomagnetic selection and either activated with stimulatory TCR Ab (anti-CD3), co-stimulated with both CD3 Ab (anti-CD3) and CD28 Ab (anti-CD28), or left unactivated. The effects of ZnO NP on plasma membrane damage were assessed using PI and flow cytometry. As shown in Figure 4A, the toxicity of ZnO NP to T cells is dependent on the activation state of the cell, with resting T cells exhibiting the greatest resistance to ZnO NP at all concentrations tested. The unactivated status of these cells was verified by their lack of appreciable CD40L protein expression, a sensitive marker of T cell activation Figure 4B. Conversely, T cells partially activated by stimulation through the TCR pathway alone displayed significantly greater sensitivity to ZnO NP at all concentrations ($p=0.0007$ for control versus CD3 at 1 mM, $p=0.0009$ at 5 mM and

p=0.0052 at 10 mM NP). The partial activation status of these cells was verified by 38% ± 6.2% of the cells expressing membrane CD40L. Importantly, T cells activated through both the TCR and CD28 co-stimulatory pathway showed an even greater sensitivity to ZnO NP toxicity (e.g. 55% viability in CD3/CD28 activated versus 69% in CD3 activated cells at 1 mM) which significantly differed from CD3 activated cultures at both 1 mM (p=0.0044) and 5 mM NP (p=0.0246) concentrations. Staining for membrane CD40L expression confirmed a greater extent of T cell activation in CD3/CD28 activated cultures (67% ± 7.0% positive staining).

Control experiments using bulk micron sized ZnO powder or NP-free supernatant showed no appreciable toxicity effect at any of the concentrations tested (e.g. viability with bulk ZnO: 95 ± 0.5% at 0 mM, 96 ± 3% at 1 mM, 91 ± 3% at 5 mM, 91 ± 1% at 10 mM; 98% viability with NP-free supernatant equivalent to 1–10 mM). In addition to PI uptake associated with disruption of plasma membrane integrity, NP-induced cell death following ZnO NP treatment was supported by an increase (~17%; MFI change of 48–56) in light side scatter characteristics indicative of increased cell granularity and a concurrent decrease (~8%; MFI change of 156–144) in forward scatter reflects a decrease in cell size at 10 mM NP concentrations. These results demonstrate significantly greater cell death in activated T cells compared to resting cells over a relatively large range of NP concentrations tested (1–10 mM), and toxicity varies with the extent of T cell activation.

Cancerous Cells Are Preferentially Killed by ZnO NP Compared to Normal Cells

Given that differential ZnO NP toxicity exists between quiescent T cells and those activated with specific signals to trigger proliferation, experiments were performed to determine whether continuously dividing cancer cells display an even greater sensitivity to ZnO NP toxicity. Jurkat leukemic and Hut-78 lymphoma T cell lines were treated with ZnO NP for 24 h and viability was determined by PI uptake (viability of cancer cell lines was performed by lab member Janet Layne). Results from these experiments demonstrate both T cell cancer lines display strikingly greater (28–35 fold) sensitivity to NP toxicity compared to resting normal T cells (Figure 5A). Significant differences were observed between Hut-78 and normal T cells ($p=0.0101$ and 0.0434 at 1 mM and 5 mM NP, respectively) and Jurkat and normal T cells (<0.0001 at both 1 and 5 mM NP). No appreciable loss of primary T cell viability was observed at NP concentrations (e.g. 0.5 mM) that effectively killed cancer T cells.

To validate experimental results, similar experiments were performed using the LIVE/DEAD® viability assay (Invitrogen, Eugene, OR). This assay allows for the simultaneous determination of live and dead cells in a sample by labeling live cells with the Calcein AM dye that fluoresces only when cleaved by intracellular esterase enzymes and the vital dye, EthD-1, which only enters dead/dying cells with disrupted cell membranes. As shown in Figure 5B, nearly identical results were obtained using this independent assay for viability, with ZnO NP displaying preferential toxicity against cancerous cells compared to normal cells of identical lineage. It should be noted that no statistically significant change in primary T cell viability occurs between untreated primary control cells and these cells treated with low NP concentrations (0.2 and 0.5

mM), while a significant decrease ($p<0.0001$) in Jurkat leukemia cell viability can readily be seen at the lowest concentration tested (~52% viable/48% dead at 0.2 mM), with no live cancer cells detectable at 5 mM NP.

Memory T Cells Display Greater Sensitivity to ZnO NP-Induced Cytotoxicity

The activation of T cells in response to specific Ag results in a cascade of intracellular signaling events and differentiation of "naïve" T cells into "memory" cells, which can become activated much more readily upon subsequent exposure to the original Ag (Surh and Sprent 2008). Given that activation thresholds and alterations in intracellular calcium and signaling responses differ between naïve and memory T cells, experiments were performed to determine whether memory T cells, display greater sensitivity to ZnO NP toxicity compared to naïve T cells. Isolated PBMC were treated with 8 nm ZnO NP for 22-24 h and viability assessed by PI uptake and flow cytometry. Naïve $CD3^+$ T cells were identified based on expression of the CD45RA ($CD45RA^+$, $CD3^+$) surface marker, while memory T cells were defined as $CD45RO^+$, $CD3^+$. The cytotoxic responses of naïve and memory $CD3^+$ T cells to ZnO NP were compared to bulk cultures of $CD3^+$ T cells (containing a mixture of both naïve and memory cells) from the same blood donor. As shown in Figure 6, memory T cells displayed significantly greater sensitivity to NP toxicity compared to either naive T cells or bulk cultures of $CD3^+$ T cells ($p=0.0044$ and $p=0.0244$) at 10 mM ZnO NP. Naïve T cells appeared more resistant to ZnO NP-induced cytotoxicity compared to total $CD3^+$ T cell samples, although statistically significant differences were not observed ($p=0.08$). These

results provide further evidence that susceptibility to ZnO NP-induced toxicity may be related to the activation threshold and/or proliferation potential of the cell.

Kinetics of ZnO NP-Mediated Toxicity to Normal and Cancerous T Cells

To further elucidate differences in normal versus cancerous immune cells, experiments were performed to determine and compare the kinetics of ZnO NP toxicity in primary versus cancerous T cells. Cells were treated with ZnO NP and concentrations chosen for each cell type (10 mM for primary T cells and 0.5 mM for Jurkat T cells) that produce at least 75% cytotoxicity by 24 h exposure. Both primary T cells and Jurkat cells display similar kinetics with appreciable losses in cell viability beginning as early as 8 h post treatment, and full toxicity effects requiring a longer treatment period of 24 h (Figure 7).

ZnO NP Cytotoxicity Is Dependent on Immune Cell Type

Our findings of differential ZnO NP toxicity based on cell type (e.g. eukaryotic versus prokaryotic) and activation/proliferative potential were extended to determine whether NP toxicity might also vary between different primary human immune cell types. Comparisons of cytotoxic responses were made between normal T cells, B cells, natural killer (NK) cells, and monocytes (Figure 8A). For these studies, freshly isolated PBMC cell cultures containing all of these cell types were used, allowing for well-controlled uniform NP exposure. Following NP treatment for 23-24 h, various cell types present in PBMC cultures were identified using Ab specific for T, B, NK or monocyte

surface markers and evaluated for toxicity by staining with PI and analyzed by flow cytometry.

As shown in Figure 8A, differences in NP-induced cytotoxicity are apparent between the immune cells present in PBMC samples. $CD3^+$ T lymphocytes, $CD4^+$ T lymphocytes and B lymphocytes display the greatest resistance to NP-mediated cytotoxicity and possess a very similar IC_{50} of ~ 5.0 mM, with no significant differences observed at any NP concentration evaluated (0.5 mM, 1 mM, 5mM and 10 mM). In addition, no significant differences were observed between $CD4^+$ T cells and $CD3^+$ T cells (e.g., 97% ± 1.5% for untreated and 28% ± 1.7% for 10 mM NP treated vs. 98% ±1.2% for untreated and 34% ± 3.2% for 10 mM NP, respectively). In contrast, NK cells were substantially more sensitive to NP-induced toxicity compared to T and B lymphocytes, with an IC_{50} of ~1.0 mM. Statistically significant differences were observed between T and B lymphocytes compared to NK cells at NP concentrations of 1 – 5 mM ($p=0.0028$ (T cells) and $p=0.0003$ (B cells) at 1 mM, $p=0.0002$ (T cells) and $p= 0.0001$ (B cells) at 2.5 mM, $p=0.0019$ (T cells) and $p=0.0031$ (B cells) at 5 mM and $p=0.05$ at 10 mM NP). Most striking is the increased NP-induced cytotoxicity observed in monocytes, with >50% of monocytes killed at the lowest NP concentration tested (0.5 mM). Statistically significant differences were observed between monocytes and NK cells (0.5 mM and 1 mM; $p=0.0002$ and $p=0.0008$, respectively), and monocytes compared to T and B lymphocytes ($p<0.0001$ for both cell types at both concentrations tested).

Because adherent monocytes appear considerably more susceptible to NP-induced cytotoxicity compared to the other immune cell subsets tested, additional experiments were performed testing lower concentrations of ZnO NP on purified monocytes in order

to determine the IC_{50} value. In these experiments, purified monocytes were treated with varying concentrations of ZnO NP (0.0625 mM, 0.25 mM, 0.5 mM and 1 mM) and viability evaluated using the fluorogenic redox Alamar Blue cytotoxicity assay. In agreement with the monocyte data obtained from PBMC cultures, these results also indicate a greater susceptibility to ZnO NP-induced toxicity in monocytes (compared to T cells, B cells and NK cells) and reveal an IC_{50} for monocytes of ~0.3 mM (Figure 8B). In addition, the Alamar Blue cytotoxicity assay was performed on purified $CD4^+$ T cells (1-10 mM) to confirm results obtained based on PI staining, and a similar IC_{50} value of ~5.4 was observed (data not shown).

Although these results indicate that monocytes are considerably more susceptible to NP-induced cytotoxicity than other immune cell types tested, it is important to note that these apparent differences may be related to significantly different cell culture conditions. While T cells, B cells and NK cells grow as suspension cultures, monocytes are adherent cells and grow as a monolayer. This difference in growth characteristic may be a factor affecting ZnO NP toxicity and thus NP treatments between adherent cells versus suspension cells may not be equivalent. Future experiments involving the growth of these cell types in 3-dimensional cultures are needed to fully investigate this issue. Nevertheless, these results indicate a significant difference in NP toxicity between different primary immune cell types, with monocytes showing the greatest susceptibility, followed by NK cells which are ~3-fold less sensitive than monocytes, and T and B cells which are ~ 17-fold and ~5-fold less sensitive than monocytes and NK cells, respectively.

Size Control of ZnO NP on Immune Cell Viability

To evaluate the relationship between ZnO NP size and its toxic potential, three different sizes of ZnO NP (4 nm, 13 nm and 20 nm) were concurrently evaluated using primary human $CD4^+$ T cells as a model system. The three sizes of NP were made by our collaborators by modification of the molar ratio of water to zinc acetate and the shape and size confirmed by TEM (Figure 9) (Reddy et al. 2007). A ZnO NP concentration of 5 mM was chosen for these experiments given the observed IC_{50} value for T cells. After 24 h of NP exposure, viability was determined by PI uptake and flow cytometry. As shown in Figure 10A, significantly greater cytotoxicity was observed with 4 nm NP (80.0% ± 2.0%) compared to either 13 nm and 20 nm sized NP ($p=0.0027$ and $p=0.0004$, respectively). Similarly, significantly less cytotoxicity was observed for 13 nm NP (70.1% ± 8.0%) compared to 20 nm particles (44.0% ± 6.8%, $p=0.05$). To verify dose-dependent ZnO NP toxicity based on NP size, we performed experiments testing 4 nm versus 20 nm sized NP at varying concentrations (1 mM, 5 mM and 10 mM). As seen in Figure 10B, significantly greater toxicity was observed using 4 nm NP compared to 20 nm NP at all concentrations tested ($p=0.015$ at 1 mM, $p=0.004$ at 5 mM and $p=0.003$ at 10 mM NP). These results demonstrate that ZnO NP-induced T cell toxicity increases with decreasing NP size.

Towards understanding the mechanism of this response, it is important to note that the band gap energy of NP is shown to increase with decreasing size (Yang, Liu, Yang, Zhang and Xi 2009). As a greater band gap energy associated with smaller NP could be expected to increase intracellular ROS production, studies were performed to address this possibility. However, initial experiments were first performed to establish

whether ZnO NP induce ROS production in immune cells and to determine the impact of ROS production on cell viability.

ZnO NP Induce ROS Production

Several types of nanomaterials, including quantum dots and metal oxide NP, have been shown to induce the generation of excess ROS, although only limited studies have evaluated the ability of ZnO NP to induce ROS in normal/non-transformed mammalian cells (Bergamini et al. 2004; Gojova, Guo, Kota, Rutledge, Kennedy and Barakat 2007). To investigate oxidative stress as a mechanism of ZnO NP-induced cellular toxicity, studies evaluated ROS production in primary $CD3^+$ lymphocytes and $CD14^+$ monocytes in mixed cell PBMC cultures and in Hut-78 T cancer cells using the cell permeable dye, DCFH-DA (Figure 11). In the presence of ROS, including hydrogen peroxide (H_2O_2) and superoxide anion (O_2^-), DCFH-DA is oxidatively modified into a highly fluorescent derivative that is readily detectable using flow cytometry. Following ZnO NP treatment for 18-24 h, a modest increase in DCFH-DA fluorescence (~7.0 fold increase—12.5/1.78) was observed in primary lymphocytes treated with 5 mM NP for 18 h (Figure 11A), and an even stronger induction was observed in Hut-78 T leukemic cells (~14-fold increase) (Figure 11B). Additionally, peripheral blood monocytes produced robust levels (~25.1 fold increase) of ROS in response to ZnO NP, consistent with the greater capacity of these cells for ROS generation (Figure 11C). Although increased ROS production was detectable as early as 8 h of NP exposure, greater levels were apparent at 18–24 h.

To investigate the kinetics of ROS production, PBMC cultures were treated with ZnO NP (1 mM and 5 mM) and ROS production measured in T cells and monocytes after

6 h and 20 h of NP exposure, using flow cytometry to distinguish between cell types. As shown in Table 1, modest amounts of ROS were detectable in monocytes (19% ROS producing cells) as early as 6 h post ZnO NP exposure, yet no detectable ROS observed in T cells at the corresponding concentration and time point. At 20 h of NP treatment, appreciable ROS production was observed in T cells treated with 5 mM ZnO NP (~38% ROS producing cells). Due to nearly complete cell death in monocyte cultures at 20 h time points, no residual cell-associated ROS signal was observable.

These findings indicate ZnO NP are capable of inducing intracellular ROS in both normal healthy immune cells (e.g. T cells and monocytes) and cancerous cells (e.g. Hut-78), and demonstrate ROS production in monocytes occurs considerably earlier compared to T cells. It is important to note that due to differing size and granularity properties of the cell types examined, different instrument voltage parameters were required which prevents direct comparisons of intrinsic levels of ROS between cell types.

ROS Production Is Dependent on ZnO NP Size

As earlier experiments demonstrated a dependence of cell viability on NP size (smaller NP display greater toxicity compared to larger NP), we speculated that smaller ZnO NP may induce greater amounts of ROS compared to larger NP. The relationship between NP size and ROS production was investigated for three different sized ZnO NP (4 nm, 13 nm and 20 nm) at two different NP concentrations (5 mM and 10 mM) in mixed PBMC cell cultures (Figure 12). Following 3 h of treatment, ROS production was evaluated using the ROS detection probe, DCFH-DA and fluorescence measured using a microplate reader. A size dependent induction of ROS was observed at both NP

concentrations, with 4 nm sized NP consistently inducing higher levels of ROS compared to 13 nm or 20 nm sized NP. At equivalent 5 mM NP concentrations, significantly higher levels of ROS were observed for 4 nm and 13 nm NP compared to 20 nm NP (~4 -fold relative increase ($p=0.0165$) and ~3-fold increase ($p=0.05$), respectively). Similarly, 10 mM NP treatment resulted in significant differences in ROS production between all sizes of NP with a 3.2-fold greater induction of ROS observed between 4 nm and 20 nm NP ($p<0.0001$), a 1.9-fold increase observed between 13 nm and 20 nm NP ($p=0.0297$) and a 1.6-fold increase observed between 4 nm and 13 nm NP ($p=0.005$).

ROS Quenchers Mitigate ZnO NP-Induced Cytotoxicity

Due to the demonstrated ability of ZnO NP to induce ROS production in immune cells, experiments were conducted to determine the causal role of NP-induced ROS as a major mechanism of toxicity. Purified human $CD14^+$ monocytes and $CD4^+$ T cells were pre-treated with N-acetyl cysteine (NAC), a tri-peptide that is readily oxidized in the presence of ROS, prior to ZnO NP exposure. NAC acts to reduce ROS-induced cell damage by augmenting cellular glutathione stores and is a well known ROS quenching agent (Valko et al. 2005). Following 24 h of ZnO NP exposure, cell viability was assessed using the Alamar Blue cytotoxicity assay and measured using a microplate reader. Results reveal that 5 mM NAC significantly protects both monocytes and T cells against NP-induced toxicity ($p = 0.0001$ and $p = 0.0481$, respectively) and implicates ROS formation as a major mechanism of ZnO NP-induced toxicity in primary immune cells.

NP Association and Uptake

To evaluate NP-cell interactions, experiments were performed using FITC-doped ZnO NP to monitor, quantify and compare NP internalization and extracellular membrane association in immune cells.

NP Preferentially Associate with Monocytes Compared to Lymphocytes

Based on results indicating monocytes are killed at lower NP concentrations compared to the other types of immune cells examined (e.g. T cells, B cells and NK cells), we performed experiments to determine if NP cytotoxicity is correlated with the degree of NP-cell association and/or NP uptake. Fluorescent FITC encapsulated ZnO NP (FITC-ZnO NP) prepared by our collaborators (Wang et al. 2009) were used to quantify the extent to which NP physically and stably associate with cells using both flow cytometric analysis and confocal microscopy. In one set of experiments, freshly isolated PBMCs were treated with 5 mM FITC-ZnO NP, or left untreated, and multi-color flow cytometry used to simultaneous identify monocytes and lymphocyte populations present in the PBMC culture, as well as evaluate relative increases in FITC-NP signal in these two cell types. As shown in Table 2, all immune cell types evaluated (T, B, and monocytes) show strong NP association, with 78-98% of cells displaying at least some level of positive FITC fluorescence compared to control cells cultured in the absence of NP. However, a 9.3-13.7 -fold increase in the number of NP associating with any given monocyte compared to individual T and B lymphocytes was observed as indicated by changes in the mean fluorescence intensity (MFI) (T and B lymphocytes displayed similar MFI values). These results demonstrate that ZnO NP preferentially associate with

monocytes (MFI: 131.2) compared to lymphocyte subpopulations (MFI: 9.84 for $CD3^+$, MFI: 14.1 for $CD4^+$ T_H and MFI: 9.61 for B cells), although whether this simply reflects initial extracellular membrane-NP interactions or intracellular NP localization is not discernable using this experimental approach.

NP Preferentially Associate with Activated T Cells

Based on differences in activated versus unactivated T cells to ZnO NP-induced toxicity and to gain further insights into mechanisms of differential cell toxicity, experiments were performed to determine whether NP preferentially associate with activated T cells compared to resting T cells. FITC encapsulated ZnO NP (FITC-ZnO NP) were prepared as described (Wang et al. 2009) and their fluorescence properties used to monitor cell uptake/association. Primary $CD4^+$ T cells were both left unactivated or activated with CD3/CD28 Ab and treated with 5 mM FITC-ZnO-NP for 4 h. Dual color flow cytometry was used to analyze changes in the FITC-NP signal on gated $CD4^+$ T cells. Results demonstrate a low NP associated fluorescence signal (12.5% FITC positive) in resting T cells, while a substantially greater FITC signal (48.4% positive) was observed for activated T cells (Figure 14). A dose-dependent uptake/association of FITC-ZnO-NP was noted with greater NP association at 5 mM compared to 1 mM concentrations (~3.3 greater attachments at 5 mM).

At the early time points evaluated in these studies, NP labeling did not appear to reflect a generalized increase in membrane permeability as no PI uptake indicative of cytotoxicity was observed following 4 h of exposure with 5 mM FITC-ZnO-NP (data not shown). However, the expected loss of cell viability (73% ±7.3% s.e., n = 3 with 1.25

mM) was detected upon extended 24 h exposure, indicating that FITC ZnO-NP behave similarly to unlabeled ZnO NP. Collectively, these results indicate that the cellular processes accompanying T cell activation (e.g. increased membrane protein expression, cell cycle progression) result in changes that promote strong physical interactions and consequent intracellular uptake of NP.

NP Uptake by Jurkat T Cells

NP uptake and internalization studies were performed using Jurkat T cells to explore NP-immune cell interactions. Jurkat T cells were treated with FITC-ZnO particles (green fluorescence) for 8 h, and washed extensively to remove unattached extracellular particles and reduce background staining. Cells were stained with an anti-CD3 PE-conjugated Ab (red fluorescence) and confocal images taken using live cells to avoid internalization artifacts resulting from cell fixation. Figure 15 (panels B-D) shows consecutive three-dimensional slices through a single Jurkat T cell and images demonstrate internalization of a green fluorescent FITC-ZnO particle with intracellular localization being confirmed by viewing along orthogonal directions. Individual confocal image slices were taken at intervals of 200 nm thickness (comparable in size to the NP), thus only one internalized particle is shown in the presented focal plane. However, at least six internalized NP were observed in this particular cell with additional internalizations likely but too proximate to the plasma membrane to accurately resolve.

The presence of such internalized FITC-ZnO particles was confirmed in multiple cells present on the culture slide. Figure 15A reflects NP background staining and was obtained by treating with an identical concentration of NP and sample washing regime as

for cell cultures (Wang et al. 2009). Although these findings do not determine specific intracellular locations of the internalized particles, they do demonstrate the ability of immune cells to endocytose/phagocytose NP and show a correlation between NP internalization/membrane association and susceptibility to ZnO NP-induce cytotoxicity.

ZnO NP Induce Apoptosis

Published research has demonstrated ZnO NP induce dose-dependent apoptotic and necrotic forms of cell death in non-human mammalian cells, with lower concentrations of ZnO NP inducing apoptosis and higher concentrations resulting in necrosis (Jeng and Swanson 2006). However, very little is known about ZnO NP-induced cell death in human cells, specifically human immune cells. To this end, experiments were performed to evaluate mechanisms of ZnO NP-induced cell death (e.g. apoptosis and necrosis) in T cells at concentrations previously determined to cause significant cell death. Jurkat cells were treated with 0.3 mM NP for 20 h and apoptosis evaluated using two different experimental approaches. In the first, cells were stained with a green fluorescent annexin V Ab which reacts against externalized phosphatidylserine, a characteristic of apoptotic cells, and the red fluorescent propidium iodide dye which stains both late-stage apoptotic and necrotic cells displaying permeable membranes (Figure 16). As expected, viable control cells show only very weak staining with annexin V Ab and no detectable staining with PI (Figure 16 panels A-C). Conversely, cells treated with ZnO NP stain positive with the apoptotic marker (e.g. two out of the four cells in panel F and four out of five cells in panel G show green fluorescence only). Some dually

stained cells were also observed as expected for late-stage apoptotic cells with permeable membranes.

To further verify NP-induced apoptosis, similar cell cultures were stained with the DNA dye, acridine orange (Figure 17), which is used to detect apoptotic morphology characterized by nuclear fragmentation, cellular shrinkage, and chromatin condensation. These morphological changes were observed in NP treated cultures (Figure 17C) and cells treated with the apoptosis inducer okadaic acid (Figure 17B), but not in control samples (Figure 17A). Collectively, results from these studies indicate ZnO NP toxicity to immune cells can occur by an apoptotic process.

ZnO NP Induce Pro-Inflammatory Cytokine Expression

The pro-inflammatory potential of NP has been shown to be dependent on a variety of factors such as nanomaterial, size, method of delivery, etc. (Duffin, Tran, Brown, Stone and Donaldson 2007). To elucidate the pro-inflammatory potential of ZnO NP on primary human immune cells, various cytokines (IFN-γ, TNF-α and IL-12) were measured in resting (unactivated) and IFN-γ-primed primary human immune cells. These cytokines were chosen because they represent critical pathways involved in both the inflammatory response and immune cell activation and differentiation. Freshly isolated PBMC were left untreated or treated with varying concentrations of 8 nm ZnO NP for 38 h. After incubation, cell-free media was harvested and cytokine levels measured using an ELISA assay (performed by Cytokine Core Laboratory, Baltimore, MD). Additionally, some cell samples were primed with IFN-γ (1000 U/mL) before addition of NP to assess

the effect of activation status on cytokine production (specifically, IL-12) in response to NP treatment.

Results from these studies demonstrate significant dose-dependent increases in IFN-γ and TNF-α in response to ZnO NP treatment at all concentrations tested (0.05 mM, 0.1 mM and 0.2 mM) (Figure 18A and B). Interestingly, while ZnO NP treatment did not induce appreciable amounts of IL-12 production in resting cells, significant dose-dependent increases were observed in IFN-γ-primed cells (Figure 18C). The inability of ZnO NP to induce IL-12 in resting cells is not altogether surprising as naturally occurring IL-12 production is typically only seen in antigenically activated immune cells (e.g. DC, monocytes, T cells) (Maranda and Robak 1998). These findings indicate ZnO NP are capable of inducing at least some key components of inflammation, and further suggests that a Th1-mediated immune response may be elicited, which is the type of immunity desirable for eradicating cancer and virally infected cells (Tau et al. 2000).

SnO_2 NP and CeO_2 NP Appear Less Toxic to T Cells Compared to ZnO NP

Initial experiments were performed to compare ZnO NP toxicity in T cells to two other common types of metal oxide NP, namely SnO_2 NP and CeO_2 NP (Figure 19). $CD4^+$ T cells were left untreated or treated with 10 mM NP of either SnO_2 NP or CeO_2 NP for 22-24 h and dual color flow cytometry was used to simultaneously identify cells and test cell viability using PI. Preliminary findings indicate both SnO_2 NP and CeO_2 NP fail to kill T cells at 10 mM of NP treatment (~90% viability), a concentration shown to cause significant ZnO NP-induced T cell death (<30% viability, Figure 8A). Interestingly, treatment with SnO_2 NP and CeO_2 NP caused a dramatic increase in cell

granularity (SSC) with no concurrent change in size (FS), and gating on these highly granular cells revealed an absence of PI signal, indicating normal cell viability. As increases in granularity (SSC) properties with no concurrent change in size (FS) may be indicative of phagocytosis/endocytosis (Coester, Nayyar and Samuel 2006; Elamanchili, Diwan, Cao and Samuel 2003), these preliminary results suggest SnO_2 NP and CeO_2 NP are taken up by T cells, but unlike ZnO NP, may not cause appreciable cell death.

DISCUSSION

Nanomaterials are of particular interest due to the unique physical, chemical and biological properties that can accompany reduction to the nanoscale (Medina, Santos-Martinez, Radomski, Corrigan and Radomski 2007). Unlike micron-sized bulk materials, the properties of nanomaterials are governed by principles of both classical and quantum physics and are attributed, at least in part by an increased surface area to volume ratio with decreasing size. This translates into distinctive size-dependent characteristics, and much research is devoted to gaining an understanding of how these characteristics impact biological and cellular systems (Fortina, Kricka, Surrey and Grodzinski 2005).

NP are being explored for a variety of different biomedical applications and are already found in many commercial products. Metal oxide NP, specifically ZnO NP, are one such type of NP frequently used in sunscreens and cosmetics due to its increased transparency and enhanced UV protection (Fan and Lu 2005). ZnO NP are also recognized as semi-conductor quantum dots, which are a class of NP which exhibits size-dependent fluorescent properties that render them useful in biosensing (e.g. tumor detection) and enhanced tissue imaging (Bawarski, Chidlowsky, Bharali and Mousa 2008). Understanding how NP interact and impact cells is of critical importance from an environmental health and safety standpoint, and also may provide for novel NP applications.

Research has provided evidence that specific properties such as size, shape and surface reactivity all contribute the cytotoxic potential of NP (Igarashi 2008). Our results

demonstrate differences in ZnO NP-induced toxicity to immune cells based on several parameters such as cell type, cell activation status, proliferative potential, NP size, the extent of NP-cell physiological interactions, and implicate ROS production as a major mechanism of cytotoxicity. Additionally, results indicate ZnO NP elicit pro-inflammatory cytokine production from immune cells. Collectively, these findings illustrate differential ZnO NP effects and suggest a potential clinical relevance for ZnO NP in the treatment of diseases such as cancer and autoimmunity based on the cell-selective cytotoxic properties of these NP.

We first evaluated the effect of ZnO NP compared to larger micron-sized ZnO on purified human $CD4^+$ T cell viability as a representative immune cell type due to the important role of T cells in regulating the immune response. Our findings demonstrate dose-dependent decreases in cell viability in response to ZnO NP treatment at concentrations of bulk ZnO where no appreciable loss in viability is observed (Figure 2). These results indicate that when reduced to the nano-scale, ZnO acquires unique size dependent properties resulting in altered toxicity thresholds compared to what is typically observed for this bulk material. To further explore this issue, T cell results were compared to ZnO NP studies performed by our collaborators, Drs. Kevin Feris and Alex Punnoose, showing bacteria (*E. coli* and *S. aureus*) inhibition in response to ZnO NP treatment, and reveal both types of bacteria are killed at lower concentrations compared to T cells (data not shown, $p<0.0001$) (Reddy et al. 2007). Although there were differences in certain experimental conditions between the bacteria and T cell studies, including media type (i.e. LB for bacteria and RPMI for T cells) and vehicle type for NP

delivery (i.e. DEG for bacteria and PBS for T cells), results are still of interest as both types of culture media contain large proteins, carbohydrates and other factors which might influence NP toxicity and no appreciable vehicle effect was observed for either cell type in control cells. Our studies further demonstrate that differences in NP-induced cytotoxicity exist between types of common bacteria, with *S. aureus* being more susceptible than *E. coli* (Figure 3) (Reddy et al. 2007). These differences in NP susceptibility observed among bacteria strains and between bacteria and human cells suggest the possibility of exploiting ZnO NP for use as novel anti-microbial agents in which potentially harmful bacteria are selectively eliminated and normal human cells are spared. As such, future research is necessary to build on these findings for further elucidation of factors underlying ZnO NP cytotoxicity and investigating ZnO NP effects on other types of bacteria.

To further explore mechanisms underlying differential ZnO NP cytotoxicity, we extended our studies to investigate whether the activation status of immune cell influences toxicity. $CD4^+$ T lymphocytes were utilized as a representative cell type given their critical role in protective immunity, the frequent negative effects of commonly used chemotherapeutic agents on cells of hematopoietic lineage, and the ability of self-reactive T cells to contribute to the development of autoimmune diseases. ZnO NP- cell responses were evaluated in normal primary resting T cells and compared to identical cultures in which cells were either activated through the T cell receptor (TCR) signaling pathway or via both TCR and CD28 co-stimulation pathways. Results demonstrate significantly greater resistance to ZnO NP-induced toxicity in quiescent T cells compared to TCR

stimulated cells, and even greater sensitivity in TCR/CD28 co-stimulated T cells (Figure 4). Additionally, we found activated T cells associate with ZnO NP to a greater extent compared to resting T cells (Figure 14), consistent with the greater susceptibility to ZnO NP-induced toxicity in activated cells compared to resting cells. The preferential killing and greater NP association observed in activated cells relative to quiescent cells of the same lineage suggests that mechanisms of ZnO NP toxicity may be related to the proliferative potential of the cell and subsequent NP-cell interactions. In a number of autoimmune diseases, including multiple sclerosis and psoriasis, self-reactive T cells are a pathogenic subset underlying disease processes and exist in a predominately activated state as they are continually exposed to specific Ag present in normal body tissue (Wagner 2007). Because only a very small percentage of the total T cell repertoire are self-reactive and pathogenic in autoimmunity, the ability of identical concentrations of ZnO NP to preferentially induce cytotoxicity in self-reactive activated T cells while leaving the unactivated T cell repertoire largely intact and immunity uncompromised represents an incredibly attractive approach for treatment. Thus, these findings may provide a foundation for the development of ZnO NP-based therapeutics, where disease-causing cells are targeted by attachment of Ab to ZnO NP directed against proteins expressed predominantly on activated T cells, such as CD40L and OX40 (Taraban et al. 2002). However, additional research is required to further elucidate factors influencing NP toxicity and *in vivo* studies are necessary to gain a more thorough understanding of how ZnO NP impact the immune system as functioning unit.

The greater toxicity of ZnO NP against activated T cells led to experiments testing the effects of ZnO NP toxicity in memory versus naïve T cells (Figure 6), since memory T cells are recognized to respond and proliferate much faster to a previously encountered Ag compared to naïve (Surh and Sprent 2008). For these experiments, bulk cultures of PBMCs were treated with ZnO NP and T cell types present in PBMC cultures (naïve, memory and a mixture of both) identified by cell-surface markers. Our results demonstrate that memory T cells are more susceptible to ZnO NP-induced cytotoxicity compared to antigenically inexperienced naïve T cells, and support the hypothesis that ZnO NP toxicity is dependent on the metabolic status and proliferative capacity of the cell.

Differences in ZnO NP cytotoxicity based on cell type (e.g. prokaryotes versus eukaryotes) and cell activation status lead to experiments in which normal cells were compared to cancerous cells of the same lineage, as cancer cells exhibit uncontrolled proliferation and robust metabolic activity (Hanley et al. 2008). Results reveal that cancerous T cells are markedly more susceptible (~28-35 times) to ZnO NP mediated toxicity compared to their normal counterparts (Figure 5), and similar kinetics were observed for NP-induced toxicity to both cancer and normal T cells (Figure 7). These findings may be of clinical importance as one of the greatest challenges facing chemotherapy is the inability of anticancer drugs to effectively distinguish between normal and transformed tissue (Nie, Xing, Kim and Simons 2007; Hellman 1980). Although many commonly used chemotherapeutic drugs target rapidly dividing cells, many suffer from a relatively low therapeutic index, that is, the ratio of toxic dose to

effective dose (Huang and Oliff 2001). This limitation frequently causes a broad range of toxicities leading to dose limiting toxicity and a concomitant reduction in antitumor efficacy. The preferential toxicity of ZnO NP towards cancerous T cells is of substantial magnitude, especially in comparison to *ex vivo* indices reported for other commonly used chemotherapeutic agents using similar cell viability assays. For example, therapeutic indices of ≤ 10 have been reported for two commonly used chemotherapeutic agents, doxorubicin and carboplatin, against a variety of tumors including acute myelogenous leukemia, non-Hodgkin's lymphoma, ovarian, and other solid tumors (Bosanquet and Bell 2004). Additionally, the similar kinetics observed in cancer and normal T cells suggests ZnO NP-induced cytotoxicity occurs in a predictable time-dependent fashion, regardless of cell type and susceptibility (Figure 7), and is a critical piece of information when considering materials for drug development.

The inherent differential toxicity of ZnO NP against activated and rapidly dividing cancer cells raises exciting opportunities for their potential use as anticancer agents, and the selectivity of these nanomaterials may be further enhanced by the covalent attachment of monoclonal Ab, peptides, and small molecules to tumor-associated proteins which would allow for selective targeting of the disease-causing cancer cells for *in vivo* studies using animal models. However, care must be taken when extrapolating these observed differential cell responses to all cell types until further studies have been conducted evaluating the effects of ZnO NP across many cell lineages.

The preferential ZnO NP-induced killing of highly proliferative cancer cells and activated T cells indicates a need to examine the effects of ZnO NP toxicity on various

types of resting primary immune cells. To assess this, the effect of ZnO NP on cell viability was measured in primary human T cells, B cells, NK cells and monocytes in mixed PBMC cell cultures and cell identification achieved by labeling cell-specific surface markers. Testing the effects of ZnO NP in bulk immune cell cultures is advantageous, as it takes intercellular interactions and cell-signaling effects into account, and is a better estimation of *in vivo* effects and physiological relevancy. Of the four cell types tested, monocytes were shown to be the most susceptible to ZnO NP-induced toxicity, with ~18-fold and ~6-fold differences in viability observed compared to T and B lymphocytes and NK cells, respectively (Figure 8). As immune cells are highly diverse and possess unique phenotypes based on specific immune cell function, our findings indicate ZnO NP toxicity may be dependent on differences in cell-specific properties such as growth characteristics, size, cell-surface receptors, mechanisms of particle uptake, capacity for ROS production, etc.

For example, unlike T, B, and NK cells which grow *in vitro* as free floating cell suspensions, monocytes are an adherent cell type and grow in culture as a surface monolayer. This property may influence the effective concentration of ZnO NP treatment for adherent monocytes as NP aggregates form and settle on top of the monocyte layer. Future studies are needed to determine the extent to which these differing attributes (e.g. adherence versus suspension) contribute to ZnO NP toxicity, and one potential approach would be altering adherent cell methodology by growing adherent cells on a 3-dimensional structure within culture media before ZnO NP addition.

Additionally, physiological differences between phagocytes and non-phagocytic cells, such as increased particle uptake by phagocytes, larger phagocyte size, and greater

capacity for ROS formation (generated for intracellular destruction of bacteria in the phagosomes) may help to explain increased ZnO NP susceptibility in monocytes compared to lymphocytes. Phagocytes may be more likely to ingest NP aggregates, and the larger cell size may allow more room for intracellular NP accumulation, and consequently, increased intrinsic ROS production. As monocytes already produce greater levels of ROS compared to lymphocytes, excess ROS generated in response to NP exposure may result in overwhelming oxidative stress mechanisms leading to cell death. The production of ROS may also factor into why NK are killed at lower concentrations of ZnO NP compared to T and B lymphocytes as published research indicates that ROS is used by cytotoxic NK cells for induction of caspase-independent induced target cell killing (Martinvalet, Zhu and Lieberman 2005), although additional research is required to substantiate this hypothesis.

Although phagocytosis is not a major defense mechanism used by T, B and NK cells, these cells are capable of intracellular uptake of certain particulate matter by endocytosis (e.g. pinocytosis and receptor-mediated endocytosis), which is used by all cells for accessing macromolecules and other essential molecules, and trafficking of cell surface receptors (Rogers and Basu 2005). To explore whether increased ZnO NP sensitivity is correlated with NP uptake and association, fluorescent FITC-doped ZnO NP were used to investigate NP-cell interactions. Consistent with our toxicity findings, observations reveal both T cells (Figure 15) and monocytes capable of NP uptake, and demonstrate greater NP association in monocytes compared to both T and B lymphocytes (Table 2). Although exact mechanisms by which nonfunctionalized NP (NP without

functionalized localization or target sequences), such as ZnO NP, interact with cells is not yet fully understood, several studies have provided evidence that both negatively and positively charged NP (specifically QD) can be endocytosed by human cells and are capable of nuclear penetration (Ryman-Rasmussen, Riviere and Monteiro-Riviere 2007; Jaiswal, Mattoussi, Mauro and Simon 2003). Based on these findings, future experiments are warranted to investigate exact mechanisms of ZnO NP uptake and association between different cell types.

Our results support other studies showing significantly greater NP QD (CdTe and CdSe/ZnS) uptake in phagocytic cells compared to NP uptake by non-phagocytic cells, and indicate that specific structural and physiological differences between different immune cell types, such as adherence and phagocytic ability, significantly contribute to ZnO NP-induced toxicity, allowing for predictions of increased NP susceptibility based on these characteristics for other cell types. The extent to which cells internalize and associate with ZnO NP may be an essential component of selective ZnO NP toxicity and although specific mechanisms of ZnO NP cellular uptake cannot be determined from these experiments, existing research indicates QD are capable of exploiting the cell's active transport machinery for NP delivery to discrete intracellular and intranuclear destinations (Nabiev et al. 2007). Future research directed at exploring specific mechanisms of ZnO NP uptake such as the contributions of receptor-mediated compared to non-receptor mediated endocytosis and factors influencing NP uptake (e.g. NP charge, dissolution, NP size, etc.) may shed further light on this issue.

Oxidative stress, as seen in excessive ROS production, is implicated in degenerative and detrimental biological processes such as aging and disease development (e.g. cancer, Alzheimer's disease), and a number of studies indicate that certain nanomaterials, including metal oxide NP, have the potential to exhibit spontaneous ROS production based on material composition and surface characteristics, while other nanomaterials trigger ROS production only in the presence of select cell systems (Xia et al 2006; Lovric, Cho, Winnik and Maysinger 2005; Long, Saleh, Tilton, Lowry and Veronesi 2006). Results from our flow cytometry experiments demonstrate ZnO NP induce ROS production in both primary and cancer immune cells (specifically T cells and monocytes) and are consistent with other reports demonstrating ROS production in biotic environments following ZnO NP exposure (Xia et al. 2008b). Our findings show ZnO NP-induced ROS formation occurs in a concentration, time, and cell-type dependent, with higher levels observed in primary monocytes compared to primary T cells, which is consistent with the ability of these cells to generate large amounts of ROS during an immune response. Interestingly, immortalized T cells produced greater levels of ROS than primary T cells which may mechanistically underlie the greater susceptibility of cancerous T cells to NP-mediated toxicity (Figure 11).

These findings have important implications regarding mechanisms of cellular toxicity, as elevated ROS production that exceeds the capacity of the cellular antioxidant defense system causes cells to enter a state of oxidative stress which results in damage of cellular components such as lipids, proteins, and DNA (Lovric et al. 2005; Xia et al. 2008b). NP-induced ROS production may activate transcription factors such as NK-kB and AP-1 that control the transcription of pro-inflammatory genes (Monteiller et al.

2007), however, it is still enigmatic under which conditions cellular demise induces an immune response or remains immunologically silent, and under which circumstances apoptotic or necrotic cells are immunostimulatory or tolerogenic (Kepp et al. 2009).

The causal role of ROS generation in NP-mediated cytotoxicity was validated by experiments using the ROS quencher, NAC. Results from these experiments demonstrated significantly greater viability in cells (e.g. primary monocytes and $CD4^+$ T cells) pre-treated with NAC before NP treatment compared to cells treated with NP alone (Figure 13). These results provide important insights implicating ZnO NP-induced ROS production as a primary mechanism of immune cell cytotoxicity and led to studies investigating the effect of NP size on ROS production.

Nano-scaled particles exhibit discontinuous crystal planes, increases in structural defects and changes in the electronic configuration, resulting in altered electronic properties on the particle surface which are directly related to particle size (Oberdorster et al. 2005). We evaluated the effect of ZnO NP size on immune cell toxicity and ROS production using 3 different sizes of ZnO NP (4 nm, 13 nm and 20 nm) at multiple concentrations. Findings from our studies demonstrate an inverse relationship between ZnO NP size and immune cell viability (Figure 10) which is consistent with reports using other NP systems and materials showing greater cytoxicity associated with smaller NP size (Nair et al. 2008). In agreement with our toxicity results, we found smaller ZnO NP (4 nm) induce greater amounts of ROS in immune cells compared to larger ZnO NP (e.g. 20 nm) (Figure 12) which may be due to smaller particles having larger reactive surface

areas compared to larger particles (Nel, Xia, Madler and Li 2006). In general, biological activity increases with decreasing particle size and the opposing trend of increased toxicity and ROS production with decreasing NP size indicates that if ZnO NP were to be employed for use in therapeutics, the smallest NP size available should be considered for use.

Particle size, shape, and chemical composition have been shown as principal factors controlling NP-cellular interactions and toxicity to mammalian cells (Yang et al. 2009). Another factor shown to contribute to the intracellular interactions with NP and NP-induced cytotoxicity is the dissolution of ions from metal and metal oxide NP, although the extent to which ion dissolution contributes to NP toxicity is unclear (Gojova et al. 2007; Cheng 2004). The dissolution of copper, cadmium and zinc ions from NP have been shown as major contributors in NP-induced toxicity to mammalian cells, especially in low pH conditions, and increasing ion dissolution has been correlated with decreasing particle size (Midander et al. 2009; Wang, Nagesha, Selvarasah, Dokmeci and Carrier 2008; Aruoja, Dubourguier, Kasemets and Kahru 2009). In one study, researchers found dissolution to play a significant role in ZnO NP-induced toxicity by disturbances in cellular zinc homeostasis resulting in lysosomal and mitochondrial damage and subsequent cell death (Xia et al. 2008a). However, conflicting research demonstrates minimal effects of Zn^{2+} ion dissolution alone on cell viability, and indicates NP size and surface chemistry as significant determinants of NP-induced toxicity (Yang et al. 2009) by ascribing the toxicological effects of ZnO NP not to particle dissolution, but to specific NP surface properties as determined by chemical composition (Yang et al. 2009).

The effects of NP size on toxicity have also been shown to be related to NP uptake (smaller NP are internalized to a greater extent compared to larger NP) and mitochondrial membrane association (Yang et al. 2009; Tarantola et al. 2009). The inconsistencies that currently exist in the scientific literature indicate that additional studies are warranted in these areas. Nonetheless, our research supports other studies by demonstrating a dependency of cytotoxicity on NP size and is novel in showing these effects specifically using ZnO NP in primary human immune cells.

The reduction in size of many materials to the nano-scale increases toxicity in many types of materials; however research suggests that other types of materials have cytoprotective properties at the nano-scale. We performed initial experiments to test differences in toxicity between CeO_2 NP and SnO_2 NP to primary T cells for comparison to results obtained using ZnO NP (Figure 19). Results from these preliminary experiments suggest that unlike ZnO NP, CeO_2 and SnO_2 are not toxic at 10 mM NP treatment, however, the increased granularity observed in response to NP treatment suggests NP uptake. These findings are in agreement with other published reports evaluating the effects CeO_2 NP on mammalian cells where it is hypothesized that the antioxidant properties of CeO_2 NP suppress ROS production and exert cellular resistance to exogenous sources of oxidative stress, thus protecting cells from oxidative injury (Chen, Patil, Seal and McGinnis 2006; Tarnuzzer, Colon, Patil and Seal 2005). Although suggestive, more research is required to further explore this issue as well as testing the effects of additional types of metal oxide NP on human immune cells.

As there is increasing evidence that elevated ROS acts as a critical signaling molecule in the induction of apoptosis by various stimuli (Jeng and Swanson 2006), studies were performed to determine mechanisms of ZnO NP-induced cell death. Results presented in Figures 16 and 17 provide strong evidence that ZnO NP cytotoxicity occurs by apoptotic processes in cells of T lymphocyte lineage at the concentrations tested. Research suggests the amount of ROS produced and intensity of oxidative stress may determine mechanisms of cell death, specifically selection between apoptosis and necrosis, with higher levels of ROS associated with the latter (Baigi et al. 2008). In contrast to apoptotic processes, necrotic forms of cell death are generally considered immunostimulatory (e.g. capable of eliciting a comprehensive immune response) and pro-inflammatory. However, the conditions under which cellular demise is immunostimulatory (e.g. elicits a comprehensive immune response) are not yet fully understood and controversy exists over whether apoptotic or necrotic cells are intrinsically immunogenic or tolerogenic (Kepp, Tesniere, Zitvogel and Kroemer 2008).

Recent evidence indicates that in contrast to scientific dogma concerning apoptotic cellular mechanisms, apoptosis (especially late stage apoptosis) may not be morphologically homogenous as evidenced by the surface expression of several proteins shown to promote antigen presentation and subsequent immune cell activation (Kepp et al. 2008). Distinguishing mechanisms of cell death (e.g. apoptosis versus necrosis) is a critical component of drug development as moderate levels of immune cell activation are beneficial for eliminating disease-causing cells, such as tumor cells, while over-stimulation of the immune response has been shown to promote tumorgenesis.

These studies indicate that a primary mechanism of ZnO NP cytotoxicity may precede ROS generation which then underlies the induction of apoptosis, a process that may be prevented by antioxidant and ROS quenchers. These observations may provide the basis for the development of new rational strategies to protect against ZnO NP toxicity or enhance the desired destruction of pathogenic cell types. Further research is needed to establish if the mechanism of ZnO NP-induced cell death (e.g. apoptosis or necrosis) occurs in a dose-dependent manner if this material is to be considered for therapeutic purposes as manipulation of this property may allow for more effective elimination of diseases-causing cells.

Certain metal oxide NP have been shown to induce pro-inflammatory responses, and some cytokines have been reported as induced by various metal oxide NP (Park and Park 2009). Additionally, the relationship between oxidative stress and inflammation is well established and studies have provided evidence which suggests ROS-induced inflammatory responses play a critical role in the cytotoxic effects (both apoptotic and necrotic) of different types of NP both in *vitro* and in *vivo* (Johar et al. 2004). We evaluated the effect of several different concentrations of ZnO NP on the expression of three different pro-inflammatory cytokines, IFN-γ, TNF-α, and IL-12, using bulk cultures of PBMCs. The role of TNF-α in inflammation is well characterized and has been shown to be an important regulator of acute inflammation, capable of influencing many aspects including infiltration of inflammatory cells into tissue, activating phagocytosis, inducing apoptosis in virally infected and tumor cells, chemotaxis of monocytes, and promoting Th1 differentiation. Notably, this cytokine received its name by the potent anti-tumor

activity it possesses when used at appropriate concentrations. However, high levels and chronic exposure to TNF-α have been shown to be detrimental and are associated with many of the symptoms associated with autoimmune disease. Our results demonstrate significant dose-dependent increases in TNF-α in response to ZnO NP compared to control cultures (Figure 18B). This dose-dependent response is important when considering ZnO NP for biomedical purposes as it allows for controlling the levels of TNF-α needed to achieve therapeutic responses without eliciting the potential damaging effects of TNF-α.

IFN-γ, secreted primarily by activated T cells, was also evaluated and is another cytokine associated with inflammation and Th1 differentiation. Similar to what was observed for TNF-α, our results demonstrate dose-dependent increases in IFN-γ in response to ZnO NP (Figure 18A). This provides further evidence that ZnO NP can induce pro-inflammatory, Th1-directed immune responses at concentrations below those required to produce significant losses of T cell viability. These results are important as IFN-γ is an important cytokine for promoting a Th1-mediated immune response, and Th1 cells are recognized as an essential cell subset for the effective elimination of cancer cells *in vivo*. The narrow range in ZnO NP concentrations necessary to increase TNF-α and IFN-γ reveals that parameters controlling ZnO NP toxicity, such as size, concentration, etc. need to be carefully controlled if ZnO NP are to be considered for used for therapeutic purposes.

The cytokine IL-12 is secreted primarily by activated monocytes, macrophages, DC cells, and to a lesser extent, T cells. IL-12 is essential in skewing the Th1/Th2 T cell responses toward a Th1-cell mediated immune response by inducing NK cells and T cells

to secrete other Th1-directed cytokines and suppressing the humoral Th2-mediated cytokines. Results from these experiments reveal that when PBMC are first primed by addition of exogenous IFN-γ, significant increases in IL-12 are observed in response to NP treatment (Figure 18C). These results suggest that a synergistic relationship between ZnO NP and the priming signals necessary to promote IL-12 secretion (e.g. IFN-γ) may occur in *in vivo* settings employing ZnO NP.

Importantly, our findings demonstrating that ZnO NP can induce TNF-α, IFN-γ, and IL-12 in activated immune cells suggest that careful titration of ZnO NP-based therapeutic interventions may be successful in elevating this key group of cytokines important for eliciting a Th1-mediated immune response with effective anti-cancer actions. Our results support other research demonstrating ZnO NP capable of inducing other pro-inflammatory cellular responses (Gojova et al. 2007; Sayes et al. 2007; Wieder et al. 2008), however this research is limited and to date, there have been no reports in which the pro-inflammatory potential of ZnO NP in primary human immune cells have been evaluated. Our results are of interest as they suggest the possibility of manipulating the immune response for utility in enhancing cancer cell targeted killing at concentrations of ZnO NP that do not cause significant cell death to normal cells.

In conclusion, results from these studies provide evidence demonstrating ZnO NP induce toxicity in a cell-specific and proliferation dependent manner with rapidly dividing, higher-ROS producing cells being the most susceptible, presumably in response to intracellular NP-mitochondrial interactions and mitochondrial damage, and quiescent cells being the least sensitive. Results also indicate cell-type dependent NP association

and intracellular localization, although additional research is required to further elucidate selective phagocytic/endocytic ZnO NP mechanisms based on specific cell susceptibility to ZnO NP-induced toxicity. ZnO NP increased the expression of the pro-inflammatory cytokines IFN-γ, TNF-α, and IL-12 at concentrations that shown minimal toxicity to primary NK, T and B cells. Manipulation of the immune response is a key element for the effective treatment of disease, and many current treatments for cancer, infection and autoimmunity are immunobased therapeutics (Becker 2006; Miao 2007).These findings suggest ZnO NP may direct Th1 mediated immune responses *in vitro* and illustrate the potential utility of ZnO NP for the treatment of diseases such as cancer, which is better eradicated by the development of a vigorous Th1-mediated immune response. Future studies will be required to investigate the effects of higher concentrations of ZnO NP on pro-inflammatory cytokine secretion and evaluate NP effects on other cytokine profiles. Additionally, expansion of these studies should include investigating mechanisms of ZnO NP adsorption, specifics of cellular uptake and intracellular localization, and the contribution of particular elements of the biotic environment that affect ZnO NP toxicity. Collectively, the findings presented in this research provide significant information that may be ultimately exploited for utilizing ZnO NP in the treatment of disease and developing next generation NP-based nanomedicines leading to improvements in lifespan, tumor growth inhibition, and decreased lethality.

APPENDIX

Figures and Tables

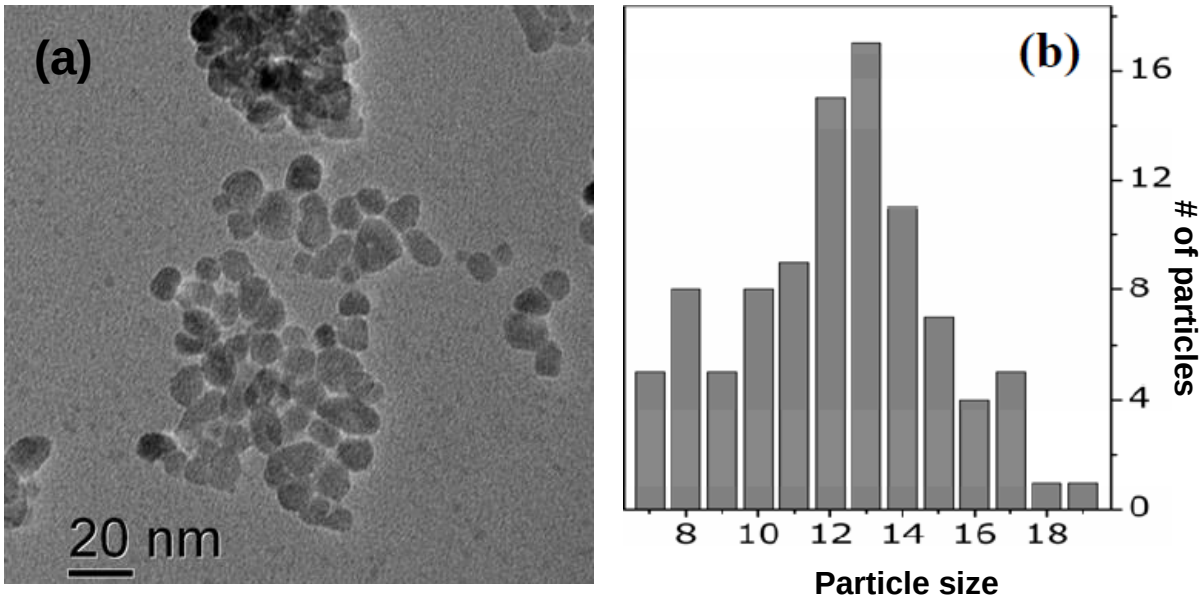

Figure 1. Transmission electron microscopy (TEM) image and size distribution of ZnO NP. A) For experiments conducted on all eukaryotic cells, ZnO NP were spun out of DEG, washed with ethanol, dried into powder form, and resuspended in an aqueous phosphate buffered saline (PBS) solution to desired stock concentration (mM). B) Plot showing particle size distribution where average NP size was determined to be ~13 nm.

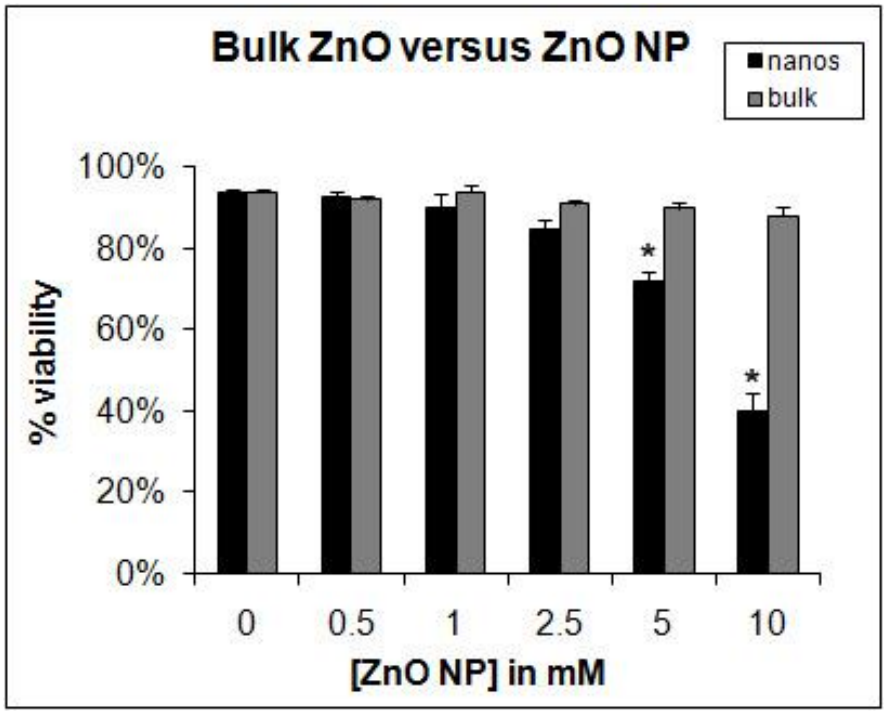

Figure 2. Effect of micron-sized bulk ZnO versus ZnO NP on $CD4^+$ T cell viability. Purified $CD4^+$ T cells (>96%) were cultured at 1 x 10^6 cells/mL and treated with varying concentrations of 13 nm ZnO NP or bulk ZnO. After 24 h of culture, cells were dually stained with PI and a FITC-labeled anti-CD4 antibody. 10,000 events gated on $CD4^+$ T cells were analyzed for changes in PI staining to allow quantification of cell death. NP were excluded from analysis based on their absence of fluorescent signal. Data from four independent experiments is presented and error bars depict standard error. To assess differences in viability between bulk ZnO and ZnO NP at each concentration, data was analyzed using a repeated measures analysis of variance (ANOVA) and asterisks denote statistically significant differences ($p < 0.05$).

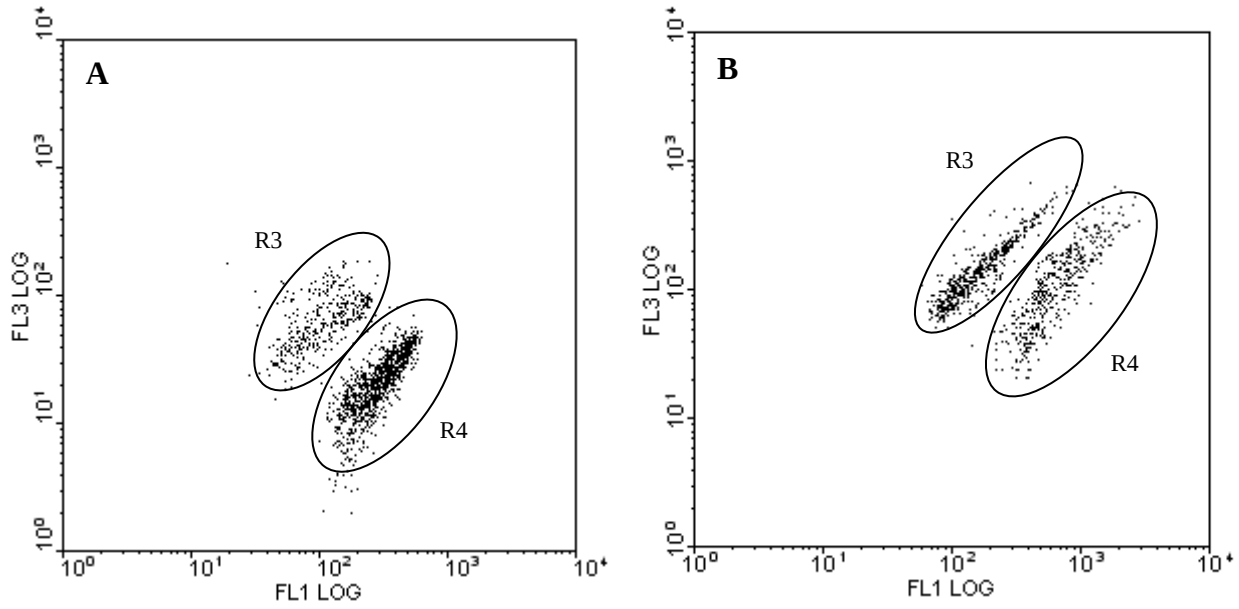

Figure 3. Dot plots of relative viability of bacterial suspensions by flow cytometry. Samples of bacteria were prepared, stained and analyzed using a 2-color live/dead BacLight® viability kit allowing for a two-parameter comparison of green and red fluorescence emission. Prior to sample analysis, the assay was validated using known mixtures of dead and live control cells. Bacteria were gated by forward scatter and side scattering light properties (R1, not shown) and nanoparticles excluded from analysis based on their absence fluorescence (R2, not shown). The R3 region depicts the region containing dead cells and the R4 region depicts the region containing live cells. A) The relative viability of *E. coli* (>30% loss of viability) treated with 5 mM ZnO nanoparticles for 15 h. B) The relative viability of *S. aureus* (>59% loss of viability) treated with 2 mM ZnO nanoparticles for 15 h.

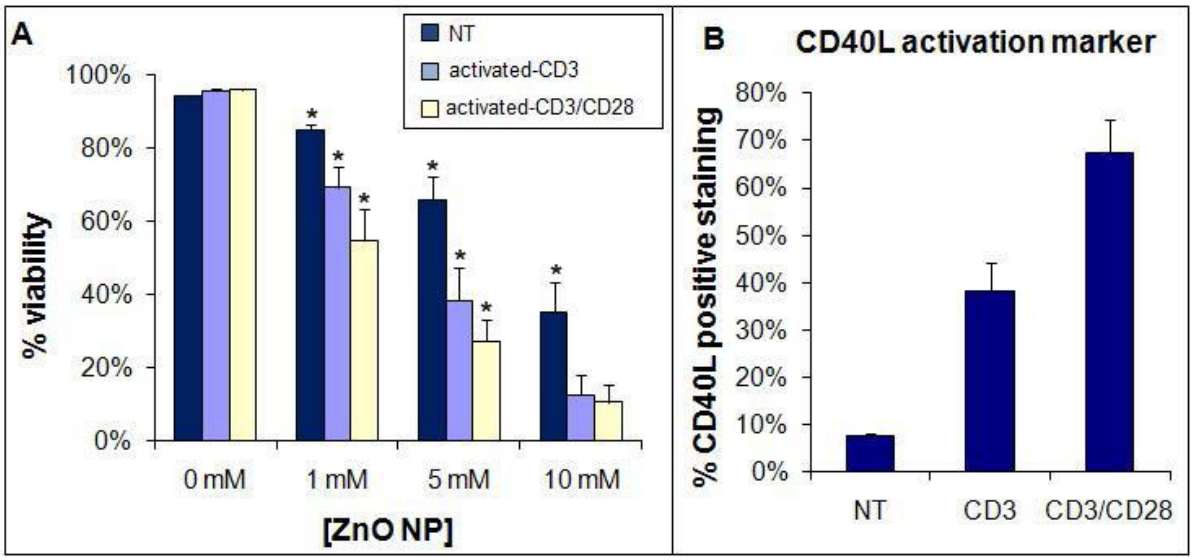

Figure 4. ZnO NP toxicity to unactivated and activated primary human $CD4^+$ T cells. A) Human peripheral blood $CD4^+$ T cells were isolated (purity >95%) and activated with anti-CD3 antibodies, a combination of anti-CD3 and anti-CD28, or left unactivated. Cultures were concurrently treated with varying concentrations of ZnO NP for 22-24 h and cell viability determined using flow cytometry and PI uptake (means ± standard error, n=6). To evaluate the relationship between cell cycle state and ZnO NP toxicity, data was analyzed using repeated measures analysis of variance and model based means post hoc test ($p < 0.05$). The two study factors are cell cycle state (unactivated, moderately activated with anti-CD3, and fully activated with anti-CD3/anti-CD28) and ZnO NP concentration (0 mM, 1 mM, 5 mM and 10 mM). Following overall statistical significance, cell viability (%) was compared among activation states at each concentration level using model-based estimates and standard errors. B) Verification of T cell activation was determined by concurrently monitoring expression of membrane CD40L protein using flow cytometry (means ± standard error, n=5).

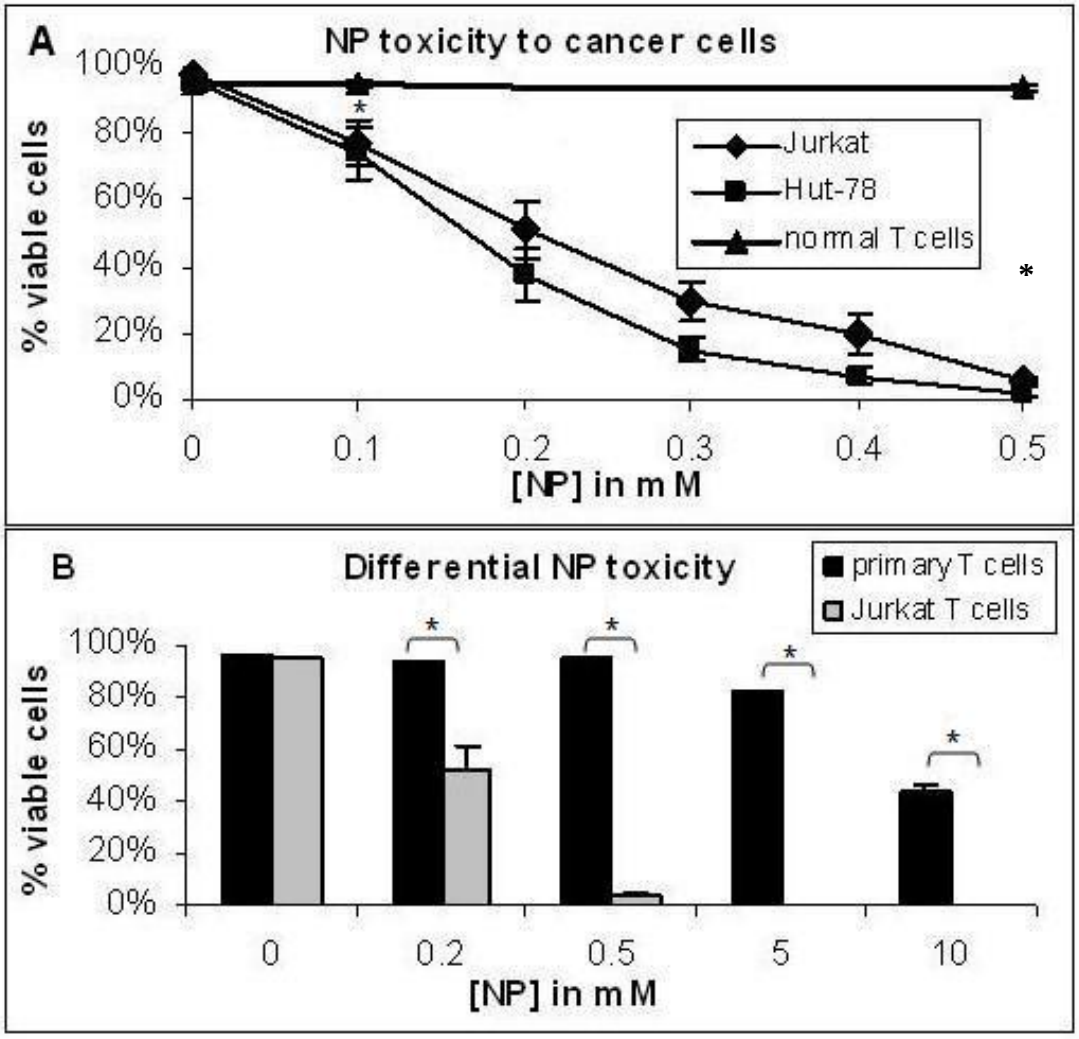

Figure 5. Differential cytotoxic effects of ZnO NP on cancerous T cell lines and primary T cells. A) Jurkat, Hut-78 T cell lines, or normal primary T cells were treated with varying concentrations of ZnO nanoparticles for 22–24 h and viability determined by monitoring PI uptake using flow cytometry. Data from seven (Jurkat), three (Hut-78), and four (normal $CD4^+$ T cells) independent experiments is presented and error bars depict standard error. Data was analyzed using a repeated measures ANOVA and model based means post test. Statistical comparisons were made between each cancer cell line and

primary T cells at 0.1 and 0.5 mM ZnO NP with significance levels defined as $p < 0.05$ and indicated by an asterisk. B) Jurkat and primary T cell viability was assessed using the LIVE/DEAD™ Viability/Cytotoxicity Kit for mammalian cells (Invitrogen, Eugene, OR). Following ZnO NP exposure for 24 h, cells were stained with calcein AM (green fluorescence) and ethidium homodimer-1 (red fluorescence) to differentiate between live and dead cells, respectively. Data from a representative experiment is presented with error bars depicting standard error, $n = 3$. A two-way analysis of variance combined with a model based means test indicates significant differences in viability between Jurkat and primary T cells for all NP concentrations tested (asterisk denotes $p < 0.0001$).

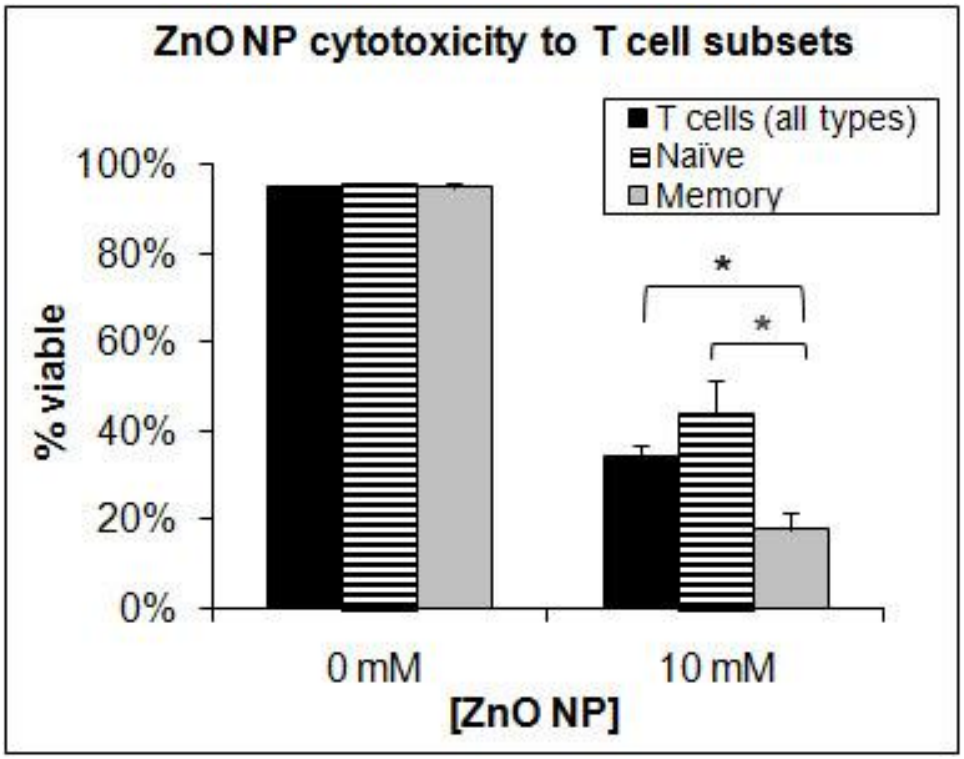

Figure 6. Differential ZnO NP cytotoxicity between naïve and memory T cells. Human peripheral blood PBMC were left untreated or treated with 10 mM ZnO NP (8 nm) for 22-24 h and viability determined by monitoring PI uptake using flow cytometry. T cells were defined as $CD3^+$, naïve T cells as $CD3^+$, $CD45RA^+$, and memory T cells as $CD3^+$, $CD45RO^+$ events. Data from three independent experiments is presented and error bars depict standard error. Asterisks denote statistically significant differences ($p < 0.05$) between NP treatment groups as determined using as a one-way repeated measures ANOVA.

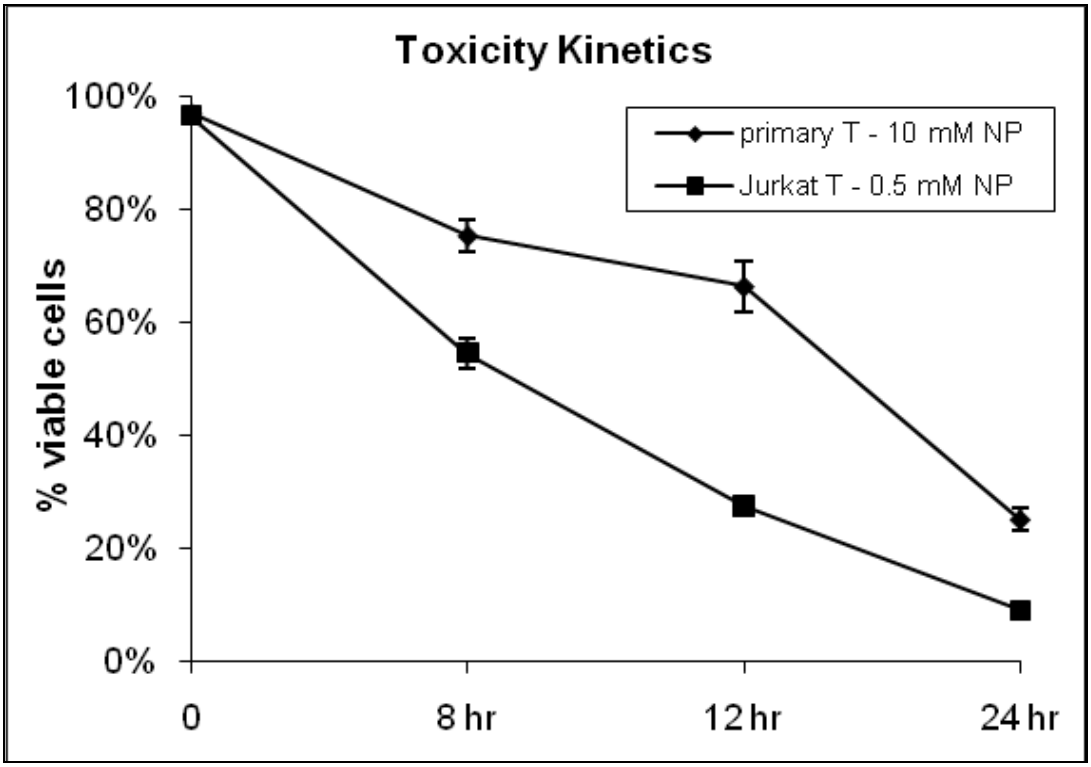

Figure 7. Kinetics of ZnO NP toxicity on normal primary T cells and Jurkat T leukemia cells. Freshly isolated $CD4^+$ T cells (purity > 96%) were treated with 10 mM ZnO NP and Jurkat T cells were treated with 0.5 mM ZnO NP for varying times and viability determined using PI uptake and flow cytometry. Means ± standard error from representative experiments are presented (n=3).

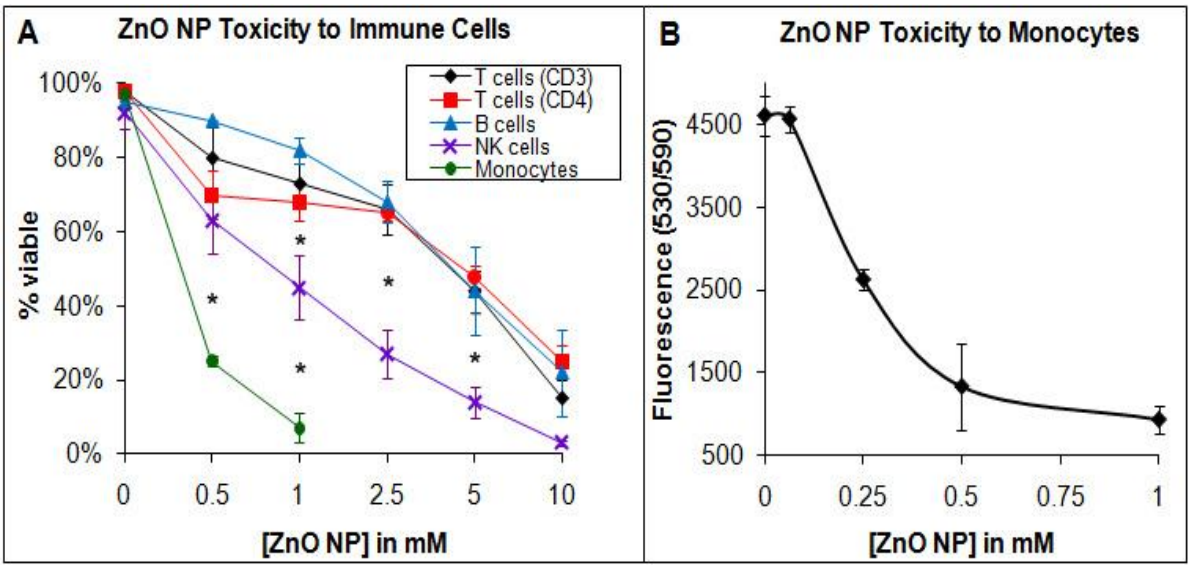

Figure 8. Differential cytotoxic effects of ZnO NP on primary immune cell subsets. A) PBMC were treated with varying concentrations (0.5 mM-10 mM) of 8 nm ZnO NP for 24 h and viability of $CD3^+$ T cells, $CD4^+$ T cells, B cells, NK cells, and monocytes present in PBMC cultures determined by monitoring PI uptake and flow cytometry. Data from three ($CD3^+$, NK cell and monocyte) and four (B cell) independent experiments is presented, with error bars depicting standard error. Data presented for purified $CD4^+$ T cells (>96%) is from one representative experiment done in triplicate with error bars depicting standard error. Asterisks denote statistically significant ($p < 0.05$) differences between $CD3^+$ T cells, B cells, NK cells and monocytes at indicated NP concentrations as determined using a repeated measures ANOVA. B) ZnO NP toxicity on purified human primary monocytes. Isolated $CD14^+$ monocytes were treated with varying concentrations of ZnO NP (0.0625 -1 mM) and viability assessed using the Alamar Blue cytotoxicity assay with error bars representing standard error (n=4).

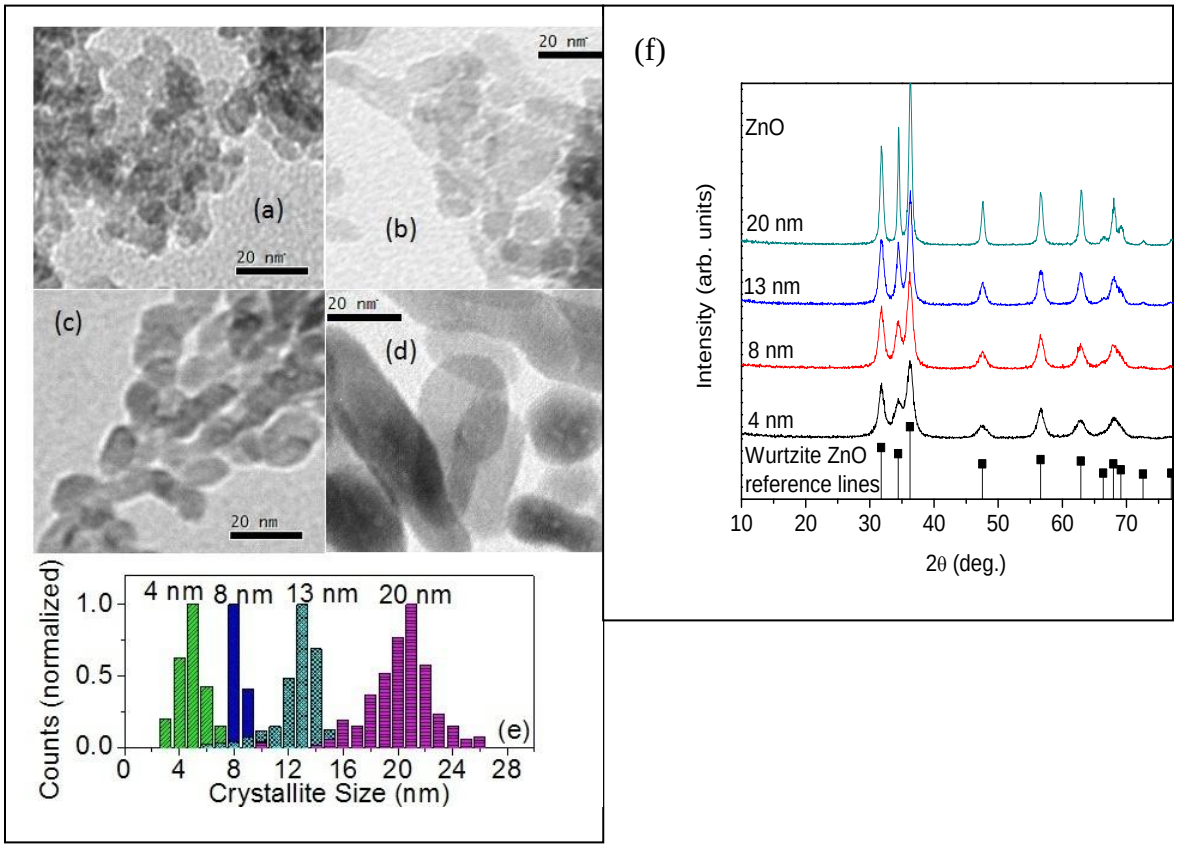

Figure 9. TEM images of different sized ZnO nanoparticle made by varying the hydrolysis molar ratio. A) 4 nm sized ZnO NP made using a water to zinc acetate ratio of 2.4. B) 8 nm sized ZnO NP made using a water to zinc acetate ratio of 6.1. C) 13 nm sized ZnO NP made using a water to zinc acetate ratio of 12.2. D) 20 nm sized ZnO NP made using a water to zinc acetate ratio of 36.6. E) Corresponding size distribution of the samples shown in panels A-D as determined by TEM. F) XRD patterns of the ZnO samples shown in panels A-D. Reference data for wurtzite ZnO is shown along the bottom.

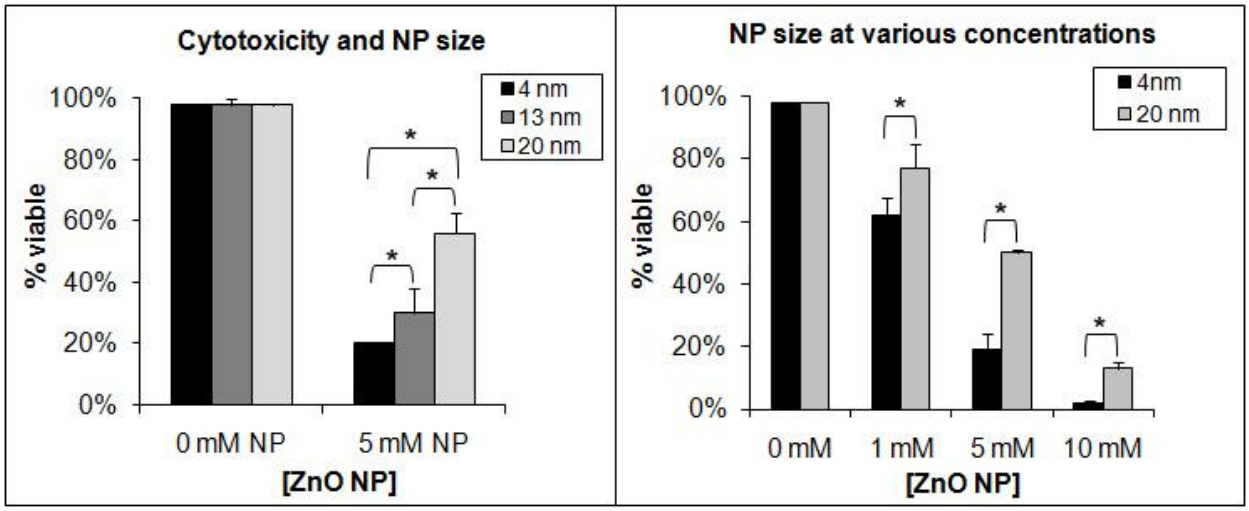

Figure 10. Effect of NP size on cytotoxicity. A) Purified human $CD4^+$ T cells (>97% purity) were left untreated or incubated with three different sizes (4nm, 13nm, and 20 nm) of ZnO NP at a final concentration of 5 mM. Following culture for 22-24 h, viability was determined using PI uptake and flow cytometry, n=4. B) Cytotoxicity studies in purified human $CD4^+$ T cells were performed using varying concentrations (1-10 mM) of 4nm and 20 nm sized ZnO NP, n=4. Error bars depict standard error and asterisks indicate statistically significant differences ($p < 0.05$) as determined by repeated measures ANOVA.

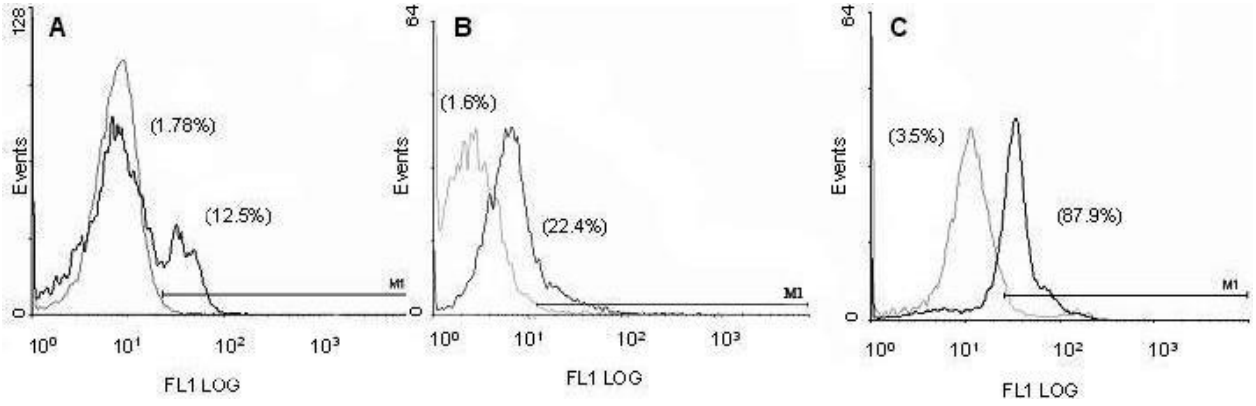

Figure 11. Cellular production of ROS following ZnO NP exposure. ROS generation was evaluated in primary T cells and monocytes and in the transformed Hut-78 T cell line following 18-24 h of ZnO NP exposure using the oxidation sensitive dye DCFH-DA and flow cytometry. A & C) Representative histograms depicting ROS production in primary T cells and monocytes. Assays were performed using freshly obtained whole blood in which red blood cells were removed following NH_4Cl lysis. T lymphocytes and monocytes were gated based on staining with fluorescently labeled CD3 and CD14 Ab and the oxidation product of DCFH-DA detected using the FL1 detector. B) Histogram depicting ROS production in the transformed Hut-78 T cell line. In each histogram, the grey line depicts fluorescence in DCFH-DA loaded cells while the black line depicts fluorescence in DCFH-DA loaded cells treated with ZnO NP for 18 h (A & C) or 24 h (B). Numbers in parentheses indicate the percentage of ROS positive cells.

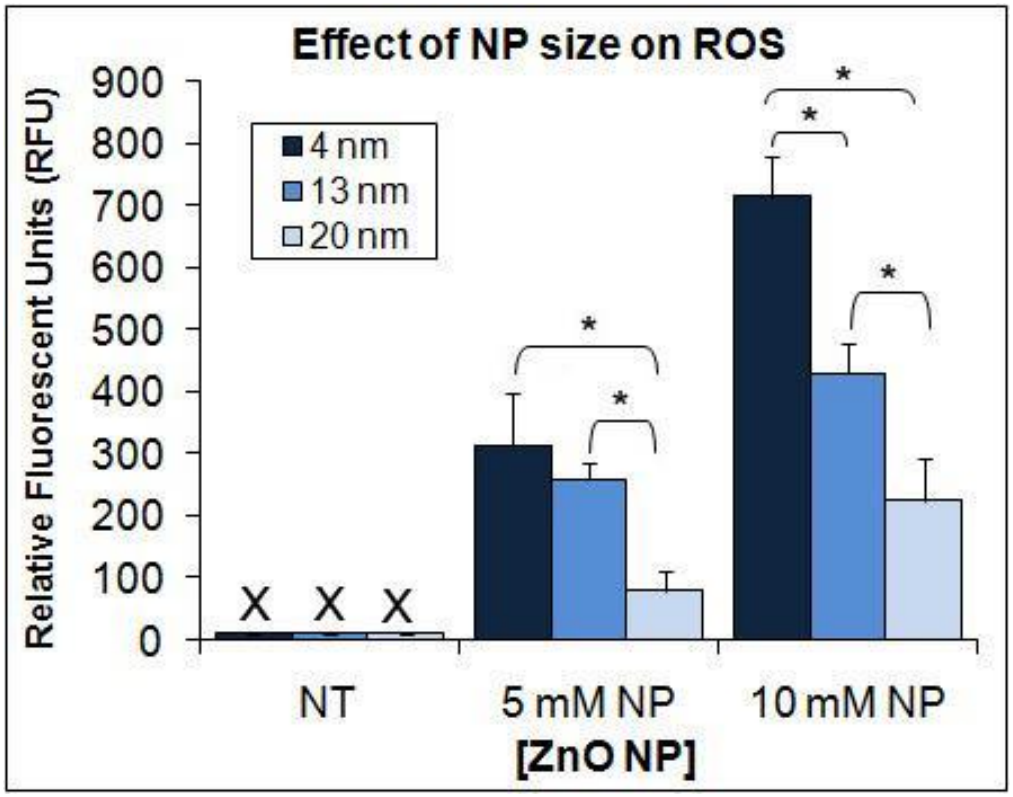

Figure 12. NP size affects ROS production in PBMC. PBMC were treated with two different concentrations (5 mM and 10 mM) of 4 nm, 13 nm and 20 nm ZnO NP for 3 h and ROS production evaluated using a fluorescent microplate reader. Data from one representative experiment is shown (n = 3) and error bars depict standard error. Data was analyzed using a 2-way ANOVA and asterisks denote statistically significant differences as defined by $p < 0.05$.

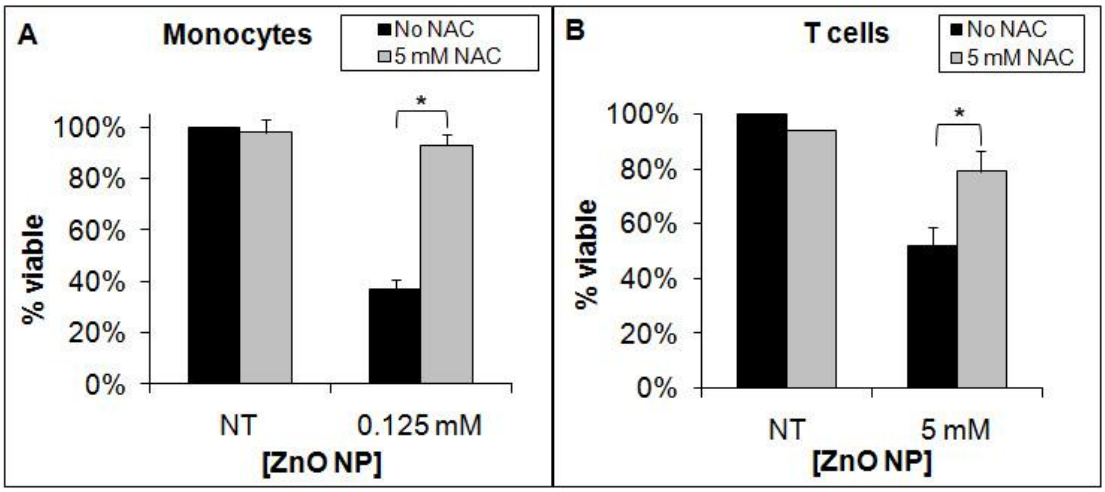

Figure 13. Quenching of ROS rescues T cells and monocytes from ZnO NP-induced cytotoxicity. Purified peripheral blood $CD14^+$ monocytes (≥ 96% purity) and $CD4^+$ T cells (≥ 95% purity) were pretreated for 4-6 h with 5 mM N-acetyl cysteine (NAC) or vehicle control and subsequently cultured with ZnO NP, or left untreated, for 22-24 h. Viability was assessed using the Alamar Blue cytotoxicity assay. A) Purified monocytes treated with 0.125 mM ZnO NP ± 5 mM NAC, n=3. B) Isolated $CD4^+$ T cells treated with 5 mM ZnO NP ± 5 mM NAC, n=3. Data for both T cells and monocytes was analyzed using a 2-way ANOVA; asterisks denote statistically significant differences ($p < 0.05$) and error bars depict standard error.

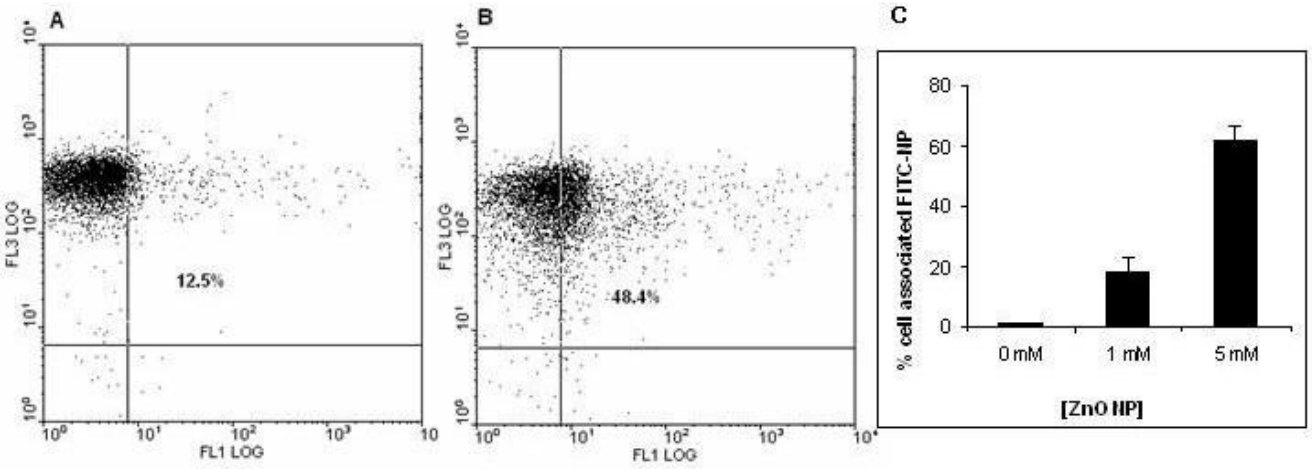

Figure 14. The activation of T cells promotes NP association. Primary $CD4^+$ T cells (>96% purity) were left untreated or activated with immobilized CD3/CD28 antibodies and cultures concurrently treated with 5 mM FITC encapsulated ZnO NP for 4 h. Cells were stained using an ECD-labeled CD4 Ab. Using flow cytometry, 10 000 events gated on $CD4^+$ cells were analyzed for changes in FITC fluorescence and data from a representative histogram is presented. A) Resting T cells cultured with FITC encapsulated NP and panel. B) Activated T cells cultured with FITC encapsulated NP. Inset numbers depict the percentage of FITC positive cells. The positioning of the quadrant on the *x*-axis was determined using T cells cultured without fluorescently labeled NP and set so 1% of cells appeared in quadrant 2. C) Depicts a dose-dependent increase in NP association with T cells, n = 3 with error bars depicting standard error.

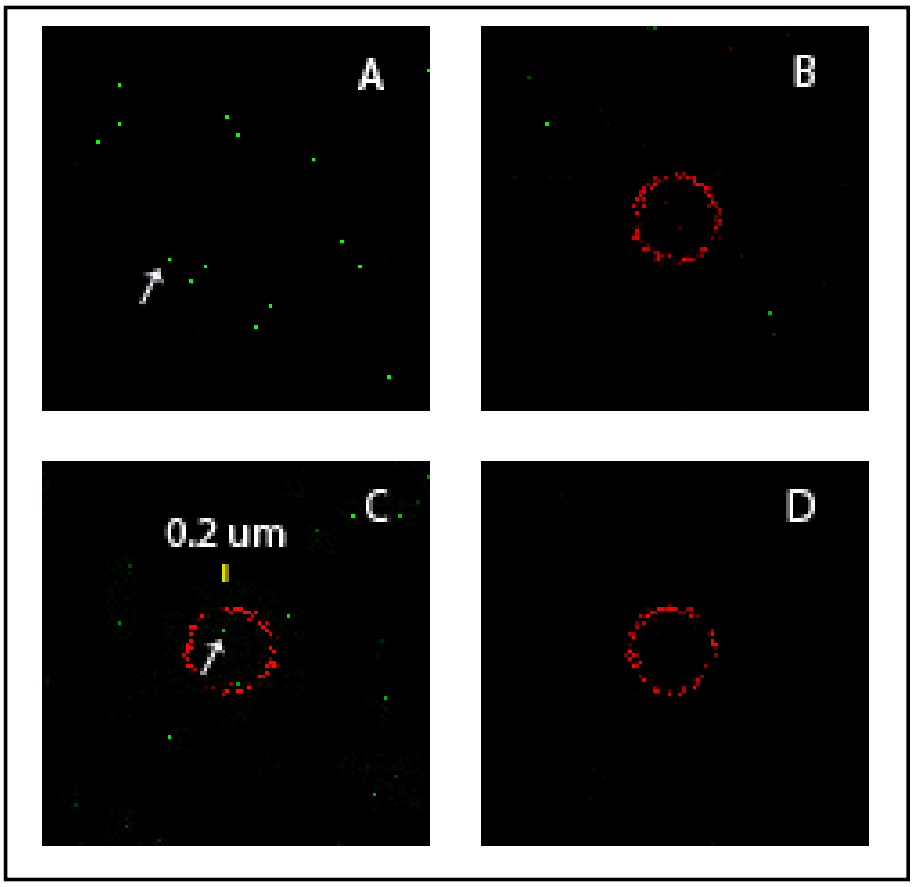

Figure 15. Uptake of FITC-ZnO particles by Jurkat T cells. Confocal fluorescence microscopic images of Jurkat T cancer cells treated with 0.25 mM FITC-ZnO particle (green fluorescence) for 8 h and stained with a PE-conjugated Ab specific to CD3 cell surface protein (red fluorescence) with extensive washing to remove extracellular NP. Panel A depicts FITC-ZnO particles alone (after identical washing steps as samples containing cells) with an arrow indicating a typical particle of ~200 nm. Panels B-D show consecutive cell images/slices of a single cell. In panel C, an internalized particle of expected 200 nm size is indicated by an arrow and orthogonal viewing was used to confirm particle intracellular localization.

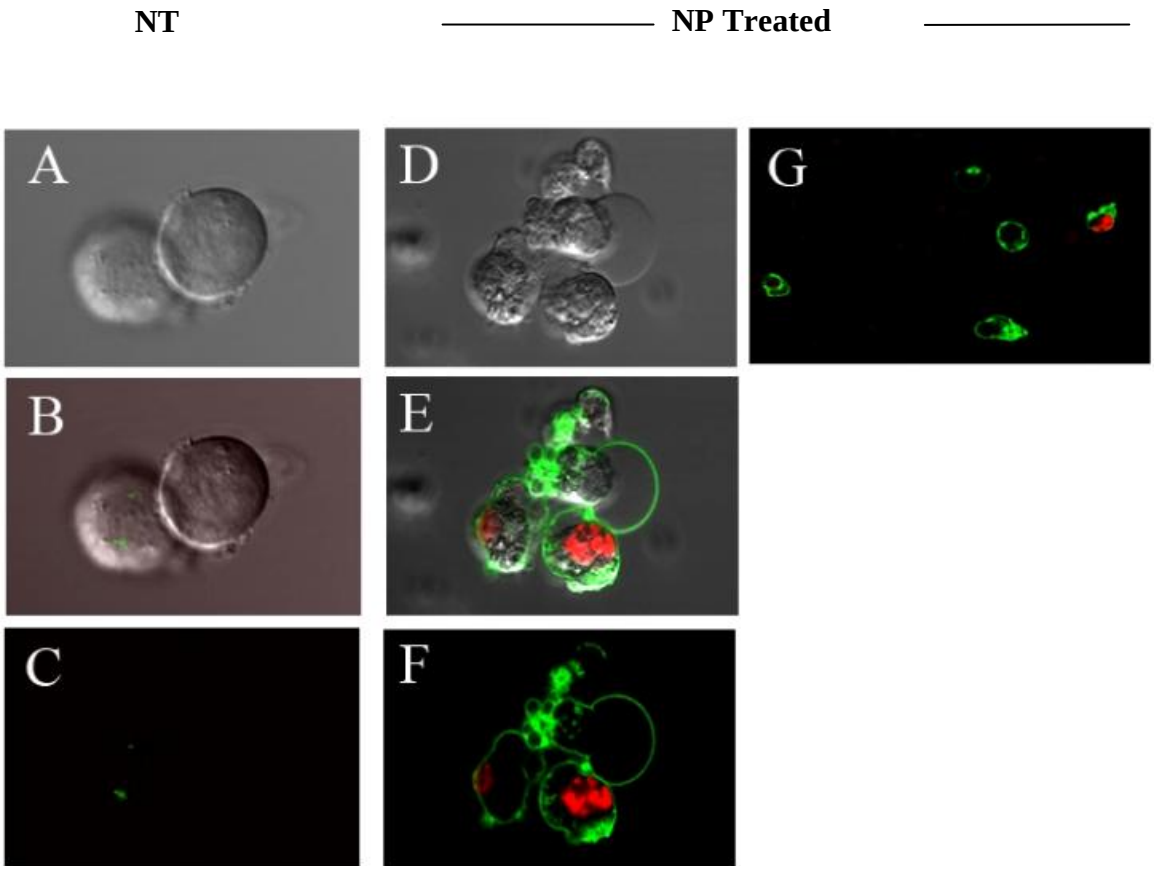

Figure 16. ZnO NP induce apoptosis in Jurkat T cells. Cells were left untreated, treated with 0.3 mM ZnO NP for 20 h, or treated with 100 nM okadaic acid for 20 h (positive control) and stained with a green fluorescent annexin V antibody to detect apoptotic membranes and the red fluorescent dye PI to detect permeable membranes using the Vybrant apoptosis assay kit #2 (Molecular Probes). Cells were visualized by confocal microscopy and representative images are shown. Panels A-C depicts control cells not treated with NP. Panel A shows control differential interference contrast (DIC image), panel B shows control DIC image with green and red fluorescence overlay, and panel C

shows control green and red fluorescence image. Panels D-G depict cells treated with NP; panel D shows NP treated DIC image, panel E shows NP treated DIC image with green and red fluorescence overly, panel F shows NP treated green and red fluorescence image, and panel G shows an additional green and red fluorescence image of NP treated cells of lower magnification.

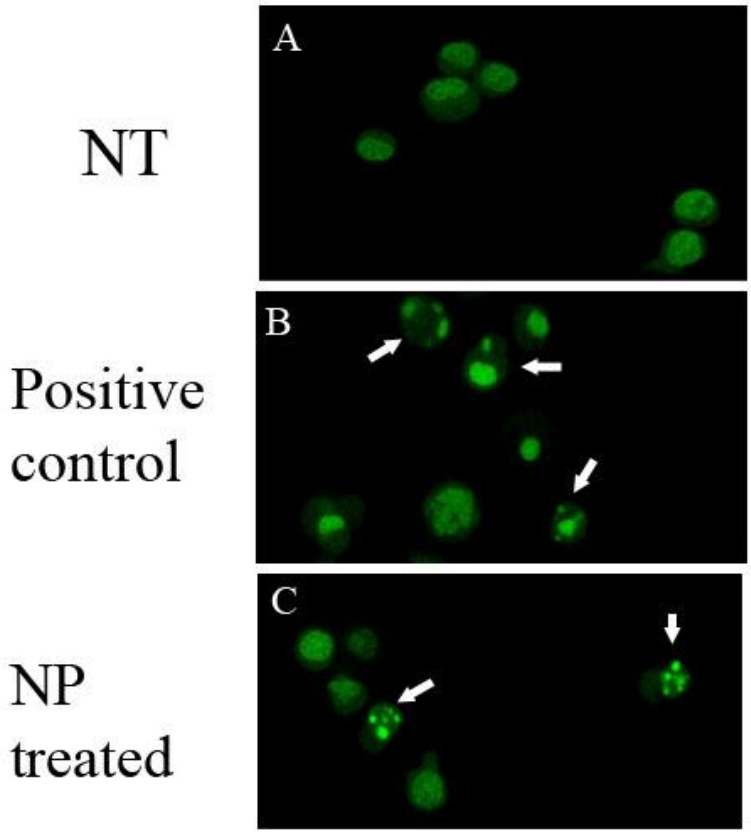

Figure 17. Detection of apoptotic morphological changes in Jurkat cells treated with ZnO NP. Cells were left untreated (A), or treated with 100 nM okadaic acid for 20 h as a positive control for apoptosis (B), or treated with 0.3 mM ZnO NP for 20 h (C) and stained with acridine orange and visualized by fluorescent microscopy. Arrows indicate typical apoptotic cells characterized by a shrunken appearance and condensed or fragmented nuclei.

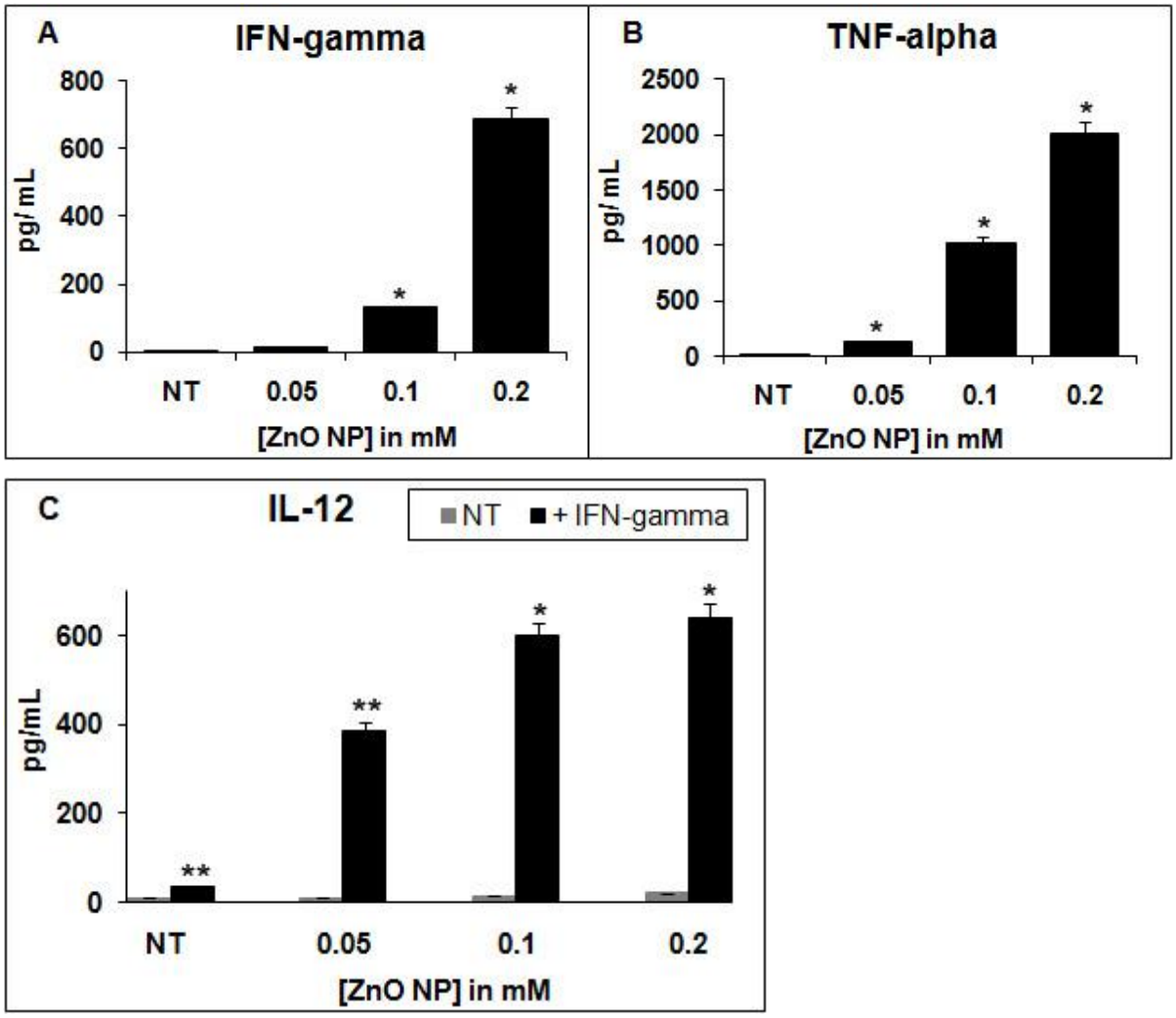

Figure 18. ZnO NP treatment increases pro-inflammatory cytokine production in PBMCs. Primary human peripheral mononuclear cells were left untreated or treated with three concentrations of 8 nm ZnO NP (0.05 mM, 0.1 mM and 0.2 mM), both alone or with the addition of exogenous IFN-γ (1000 U/mL) for 38 h. Cytokine production was evaluated by ELISA and measured in pg/mL. Data was analyzed using a 2-way ANOVA with error bars depicting standard error from the mean. Asterisks denote statistically significant differences as defined as $p < 0.05$. ** = significant differences between all treatment groups (including NT), * = significant differences compared to 0.05 mM and

NT. No significant differences were observed for any samples not primed with exogenous IFN-γ.

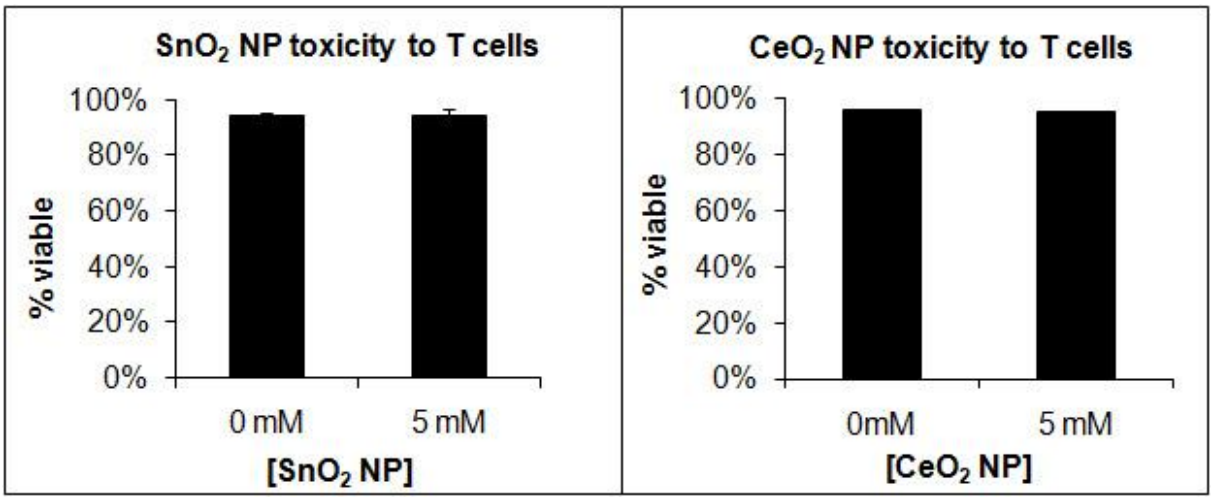

Figure 19. Effect of SnO_2 NP and CeO_2 NP on T cell viability. Purified human $CD4^+$ T cells (> 97% purity) were left untreated or incubated with two different concentrations of either SnO_2 NP or CeO_2. Following culture for 22-24 h, viability was determined using PI uptake and flow cytometry, n=3 from one representative experiment and error bars depict standard error. A) T cells left untreated or treated with 5 mM SnO_2 NP. B) T cells left untreated or treated with 5 mM CeO_2 NP.

Table 1. Freshly isolated PBMC were treated with either 1mM or 5 mM of 8 nm sized ZnO NP and ROS production measured using the oxidation sensitive fluorescent probe, DCFH-DA. Following NP treatment for 6 h or 20 h, cells were stained with fluorescently labeled CD3 (T cells) and CD14 (monocytes) Ab and loaded with DCFH-DA. Flow cytometry was used to simultaneously evaluate ROS production and distinguish T cells and monocytes present in PBMC cultures. Values represent the percentage of ROS producing cells ± standard error from the mean.

Table 1. NP-induced ROS production

Time	***Cells**	**0 mM NP**	**1 mM NP**	**5 mM NP**
6h	T cells	1.4% ± 0.1%	1.3% ± 0%	***ND
6h	mono	1.4% ± 0.13%	19.3% ± 2.6%	***ND
20h	T cells	6.5% ± 2.8%	3.4% ± 1.1%	38.5% ± 1.8%
20h	mono	8.1% ± 3.4%	**<3% viable cells	**<1% viable cells

* $CD3^+$ T cells and $CD14^+/CD3^-$ monocytes (monos) present in PBMCs
** NP-induced cell destruction precludes collection of FS/SSC gated cellular events and subsequent ROS signal
***Values not determined (ND)

Table 2. Freshly isolated PBMCs were left untreated or exposed to 5 mM FITC-encapsulated ZnO NP for 16h. The cell mixture was then stained with fluorescently labeled CD3, CD4, CD19, CD14 Ab to identify subsets, washed to remove excess Ab and unbound NP, and the level of NP association determined based on FITC fluorescent signal using flow cytometry. Data was obtained by gating on 10 000 events, n=3.

Table 2.	**NP association with various immune cells**	
	Control (% / MFI)[a]	**+ FITC-NP (% / MFI)[b]**
$CD3^+$ T cells	1.79% / 1.15	84.2% / 9.84
$CD4^+$ T cells	1.61% / 1.23	82.5% / 14.1
$CD19^+$ B cells	2.0% / 2.85	78.1% / 9.61
$CD14^+$ Monocytes	1.7% / 5.80	98.0% / 131.2

[a]Values shown represent the background autofluorescence signal for control cells (percent FITC positive cells/mean fluorescent intensity (MFI)
[b]The percentage of FITC positive cell and MFI for cells treated with FITC-doped ZnO NP

REFERENCES

Alam R. 1998. A brief review of the immune system. Prim Care 25(4):727-38.

Alfano M, Poli G. 2005. Role of cytokines and chemokines in the regulation of innate immunity and HIV infection. Mol Immunol 42(2):161-82.

Angeli E, Buzio R, Firpo G, Magrassi R, Mussi V, Repetto L, Valbusa U. 2008. Nanotechnology applications in medicine. Tumori 94(2):206-15.

Aruoja V, Dubourguier HC, Kasemets K, Kahru, A. 2009. Toxicity of nanoparticles of CuO, ZnO and TiO2 to microalgae Pseudokirchneriella subcapitata. Science of the Total Environment 407(4):1461-8.

Ashammakhi N. 2006. Nanosize, mega-impact, potential for medical applications of nanotechnology. J Craniofac Surg 17(1):3-7.

Bacic G, Spasojevic I, Secerov B, Mojovic M. 2008. Spin-trapping of oxygen free radicals in chemical and biological systems: new traps, radicals and possibilities. Spectrochim Acta A Mol Biomol Spectrosc 69(5):1354-66.

Baigi MG, Brault L, Néguesque A, Beley M, El Hilali R, Gaüzère F, Bagrel D. 2008. Apoptosis/necrosis switch in two different cancer cell lines: influence of benzoquinone- and hydrogen peroxide-induced oxidative stress intensity, and glutathione. Toxicology in Vitro 22(6):1547-1554

Bawarski W, Chidlowsky E, Bharali D, Mousa S. 2008. Emerging nanopharmaceuticals. Nanomedicine 4(4): 273-282

Becker Y. 2006. Molecular immunological approaches to biotherapy of human cancers--a review, hypothesis and implications. Anticancer Res 26(2A):1113-34.

Behrens G, Li M, Smith CM, Belz GT, Mintern J, Carbone FR, Heath WR. 2004. Helper T cells, dendritic cells and CTL Immunity. Immunol Cell Biol 82(1):84-90.

Beilhack A, Rockson SG. 2003. Immune traffic: a functional overview. Lymphat Res Biol 1(3):219-34.

Bellanti JA, Kadlec JV, Escobar-Gutierrez A. 1994. Cytokines and the immune response. Pediatr Clin North Am 41(4):597-621.

Benzie IF. 2000. Evolution of antioxidant defense mechanisms. Eur J Nutr 39(2):53-61.

Bergamini CM, Gambetti S, Dondi A, Cervellati C. 2004. Oxygen, reactive oxygen species and tissue damage. Curr Pharm Des 10(14):1611-26.

Blair PJ, Riley JL, Carroll RG, St Louis DC, Levine BL, Saha B, Lee KP, Perrin PJ, Harlan DM, June CH. 1997. CD28 co-receptor signal transduction in T-cell activation. Biochem Soc Trans 25(2):651-7.

Bogunia-Kubik K, Sugisaka M. 2002. From molecular biology to nanotechnology and nanomedicine. Biosystems 65(2-3):123-38.

Bosanquet AG, Bell PB. 2004. Ex vivo therapeutic index by drug sensitivity assay using fresh human normal and tumor cells. J Exp Ther Oncol 4(2):145-54.

Bour-Jordan H, Blueston JA. 2002. CD28 function: a balance of costimulatory and regulatory signals. J Clin Immunol 22(1):1-7.

Bowers W. 2006a. Immunology - Cells Involved in Immune Responses. Microbiology and Immunology On-line Textbook. USC School of Medicine.

Bowers W. 2006b. Immunology - Immunoregulation. In: USC School of Medicine, editor. Microbiology and Immunology On-line Textbook. USC School of Medicine

Brayner R, Ferrari-Iliou R, Brivois N, Djediat S, Benedetti MF, Fievet F. 2006. Toxicological impact studies based on Escherichia coli bacteria in ultrafine ZnO nanoparticles colloidal medium. Nano Lett 6(4):866-70.

Burns A, Ow H, Wiesner U. 2006. Fluorescent core-shell silica nanoparticles: towards "Lab on a Particle" architectures for nanobiotechnology. Chem Soc Rev 35:1028-42.

Caligiuri MA. 2008. Human natural killer cells. Blood 112(3):461-9.

Cao G. 2004. Nanostructures and nanomaterials: synthesis, properties and applications. London: Imperial College Press. 1 p.

Chaplin DD. 2006. 1. Overview of the human immune response. J Allergy Clin Immunol 117(2 Suppl Mini-Primer):S430-S435.

Chen J, Patil S, Seal S, McGinnis JF. 2006. Rare earth nanoparticles prevent retinal degeneration induced by intracellular peroxides. Nat Nanotechnol 1(2):142-50.

Chen X, Schluesener HJ. 2008. Nanosilver: a nanoproduct in medical application. Toxicol Lett 176(1):1-12.

Cheng M. 2004. Effects of nanophase materials (< or = 20 nm) on biological responses. J Environ Sci Health A Tox Hazard Subst Environ Eng 39(10):2691-705.

Cho K, Wang X, Nie S, Chen Z, Shin D. 2008. Therapeutic nanoparticles for drug delivery in cancer. Clin Cancer Res 14(5):1310-6.

Coester C, Nayyar P, Samuel, J. 2006. In vitro uptake of gelatin nanoparticles by murine dendritic cells and their intracellular localisation. European Journal of Pharmaceutics and Biopharmaceutics 62(3):306-14.

Cohn M. 2005. A biological context for the self-nonself discrimination and the regulation of effector class by the immune system. Immunol Res 31(2):133-50.

Coligan J.E. 1995. Current Protocals in Immunology. New York: Greene Publishing Associates and Wiley-Interscience. Chapt. 5.1 p.

Cross S, Innes B, Roberts M, Tsuzuki T, Robertson T, McCormick, P. 2007. Human skin penetration of suncreen nanoparticles: in-vitro assessment of a novel micronized zinc oxide formulation. Skin Pharmacol Physiol 20(3):148-54.

Davies KJ. 2000. An overview of oxidative stress. IUBMB Life 50(4-5):241-4.

Decuzzi P, Ferrari M. 2007. The role of specific and non-specific interactions in receptor-mediated endocytosis of nanoparticles. Biomaterials 28(18):2915-2922

Decuzzi P, Ferrari M. 2008. The receptor-mediated endocytosis of nonspherical particles. Biophysical Journal 94(10):3790-3797

Devasagayam TP, Tilak JC, Boloor KK, Sane KS, Ghaskadbi SS, Lele, RD. 2004. Free radicals and antioxidants in human health: current status and future prospects. J Assoc Physicians India 52:794-804.

Dinauer N, Balthasar S, Weber C, Kreuter J, Langer K, von Briesen H. 2005. Selective targeting of antibody-conjugated nanoparticles to leukemic cells and primary T-lymphocytes. Biomaterials 26(29):5898-906.

Djordjevic VB. 2004. Free radicals in cell biology. Int Rev Cytol 237:57-89.

Dobrovolskaia M, McNeil S. 2007. Immunological properties of engineered nanomaterials. Nature Nanotechnology 2:469-478.

Doherty G, McMahon H. 2009. Mechanisms of endocytosis. Annual Review of Biochemistry 78: ahead of print

Donaldson K. 2006. Resolving the nanoparticles paradox. Nanomed 1(2):229-34.

Duffin R, Tran L, Brown D, Stone V, Donaldson K. 2007. Proinflammogenic effects of low-toxicity and metal nanoparticles in vivo and in vitro: highlighting the role of particle surface area and surface reactivity. Inhal Toxicol 19(10):849-56.

Elamanchili P, Diwan M, Cao M, Samuel J. 2003. Characterization of poly(D,L -lactic-co-glycolic acid) based nanoparticulate system for enhanced delivery of antigens to dendritic cells. Vaccine 22(19):2406-12.

Elmore S. 2007. Apoptosis: a review of programmed cell death. Toxicol Pathol 35(4):495-516.

Emerich DF, Thanos CG. 2007. Targeted nanoparticle-based drug delivery and diagnosis. J Drug Target 15(3):163-83.

Erhardt D. 2003 Aug. Materials conservation: Not-so-new technology. Nature Materials; 509 p. Available from.

Fan Z, Lu JG. 2005. Zinc oxide nanostructures: synthesis and properties. J Nanosci Nanotechnol 5(10):1561-73.

Feito MJ, Jimenez-Perianez A, Ojeda G, Sanchez A, Portoles P, Rojo JM. 2002. The TCR/CD3 complex: molecular interactions in a changing structure. Arch Immunol Ther Exp (Warsz) 50(4):263-72.

Feringa BL. 2000. Nanotechnology. In control of molecular motion. Nature 408(6809):151, 153-1, 154.

Feynman R. "There's Plenty of Room at the Bottom". Caltech . 1959. Engineering and Science.
Ref Type: Electronic Citation

Fischer HC, Chan WC. 2007. Nanotoxicity: the growing need for in vivo study. Curr Opin Biotechnol 18(6):565-71.

Fishman MA, Perelson AS. 1999. Th1/Th2 differentiation and cross-regulation. Bull Math Biol 61(3):403-36.

Foell J, Hewes B, Mittler R. 2007. T cell costimulatory and inhibitory receptors as therapeutic targets for inducing anti-tumor immunity. Curr Cancer Drug Targets 7:55-70.

Fortina P, Kricka LJ, Surrey S, Grodzinski P. 2005. Nanobiotechnology: the promise and reality of new approaches to molecular recognition. Trends Biotechnol 23(4):168-73.

Gaur U, Aggarwal BB. 2003. Regulation of proliferation, survival and apoptosis by members of the TNF superfamily. Biochem Pharmacol 66(8):1403-8.

Godfrey DI, Rossjohn J, McCluskey J. 2008. The fidelity, occasional promiscuity, and versatility of T cell receptor recognition. Immunity 28(3):304-14.

Gojova A, Guo B, Kota RS, Rutledge JC, Kennedy IM, Barakat AI. 2007. Induction of inflammation in vascular endothelial cells by metal oxide nanoparticles: effect of particle composition. Environ Health Perspect 115(3):403-9.

Goldsby RA, Kindt T, Osborne B, Kirby J. 2003. Immunology. 5 ed. New York: W.H. Freeman and Company. 119 p.

Goriely S, Goldman M. 2007. The interleukin-12 family: new players in transplantation immunity? Am J Transplant 7(2):278-84.

Guo D, Wu C, Jiang H, Li Q, Wang X, Chen B. 2008. Synergistic cytotoxic effect of different sized ZnO nanoparticles and daunorubicin against leukemia cancer cells under UV irradiation. Journal of Photochemistry and Photobiology B: Biology 93: 119-126

Guo H, Qiao Z, Zhu L, Wang H, Su L, Lu Y, Cui Y, Jiang B, Zhu Q, Xu L. 2004. Th1/Th2 cytokine profiles and their relationship to clinical features in patients following nonmyeloablative allogeneic stem cell transplantation. Am J Hematol 75(2):78-83.

Hanley C, Layne J, Punnoose A, Reddy KM, Coombs I, Coombs A, Feris K, Wingett D. 2008. Preferential killling of cancer cells and activated human T cells using zinc oxide nanoparticles. Nanotechnology 19(29):295103-13.

Hellman S. 1980. Improving the therapeutic index in breast cancer treatment: the Richard and Hinda Rosenthal Foundation Award lecture. Cancer Res 40(12):4335-42.

Hong H, Liu GQ. 2004. Protection against hydrogen peroxide-induced cytotoxicity in PC12 cells by scutellarin. Life Sci 74(24):2959-73.

Huang P, Oliff A. 2001. Drug-targeting strategies in cancer therapy. Current Opinion in Genetic Development 11(1):104-10.

Hummell DS. 1994. The role of T-cell receptors in health and disease. Compr Ther 20(11):616-22.

Huston DP. 1997. The biology of the immune system. JAMA 278(22):1804-14.

Igarashi E. 2008. Factors affecting toxicity and efficacy of polymeric nanomedicines. Toxicol Appl Pharmacol 229(1):121-34.

Jaiswal JK, Mattoussi H, Mauro JM, Simon SM. 2003. Long-term multiple color imaging of live cells using quantum dot bioconjugates. Nat Biotechnol 21(1):47-51.

Jeng H, Swanson J. 2006. Toxicity of metal oxide nanoparticles in mammalian cells. Journal of Environmental Science and Health: Part A 41:2699-711.

Jiang W, Mashayekhi H, Xing B. 2009. Bacterial toxicity comparison between nano- and micro-scaled oxide particles. Environ Pollut.

Johar D, Roth JC, Bay GH, Walker JN, Kroczak TJ, Los M. 2004. Inflammatory response, reactive oxygen species, programmed (necrotic-like and apoptotic) cell death and cancer. Rocz Akad Med Bialymst 49:31-9.

Kam PC, Ferch NI. 2000. Apoptosis: mechanisms and clinical implications. Anaesthesia 55(11):1081-93.

Kantari C, Pederzoli-Ribeil M, Witko-Sarsat V. 2008. The role of neutrophils and monocytes in innate immunity. Contrib Microbiol 15:118-146

Kepp O, Tesnierea A, Zitvogel L, Kroemer G. 2008. The immunogenicity of tumor cell death. Current Option in Oncology 21:71-76.

Kepp O, Tesniere A, Schlemmer F, Michaud M, Senovilla L, Zitvogel L, Kroemer G. 2009. Immunogenic cell death modalities and their impact on cancer treatment. Apoptosis 14:364-375.

Kondo T. 2003. [Differentiation, crossregulation and roles of Th1 and Th2 cells in multiple sclerosis]. Nippon Rinsho 61(8):1409-15.

Krogsgaard M, Davis MM. 2005. How T cells 'see' antigen. Nat Immunol 6 (3):239-45.

Le Page C, Genin P, Baines MG, Hiscott J. 2000. Interferon activation and innate immunity. Rev Immunogenet 2 (3):374-86.

Lenschow DJ, Walunas TL, Bluestone JA. 1996. CD28/B7 system of T cell costimulation. Annu Rev Immunol 14:233-58.

Li KG, Chen JT, Bai SS, Wen X, Song SY, Yu Q, Li J, Wang YQ. 2009. Intracellular oxidative stress and cadmium ion release induce cytotoxicity of unmodified cadmium sulfide quantum dots. Toxicology in Vitro: in press.

Liberman AC, Refojo D, Arzt E. 2003. Cytokine signaling/transcription factor cross-talk in T cell activation and Th1-Th2 differentiation. Arch Immunol Ther Exp (Warsz) 51 (6):351-65.

Limbach LK, Wick P, Manser P, Grass RN, Bruinink A, Stark WJ. 2007. Exposure of engineered nanoparticles to human lung epithelial cells: influence of chemical composition and catalytic activity on oxidative stress. Environ Sci Technol 41 (11):4158-63.

Lindquist JA, Schraven B. 2006. Systems biology of T cell activation. Ernst Schering Found Symp Proc 3:43-61.

Lissoni P, Pittalis S, Roselli MG, Rovelli F, Vigano MG. 1996. Comparison between interleukin-2 and interleukin-12: effects on monocyte functions and their possible importance in the clinical significance of neopterin. Int J Biol Markers 11 (1):58-9.

Locksley RM, Killeen N, Lenardo MJ. 2001. The TNF and TNF receptor superfamilies: integrating mammalian biology. Cell 104 (4):487-501.

Lodish H, Beck A, Zipurksy L, Matsudaira P, Baltimore D, Darnell J. 2000. Molecular Cell Biology Fourth edition, W.H. Freeman and Company, New York.

Long TC, Saleh N, Tilton RD, Lowry GV, Veronesi B. 2006. Titanium dioxide (P25) produces reactive oxygen species in immortalized brain microglia (BV2): implications for nanoparticle neurotoxicity. Environ Sci Technol 40(14):4346-52.

Lovric J, Cho SJ, Winnik FM, Maysinger D. 2005. Unmodified cadmium telluride quantum dots induce reactive oxygen species formation leading to multiple organelle damage and cell death. Chem Biol 12(11):1227-34.

Lowe CR. 2000. Nanobiotechnology: the fabrication and applications of chemical and biological nanostructures. Curr Opin Struct Biol 10(4):428-34.

Luo J, Li N, Paul RJ, Shi R. 2002. Detection of reactive oxygen species by flow cytometry after spinal cord injury. J Neurosci Methods 120(1):105-12.

Lux Research Inc. 2009 Jan. Profits in nanotech come from intermediate products, not raw materials. Lux Research,Inc. <http://www.luxresearchinc.com>

Mackay CR. 2001. Chemokines: immunology's high impact factors. Nat Immunol 2(2):95-101.

Mannie MD. 1999. Immunological self/nonself discrimination: integration of self vs nonself during cognate T cell interactions with antigen-presenting cells. Immunol Res 19(1):65-87.

Maranda E, Robak T. 1998. Biological properties and clinical significance of interleukins 12 (IL-12). Postepy Hig Med Dosw 52(5):489-506.

Martin P, Leibovich SJ. 2005. Inflammatory cells during wound repair: the good, the bad and the ugly. Trends Cell Biol 15(11):599-607.

Martinvalet D, Zhu P, Lieberman J. 2005. Granzyme A induces caspase-independent mitochondrial damage, a required first step for apoptosis. Immunity 22:355-370

Maxwell JC, Niven WD. 2003. The Scientific Papers of James Clerk Maxwell. Courier Dover Publications. 1 p.

Mayer G. 2006. Immunology - Innate (non-specific) Immunity. In: USC School of Medicine, editor. Microbiology and Immunology On-Line Textbook.

May RC, Machesky LM. 2001. Phagocytosis and the actin cytoskeleton. J. Cell Sci. 114(Pt 6):1061-1077

Maysinger D. 2007. Nanoparticles and cells: good companions and doomed partnerships. Org Biomol Chem 5(15):2335-42.

McNeil SE. 2005. Nanotechnology for the biologist. Journal of Leukocyte Biology 78:585-94.

Medema JP, Borst J. 1999. T cell signaling: a decision of life and death. Hum Immunol 60(5):403-11.

Medina C, Santos-Martinez MJ, Radomski A, Corrigan OI, Radomski MW. 2007. Nanoparticles: pharmacological and toxicological significance. Br J Pharmacol 150(5):552-8.

Miao CH. 2007. Recent advances in immune modulation. Curr Gene Ther 7(5):391-402.

Midander K, Cronholm P, Karlsson HL, Elihn K, Moller L, Leygraf C, Wallinder IO. 2009. Surface characteristics, copper release, and toxicity of nano- and micrometer-sized copper and copper (II) oxide particles: a cross-disciplinary study. Small 5(3):389-99.

Middleton D, Curran M, Maxwell L. 2002. Natural killer cells and their receptors. Transpl Immunol 10(2-3):147-64.

Mocellin S, Nitti D. 2008. TNF and cancer: the two sides of the coin. Front Biosci 13:2774-83.

Modlin RL, Sieling PA. 2005. Immunology. Now presenting: gammadelta T cells. Science 309(5732):252-3.

Moghimi SM, Hunter AC, Murray JC. 2005. Nanomedicine: current status and future prospects. FASEB Journal 19 (3):311-30.

Monteiller C, Tran L, MacNee W, Faux S, Jones A, Miller B, Donaldson K. 2007. The pro-inflammatory effects of low-toxicity low-solubility particles, nanoparticles and fine particles, on epithelial cells in vitro: the role of surface area. Occup Environ Med 64: 609-615.

Mulloy B, Rider CC. 2006. Cytokines and proteoglycans: an introductory overview. Biochem Soc Trans 34 (Pt 3):409-13.

Nabiev I, Mitchell S, Davies A, Williams Y, Kelleher D, Moore R, Gun'ko YK, Byrne S, Rakovich YP, Donegan JF, Sukhanova A, Conroy J, Cottell D, Gaponik N, Rogach A, Volkov Y. 2007. Nonfunctionalized nanocrystals can exploit a cell's active transport machinery delivering them to specific nuclear and cytoplasmic compartments. Nano Letters 7 (11):3452-61.

Nair S, Sasidharan A, Rani-Divya VV, Menon D, Nair S, Manzoor K, Raina S. 2008. Role of size scale of ZnO nanoparticles and microparticles on toxicity toward bacteria and osteoblast cancer cells. Journal of Material Science: Materials in Medicine DOI 10.1007/s10856-008-3548-5.

Navalakhe RM, Nandedkar TD. 2007. Application of nanotechnology in biomedicine. Indian J Exp Biol 45 (2):160-5.

Nel A, Xia T, Madler L, Li N. 2006. Toxic potentials of materials at the nanolevel. Science 311:622-7.

Nie S, Xing Y, Kim GJ, Simons JW. 2007. Nanotechnology applications in cancer. Annu Rev Biomed Eng 9:257-88.

NNI. 2009. National Nanotechnology Initiative FY 2008 Budgets and Highlights. National Science and Technology Council. <www.nano.gov/NNI_FY09_budget_summary.pdf>. Accessed 2009 Feb 8.

Nohynek GJ, Dufour EK, Roberts MS. 2008. Nanotechnology, cosmetics and the skin: is there a health risk? Skin Pharmacol Physiol 21(3):136-49.

Oberdorster G, Oberdorster E, Oberdorster J. 2005. Nanotoxicology: an emerging discipline evolving from studies of ultrafine particles. Environ Health Perspect 113(7):823-39.

Oesterling E, Chopra N, Gavalas V, Arzuaga X, Lim EJ, Sultana R, Butterfield DA, Bachas L, Hennig B. 2008. Alumina nanoparticles induce expression of endothelial cell adhesion molecules. Toxicol Lett 178(3):160-6.

Onaran I, Sencan S, Demirtas H, Aydemir B, Ulutin T, Okutan M. 2008. Toxic-dose warfarin-induced apoptosis and its enhancement by gamma ionizing radiation in leukemia K562 and HL-60 cells is not mediated by induction of oxidative stress. Naunyn Schmiedebergs Arch Pharmacol 378(5):471-81.

Osman T, Rardon D, Friedman L, Fanor Vega L. 2006. The commercialization of nanomaterials: today and tomorrow. Journal of the Minerals, Metals and Materials Society 58(4):21-4.

Pancer Z, Cooper MD. 2006. The evolution of adaptive immunity. Annu Rev Immunol 24:497-518.

Parham P. 2005. The Immune System. New York: Garland Science Publishing.

Park EJ, Park K. 2009. Oxidative stress and pro-inflammatory responses induced by silica nanoparticles in vivo and in vitro. Toxicol Lett 184(1):18-25.

Parkin J, Cohen B. 2001. An overview of the immune system. Lancet 357(9270):1777-89.

Proskuryakov SY, Gabai VL, Konoplyannikov AG, Zamulaeva IA, Kolesnikova AI. 2005. Immunology of apoptosis and necrosis. Biochemistry (Mosc) 70(12):1310-20.

Reddy KM, Feris K, Bell J, Wingett DG, Hanley C, Punnoose A. 2007. Selective toxicity of zinc oxide nanoparticles to prokaryotic and eukaryotic systems. Applied Physics Letters 90:213902-3.

Riehemann K, Schneider S, Luger T, Godin B, Ferrari M, Fuchs H. 2009. Nanomedicine-challenge and perspectives. Diagnostics and Drug Delivery 48:872-897

Roca M, Haes AJ. 2008. Probing cells with noble metal nanoparticle aggregates. Nanomedicine 3(4):555-65.

Roco M. 2003. Nanotechnology: convergence with modern biology and medicine. Current Opinion in Biotechnology 14: 337-346.

Rogers W, Basu P. 2005. Factors regulating macrophage endocytosis of nanoparticles: implications for targeted magnetic resonance plaque imaging. Atherosclerosis (178):67-73

Rojo JM, Bello R, Portoles P. 2008. T-cell receptor. Adv Exp Med Biol 640:1-11.

Ryman-Rasmussen JP, Riviere JE, Monteiro-Riviere NA. 2007. Surface coatings determine cytotoxicity and irritation potential of quantum dot nanoparticles in epidermal keratinocytes. J Invest Dermatol 127(1):143-53.

Salata OV. 2004. Applications of nanoparticles in biology and medicine. Journal of Nanobiotechnology 2(3).

Sallusto F, Palermo B, Hoy A, Lanzavecchia A. 1999. The role of chemokine receptors in directing traffic of naive, type 1 and type 2 T cells. Curr Top Microbiol Immunol 246:123-8.

Sayes CM, Reed KL, Warheit DB. 2007. Assessing toxicity of fine and nanoparticles: comparing in vitro measurements to in vivo pulmonary toxicity profiles. Toxicological Sciences 97(1):163-80.

Schepers K, Arens R, Schumacher TN. 2005. Dissection of cytotoxic and helper T cell responses. Cell Mol Life Sci 62(23):2695-710.

Schmid G. 2004. Nanoparticles: From Theory to Application. Wiley-VCH.

Schroder K, Hertzog PJ, Ravasi T, Hume DA. 2004. Interferon-gamma: an overview of signals, mechanisms and functions. J Leukoc Biol 75(2):163-89.

Seabra MC, Mules EH, Hume AN. 2002. Rab GTPases, intracellular traffic and disease. Trends Mol Med 8(1):23-30.

Singh S, Nalwa HS. 2007. Nanotechnology and health safety--toxicity and risk assessments of nanostructured materials on human health. J Nanosci Nanotechnol 7(9):3048-70.

Surh CD, Sprent J. 2008. Homeostasis of naive and memory T cells. Immunity 29(6):848-62.

Takata N, Lee SH, Lim CY, Kim SS, Tsuji N. 2007. Nanostructured bulk copper fabricated by accumulative roll bonding. J Nanosci Nanotechnol 7(11):3985-9.

Taraban V, Rowley T, O'Brien L, Chan C, Haswell L, Green M, Tuft A, Glennie M, Al-Shamkhani A. 2002. Expression and costimulatory effects of the TNF receptor superfamily members CD134 (OX40) and CD137 (4-1BB), and their role in the generation of anti-tumor responses. European Journal of Immunology 32(12):3617-27.

Tarantola M, Schneider D, Sunnick E, Adam H, Pierrat S, Rosman C, Breus V, Sonnichsen C, Basche T, Wegener J, Janshoff A. 2009. Cytotoxicity of metal and semiconductor nanoparticles indicated by cellular micromotility. ACS Nano 3(1):213-22.

Tarnuzzer RW, Colon J, Patil S, Seal S. 2005. Vacancy engineered ceria nanostructures for protection from radiation-induced cellular damage. Nano Lett 5(12):2573-7.

Tau GZ, von der WT, Lu B, Cowan S, Kvatyuk M, Pernis A, Cattoretti G, Braunstein NS, Coffman RL, Rothman PB. 2000. Interferon gamma signaling alters the function of T helper type 1 cells. J Exp Med 192(7):977-86.

Townsend DM, Tew KD, Tapiero H. 2003. The importance of glutathione in human disease. Biomed Pharmacother 57(3-4):145-55.

U.S.Department of Health and Human Services, National Institutes of Health, National Institute of Allergy and Infectious Disease, National Cancer Institute. 2003 Sep. Understanding the Immune System: How It Works. Report nr 03-5423. <www.niaid.nih.gov/Publications/immune/the_immune_system.pdf>. Accessed 2009 Feb 18.

Uthaisangsook S, Day NK, Bahna SL, Good RA, Haraguchi S. 2002. Innate immunity and its role against infections. Ann Allergy Asthma Immunol 88(3):253-64.

Valko M, Leibfritz D, Moncol J, Cronin MT, Mazur M, Telser J. 2007. Free radicals and antioxidants in normal physiological functions and human disease. Int J Biochem Cell Biol 39(1):44-84.

Valko M, Morris H, Cronin MT. 2005. Metals, toxicity and oxidative stress. Curr Med Chem 12(10):1161-208.

Vashist S, Tewari R, Bajpai R, Bharadwaj L, Raiteri R. 2006. Review of quantum dot technologies for cancer detection and treatment. Journal of Nanotechnology Online 2:1-14.

Volk HD, Reinke P, Docke WD. 1999. Immunological monitoring of the inflammatory process: Which variables? When to assess? Eur. J. Surg. Suppl 584:70-72

Wagner DH, Jr. 2007. Re-shaping the T cell repertoire: TCR editing and TCR revision for good and for bad. Clin Immunol 123(1):1-6.

Wajant H, Pfizenmaier K, Scheurich P. 2003. Tumor necrosis factor signaling. Cell Death Differ 10(1):45-65.

Wang H, Wingett D, Engelhard MH, Feris K, Reddy KM, Turner P, Layne J, Hanley C, Bell J, Tenne D, Wang C, Punnoose A. 2009. Fluorescent dye encapsulated ZnO particles with cell-specific toxicity for potential use in biomedical applications. J Mater Sci Mater Med 20(1):11-22.

Wang L, Nagesha DK, Selvarasah S, Dokmeci MR, Carrier RL. 2008. Toxicity of CdSe Nanoparticles in Caco-2 Cell Cultures. J Nanobiotechnology 6:11.

Wieder T, Braumuller H, Kneilling M, Pichler B, Rocken M. 2008. T cell-mediated help against tumors. Cell Cycle 7(19):2974-7.

Wilkinson CD. 2004. Making structures for cell engineering. Eur Cell Mater 8:21-5.

Willcox JK, Ash SL, Catignani GL. 2004. Antioxidants and prevention of chronic disease. Crit Rev Food Sci Nutr 44(4):275-95.

Wilson R. 2008. The use of gold nanoparticles in diagnostics and detection. Chem Soc Rev 37(9):2028-45.

Winoto A. 1997. Cell death in the regulation of immune responses. Curr Opin Immunol 9(3):365-70.

Xia T, Kovochich M, Brant J, Hotze M, Sempf J, Oberley T, Sioutas C, Yeh JI, Wiesner MR, Nel AE. 2006. Comparison of the abilities of ambient and manufactured nanoparticles to induce cellular toxicity according to an oxidative stress paradigm. Nano Lett 6(8):1794-807.

Xia T, Kovochich M, Liong M, Madler L, Gilbert B, Shi H, Yeh J, Zink J, Nel AE. 2008a. Comparison of the mechanism of toxicity of zinc oxide and cerium oxide nanoparticles based on dissolution and oxidative stress properties. ACS Nano 2(10):2121-34.

Xia T, Kovochich M, Liong M, Zink J, Nel A. 2008b. Cationic polystyrene nanosphere toxicity depends on cell-specific endocytic and mitochondrial injury pathways. ACS Nano 2(1):85-96.

Yang H, Liu C, Yang D, Zhang H, Xi Z. 2009. Comparative study of cytotoxicity, oxidative stress and genotoxicity induced by four typical nanomaterials: the role of particle size, shape and composition. J Appl Toxicol 29(1):69-78.

Zhang L, Gu FX, Chan JM, Wang AZ, Langer RS, Farokhzad OC. 2008. Nanoparticles in medicine: therapeutic applications and developments. Clin Pharmacol Ther 83(5):761-9.

Ziegler-Heitbrock, L. 2007. The $CD14^{+}CD16^{+}$ blood monocytes: their role in infection and inflammation. J Leuko Biol 81(3):584-592

Zimmermann C, Prevost-Blondel A, Blaser C, Pircher H. 1999. Kinetics of the response of naive and memory CD8 T cells to antigen: similarities and differences. Eur J Immunol 29(1):284-90.